

UNIVERSITY OF SOUTHAMPTON

**QCD Physics from the AdS/CFT  
Correspondence**

by

Tom Richard Waterson

A thesis submitted for the degree of

Doctor of Philosophy

School of Physics and Astronomy

October 2006

*Dedicated to my father Ian Waterson*

UNIVERSITY OF SOUTHAMPTON

ABSTRACT

FACULTY OF SCIENCE

SCHOOL OF PHYSICS AND ASTRONOMY

Doctor of Philosophy

QCD PHYSICS FROM THE ADS/CFT

CORRESPONDENCE

Tom Richard Waterson

The AdS/CFT correspondence has long been used as a tool for understanding non-perturbative phenomena in QCD-like theories. In its original form, the correspondence proposes a duality between type IIB string theory on  $\text{AdS}_5 \times \text{S}^5$  and  $\mathcal{N} = 4$  supersymmetric Yang-Mills gauge theory. In this thesis, we investigate extensions to the original correspondence that allow one to construct dual supergravity theories to other gauge theories that are more similar to QCD. We study renormalisation group flow as a smooth deformation of the supergravity background. We then investigate dual models including quarks and chiral symmetry breaking in certain D3-D7-brane systems and propose a simple test to determine which supergravity backgrounds will exhibit chiral symmetry breaking behaviour. We go on to describe how improved action ideas from lattice QCD can be incorporated into the correspondence to improve the ultra-violet region of the dual theories. Finally we calculate meson and glueball spectra in the AdS/QCD approach, finding results in good agreement with experimental and lattice data.

# Contents

<b>1</b>	<b>QCD &amp; Quantum Field Theory</b>	<b>1</b>
1.1	QCD . . . . .	1
1.1.1	Confinement & Asymptotic Freedom . . . . .	3
1.2	Chiral Symmetries in QCD . . . . .	5
1.2.1	Chiral Symmetry . . . . .	5
1.2.2	Chiral Symmetry Breaking . . . . .	7
1.3	The 't Hooft Expansion . . . . .	9
<b>2</b>	<b>Superstring Theory</b>	<b>12</b>
2.1	Superstring Theory . . . . .	12
2.2	Supergravity . . . . .	19
2.3	D-Branes . . . . .	22
<b>3</b>	<b>The AdS/CFT Correspondence</b>	<b>25</b>
3.1	Maldacena's Conjecture . . . . .	26
3.2	Deformations and Renormalisation Group Flow . . . . .	32

3.3	Operator Matching . . . . .	34
3.4	Introducing Fundamental Matter . . . . .	36
<b>4</b>	<b>Leigh-Strassler Off Moduli Space</b>	<b>38</b>
4.0.1	Brane Probing . . . . .	38
4.0.2	The Calculation . . . . .	40
<b>5</b>	<b>Gravitational Dual Theories of Chiral Symmetry Breaking</b>	<b>48</b>
5.1	A Geometric Picture of Chiral Symmetry Breaking . . . . .	48
5.2	A Test for Chiral Symmetry Breaking . . . . .	51
5.2.1	D7 Branes and $\mathcal{N} = 4$ Geometries . . . . .	54
5.2.2	Quarks in a Dilaton Flow Geometry . . . . .	60
5.2.3	Spherical D7 Embedding . . . . .	63
5.2.4	A Non-supersymmetric Scalar Deformation . . . . .	68
5.2.5	$N=2^*$ Geometry . . . . .	75
5.2.6	The Yang Mills* Geometry . . . . .	80
5.2.7	Summary . . . . .	87
<b>6</b>	<b>Improving the Glueball Spectrum in Finite Temperature QCD<sup>1</sup></b>	<b>91</b>
6.1	AdS-Schwarzschild Geometries and Finite Temperature QCD . . . . .	92
6.1.1	The $0^{++}$ Mass Spectrum . . . . .	94
6.2	Improving the Ultra-Violet . . . . .	96
6.2.1	The Improved Geometry . . . . .	99
6.2.2	The $0^{++}$ Mass Spectrum . . . . .	100

6.2.3	The $0^{-+}$ Mass Spectrum . . . . .	103
6.3	Conclusions . . . . .	104
<b>7</b>	<b>The AdS/QCD Approach</b>	<b>106</b>
7.1	Improving the Infra-red . . . . .	110
7.1.1	Results . . . . .	123
7.1.2	Conclusions . . . . .	124
7.2	Glueballs in AdS/QCD . . . . .	126
7.2.1	AdS/QCD Glueball Model . . . . .	127
7.2.2	Dilaton Geometry . . . . .	129
7.2.3	Conclusions . . . . .	132
<b>8</b>	<b>Conclusions</b>	<b>140</b>

# List of Figures

2.1	D <sub>p</sub> -brane emitting a closed string . . . . .	23
3.1	Constructing a non-Abelian gauge theory from open strings attached to a stack of D-branes . . . . .	27
3.2	Minkowski space as a radial slice of AdS <sub>5</sub> . . . . .	33
3.3	Fundamental and adjoint fields in a D3-D7 system. . . . .	37
4.1	Direction field for the supergravity fields $\rho(r)$ and $\varphi(r) = \cosh^2 \chi(r)$ showing UV and IR fixed points . . . . .	44
5.1	Geometric chiral symmetry breaking in a D3-D7 system. . . . .	51
5.2	D7 brane flow in the FGPW geometry. The solid lines are the numer- ical solutions and the dashed lines the coordinate transform of the full analytic solutions. The singularity of the geometry is shown as a black circle. . . . .	58
5.3	Apparent values of the quark mass and condensate extracted asymptot- ically from the flows in Figure 5.2. . . . .	58

5.4	Numerical solutions for D7 embeddings in the Constable-Myers geometry with $b = 1$ . The shaded area corresponds to the singularity in the metric. Also plotted is the value of the quark condensate vs the mass extracted asymptotically from those flows. . . . .	63
5.5	Plot of the minimum action spherical D7 embedding and the massless quark embeddings in the Constable Myers Geometry. The black circle represents the singularity in the geometry. . . . .	66
5.6	Plot of the minimum action spherical D7 embedding and a local minimum embedding action for a massive quark in the Constable Myers Geometry. . . . .	66
5.7	4 different flows of the SUGRA field $\lambda(r)$ all of which become singular at $r=0$ . $\lambda_1$ and $\lambda_2$ are the turning point flows between the flows of the form $\lambda_3$ and $\lambda_4$ . . . . .	69
5.8	Sample solutions for a D7 brane embedding in the non-supersymmetric scalar deformation geometry showing the absence of a gap between the solutions and the singularity. . . . .	71
5.9	Sample result of a numerical solution for the determination of a spherical D7 brane embedding $r$ vs $\alpha$ that wraps the $YM^*$ singularity shown by the lower straight line. . . . .	87

5.10 A sketch of how a flat D7 brane embedding is expected to behave in $YM^*$ as the brane is brought close to the singularity. The repulsive potential away from $\alpha = n\pi/2$ will induce a chiral symmetry breaking like configuration although the D7 may collapse into the singularity at $\alpha = \pi/2$ .	88
6.1 Direction field for the supergravity fields $\rho(r)$ and $\varphi(r) = \cosh^2 \chi(r)$ showing UV and IR fixed points	98
6.2 QCD <sub>4</sub> Schrödinger potential for the $0^{++}$ glueballs $\alpha = 0$ to $\alpha = 0.01$	101
6.3 $m_{0^{++*}}/m_{0^{++}}$ for different values of $\alpha$	104
7.1 A plot of the embedding of the D7 brane as a function of the radial coordinate $r$	118
7.2 Plot of $(m_\pi^2 f_\pi^2)/(2c)$ against $m$ . For the Gell-Mann-Oakes-Renner relation to hold, this must be a straight line. As expected, the graph diverges from this straight line behaviour for large $m$	121

# List of Tables

2.1	Summary of the massless states in type IIA and type IIB string theory . . . . .	18
6.1	QCD <sub>4</sub> 0 <sup>++</sup> glueball masses from AdS ( $\alpha = 0$ ) and Improved ( $\alpha = 0.0855$ ) geometries along with lattice data [64, 65]. Normalisation is such that the ground state mass is set to one. . . . .	103
6.2	QCD <sub>4</sub> 0 <sup>−+</sup> glueball masses from AdS ( $\alpha = 0$ ) and Improved ( $\alpha = 0.0855$ ) geometries along with lattice data [64]. All states are normalised to the 0 <sup>++</sup> ground state. . . . .	105
7.1	Results for meson variables in the models discussed in the text. Model A is the new model in the paper with parameters fixed to the starred measurements. AdS A is the equivalent pure AdS model results with a hard IR cut off and the value of the condensate being fitted. Model B is a global fit in the new model and AdS B is the equivalent fit result in pure AdS. . . . .	122
7.2	4d glueball masses from simple AdS slice model. All masses are normalised to $m(0^{++})$ . . . . .	134

7.3	4d glueball masses from AdS slice compared to $N_c = 3$ lattice data [64]. All masses are normalised to $m(0^{++})$ . The total rms error is 12.9% . . . . .	135
7.4	4d glueball masses from AdS plus dilaton geometry. All masses are normalised to $m(0^{++})$ . . . . .	136
7.5	4d glueball masses from AdS plus dilaton geometry compared to $N_c = 3$ lattice data [64]. All masses are normalised to $m(0^{++})$ . The total rms error is 13.4% . . . . .	137
7.6	4d glueball masses from AdS plus dilaton geometry, identifying even(odd) parity solutions with even(odd) values of $n$ . All masses are normalised to $m(0^{++})$ . . . . .	138
7.7	4d glueball masses from AdS plus dilaton geometry, identifying even(odd) parity solutions with even(odd) values of $n$ , compared to $N_c = 3$ lattice data [64]. All masses are normalised to $m(0^{++})$ . The total rms error is 3.9% . . . . .	139

# Motivation

During the last century great strides have been taken in the quest to understand the fundamental forces of nature. The discovery of quantum mechanics and special relativity revolutionized our understanding of fundamental physics, and out of these two great theories was born quantum field theory. One of the first quantum field theories was the theory of quantum electrodynamics or QED [1], discovered in the 1920s and subsequently yielding a Nobel prize for its founders. This remarkable theory of photons and electrons can be argued to be the most successful theory of modern physics, with its predictions verified by experiment to 10 decimal places [2, 3]. QED is an example of a gauge theory. Since its discovery, there has been a great effort to unify all fundamental interactions into a single gauge theory. In the 1950s, Gell-Mann introduced a non-Abelian gauge theory [4] called quantum chromodynamics or QCD, which described the strong nuclear force. Soon after, Weinberg, Glashow and Salam unified the QED with a theory for the weak nuclear force in the so-called Electroweak model [4]. These discoveries were brought together along with the Higgs mechanism [5] for dynamical mass generation into what is known as the Standard Model of particle physics.

This is a unified quantum field theory of the electromagnetic and the strong and weak nuclear forces. This model has proven to be remarkably successful in predicting many properties of nature including for instance the mass of the weak gauge bosons to within a 0.1% error [6].

Despite the success of the Standard Model, there are many criticisms that might be aimed at it. The first most obvious point is that the theory does not include a description of the gravitational force. All attempts to unify general relativity with the current Standard Model into a unified gauge theory have failed. This is largely due to the fact that general relativity is not *renormalisable*. On a more aesthetic note, there are many parameters in the standard model that have to be entered by hand. One would like to have some explanation as to where these numbers come from. For instance, the fact that the proton and electron have equal and opposite charge is an input to the theory and not a prediction. A more subtle point is the problem of fine tuning [7]. The value of the Higgs mass needs to be tuned to around 16 significant figures in order for the theory to give sensible results.

On a practical level, making predictions from the Standard Model, particularly in the theory of the strong interactions, QCD, has proven to be difficult. Currently, QCD can only be solved perturbatively in powers of the strong coupling constant. This is fine for high energy calculations where the value of the coupling is small. However, the value of the coupling increases for low energies. This is the reason that we can't see individual quarks, only bound states of quarks such as the proton. The strength of the coupling constant at low energies means that perturbation theory breaks down and we

are no longer able to make reliable predictions. Although in theory QCD should be able to predict low energy results such as the mass of the proton, in practice there is no calculational tool yet developed that can be used to solve the theory analytically for all energy scales (although one can make some non-perturbative predictions using computational lattice QCD methods [8].)

It was out of an attempt to understand strongly coupled QCD that a new fundamental theory of nature was discovered called String Theory [9, 10]. In string theory, the fundamental building blocks are no longer point-like particles as in the Standard Model, but instead one dimensional “strings”. The different particles of the Standard Model are different modes of vibration of the string. The action of the theory is just the area swept out by the string as it propagates, called the string world-sheet; thus the Euler-Lagrange equations of motion are found by minimizing the area of the world-sheet. From this extremely simple starting point comes a rich theory which shows tantalizing signs of being able to unify all of the fundamental forces including gravity into a single theory. In addition, unlike the standard model, there are no free parameters of the theory, which is remarkable.

Of course there is a catch. One of the predictions from string theory is that the universe should actually be ten-dimensional. This is clearly in violation of current experimental data. One solution might be that the extra dimensions are compactified on a scale that we are currently unable to probe. The shape of the compact space is unknown, and the problem is that different compact spaces give entirely different predictions from string theory. The current dilemma within string theory is which

space to choose in order to give a low energy theory that looks like the standard model plus gravity. The current estimate on the number of possible different spaces is of the order of  $10^{100}$ .

A less ambitious line of development is the theory of Supersymmetry [7, 11], and the supersymmetric standard model. Supersymmetry was discovered in the development of string theory, but can be developed as a theory in its own right. It is a symmetry between bosons and fermions. It is a remarkable symmetry in that it non-trivially combines both space-time and internal symmetry groups, bypassing the so-called “no-go” theorems [12] by adding non-commuting elements to the space-time algebra. One of the major achievements of supersymmetry is that it solves, at least partially, the fine-tuning problem of the standard model. Another nice prediction is that of gauge coupling unification at high energies, a feature not present in the non-supersymmetric standard model. The drawback of this model, though, is that it introduces yet more free parameters and additional particles that are yet to be discovered. It is hoped that some of these extra particles may be found by the Large Hadron Collider [13] when it begins collecting data in around 2008.

Recently, an exciting new link between ten-dimensional string theory and four-dimensional gauge theories has been proposed by Maldacena. In his revolutionary paper [14], Maldacena proposed that there is a duality between the low energy, weak coupling limit of Type IIB string theory compactified on the space  $\text{AdS}_5 \times \text{S}^5$ , and the four-dimensional  $\mathcal{N}=4$  supersymmetric Yang-Mills gauge theory in the strong coupling limit. By duality it is meant that any observable on one side of the correspondence can

be calculated by some method in the dual theory. This is remarkable for two reasons. Firstly, it is providing a link between string theory, believed to be a strong candidate for a unified field theory, and a four-dimensional gauge theory, which have proven to be extremely successful in describing the fundamental forces excluding gravity. Secondly, the correspondence gives us a tool for investigating the strong coupling limit of a gauge theory with many similarities to QCD.

It is believed that the original duality proposed by Maldacena is just one example of a whole class of gauge/string dualities. The belief is that every four dimensional gauge theory can be described by an equivalent higher dimensional string theory including gravity. This is known as the holographic principle. A lot of work has gone into modifying the correspondence in order to find gravitational duals of many gauge theories. The ultimate goal of this approach is to find a dual theory to QCD so that we may finally be able to make predictions in the low energy, strong coupling limit.

# Outline

The outline for this thesis is as follows: In Chapter 1 we first review the theory of QCD and then go on to look at the theory of chiral symmetry breaking. In Chapter 2 String Theory, D-branes and Supergravity are briefly reviewed. In Chapter 3 we give an introduction to AdS/CFT correspondence and modifications of this, which will be the focus of this thesis in studying aspects of QCD at strong coupling. No claim to originality is made for the content of these first three chapters which were compiled using a variety of sources.

In Chapter 4 we look at an example of a deformed geometry in supergravity that is dual to  $\mathcal{N} = 4$  super Yang-Mills in the UV and flowing to an  $\mathcal{N} = 1$  theory in the IR. We show an explicit matching between the dual theories at fixed points along the renormalisation group flow. In Chapter 5 we use the AdS/CFT correspondence to study chiral symmetry breaking from a geometric point of view in a dual higher dimensional gravitational theory. In Chapter 6 we look at glueballs in finite temperature field theory, and how one can improve on predictions from the standard correspondence by introducing an improved action. Finally, in Chapter 7 we move on to the so-called

AdS/QCD approach, which is a “bottom up” approach to finding a gravitational dual theory to QCD.

The work described in Chapters 5 and 6 was carried out in collaboration with Dr. N. J. Evans and Dr. J. P. Shock, and the work in Chapter 7 with Dr. N. J. Evans. References for the published material covering some of the original work in these chapters are

- Chapter 5: N. Evans, J. Shock and T. Waterson, “D7 brane embeddings and chiral symmetry breaking,” *JHEP* **0503** (2005) 005 [[arXiv:hep-th/0502091](https://arxiv.org/abs/hep-th/0502091)].
- Chapter 6: N. Evans, J. Shock and T. Waterson, “Towards a perfect QCD gravity dual,” *Phys. Lett. B* **622** (2005) 165 [[arXiv:hep-th/0505250](https://arxiv.org/abs/hep-th/0505250)].
- Chapter 7: N. Evans and T. Waterson, “Improving the infra-red of holographic descriptions of QCD,” [[arXiv:hep-ph/0603249](https://arxiv.org/abs/hep-ph/0603249)].

# Acknowledgements

Firstly, I would like to thank my supervisor Nick Evans whose guidance and experience have been invaluable. I would also like to thank my other collaborator Jon Shock who was always available to answer my questions with patience and enthusiasm.

I have greatly enjoyed my time here at Southampton and would like to thank all of the staff, students and postdocs in the SHEP group for providing a great working and social environment. Also, thanks to PPARC for funding my studentship and trips to Plymouth and Seattle.

Thanks to Jon, Nick, Mum and Sarah for helping to proofread this thesis. Any remaining mistakes that you find - blame them!

I am grateful to my Dad for getting me interested in physics in the first place, and to both my parents for supporting me throughout my academic career.

Lastly, I would like to thank Angela and Noah for their constant support and putting up with me during the course of writing this thesis.

# Chapter 1

## QCD & Quantum Field Theory

### 1.1 QCD

Since we will be trying to understand aspects of QCD through the AdS/CFT Correspondence, it will be useful to briefly summarize the theory here.

In the theory of QCD, quarks have a *colour* quantum number. There are three colours typically labelled as Red, Blue and Green. The quarks transform in the fundamental **3** representation of an  $SU(3)$  symmetry group associated with the colour quantum number, and the anti-quarks transform in the  $\bar{\mathbf{3}}$  representation. Unlike electric charge, we do not observe colour charge. This is due to confinement, which will be explained later. The particles we observe are all singlets under the colour group, such as mesons ( $\mathbf{3} \otimes \bar{\mathbf{3}} = \mathbf{1} + \dots$ ) and baryons ( $\mathbf{3} \otimes \mathbf{3} \otimes \mathbf{3} = \mathbf{1} + \dots$ ).

The Dirac Lagrangian for the quarks is

$$\mathcal{L} = \bar{q}_a (i\gamma^\mu \partial_\mu - m) q^a, \quad (1.1)$$

where  $a = 1, 2, 3$  and  $\mu = 0, \dots, 3$ . This is invariant under the transformation  $q^a \rightarrow U_b^a q^b$ , where  $U_b^a$  is a constant matrix representation of the  $SU(3)$  symmetry. If this global symmetry is now promoted to a local symmetry by letting  $U$  be a function of  $x$ , this will generate additional terms in the Lagrangian which will need to be cancelled by introducing a covariant derivative

$$\mathbf{D}_\mu(x) = \mathbf{I}\partial_\mu + ig\mathbf{T}^a A_\mu^a(x), \quad (1.2)$$

where  $\mathbf{T}^a$  are the Gell-Mann matrices which are generators of  $SU(3)$ ,  $g$  is the  $SU(3)$  charge, and  $A_\mu^a(x)$  are the connection fields. For the Lagrangian to be invariant, we require that under transformations

$$\mathbf{D}'_\mu = \mathbf{U}^{-1}\mathbf{D}_\mu\mathbf{U}. \quad (1.3)$$

This means that the connection fields must transform in the following way

$$\mathbf{A}'_\mu = \mathbf{U}^{-1}\mathbf{A}_\mu\mathbf{U} + \frac{1}{g}\mathbf{U}^{-1}\partial_\mu\mathbf{U}. \quad (1.4)$$

The fields  $A_\mu^a(x)$  transform in the adjoint representation of the  $SU(3)$  and are the gluons. We can define the field strength tensor as the commutator of two covariant derivatives

$$\mathbf{F}_{\mu\nu} = -\frac{i}{g} [\mathbf{D}_\mu, \mathbf{D}_\nu]. \quad (1.5)$$

This gives

$$F_{\mu\nu}^a = \partial_\mu A_\nu^a - \partial_\nu A_\mu^a - if_{bc}^a A_\mu^b A_\nu^c, \quad (1.6)$$

where  $if^{abc}\mathbf{T}^c = [\mathbf{T}^a, \mathbf{T}^b]$ . The kinetic term for the gluons is therefore

$$-\frac{1}{4}\text{Tr}F_{\mu\nu}F^{\mu\nu}, \quad (1.7)$$

where the trace is taken over the colour group index. This is indeed gauge invariant as can be seen from (1.3), (1.5) and the cyclic property of the trace.

### 1.1.1 Confinement & Asymptotic Freedom

A key feature of this theory is the self interaction of the gluons. Define the  $\beta$ -function as the derivative of the coupling with respect to the log of the defining energy scale  $\mu$ :

$$\beta(g) = \frac{\partial g}{\partial \ln \mu} \quad (1.8)$$

The one-loop  $\beta$  function for QCD is [15]

$$\beta(g) = -\frac{g^3}{(4\pi)^2} \left[ \frac{11}{3}N - \frac{2}{3}N_f \right], \quad (1.9)$$

where  $N$  is the number of colours and  $N_f$  the number of flavours. The first term inside the brackets comes from the self interaction of the gluons and the second term from quark/gluon interactions. In QCD,  $N = N_f = 3$ . This means that the dominant term is the gluon self interaction term and the overall sign of the  $\beta$  function is negative. This has some important consequences for the theory.

At large interaction energies the coupling goes to zero and the quarks essentially become non-interacting. This property is known as *asymptotic freedom* [16, 17]. When the theory of QCD was first proposed in the 1970s there was experimental evidence through deep inelastic scattering reactions such as  $e + p \rightarrow e + \text{anything}$  that cross sections were scale invariant at high energies. This could be explained if the quarks were acting as free particles at high energies. Historically, it was the discovery of asymptotic freedom in QCD that led to it becoming the leading theory of the strong

interactions.

At small interaction energies the coupling becomes large. This gives a possible theoretical interpretation for the confinement of the quarks: the strength of the strong interaction between a pair of quarks increases as their separation increases. The energy required to separate a pair of quarks is greater than the energy required to create a quark/anti-quark pair from the vacuum, therefore we don't observe free quarks. Any attempt to split hadrons will just create more hadrons. Although a rigorous proof of confinement in QCD (or indeed any four-dimensional non-Abelian Yang-Mills theory) is yet to be found, there is compelling numerical evidence coming from lattice QCD that supports this picture.

The fact that the coupling becomes large at small interaction energies also has major consequences when it comes to making concrete numerical predictions from QCD at these energies. The main calculational tool that has been used to date in field theory is perturbation theory, with the expansion parameter in the perturbation series being the coupling constant. When this coupling becomes large, as it does for QCD at low energy, perturbation theory breaks down and we are no longer able to use it to make predictions. This means that, although QCD may be the favoured theory of the strong interactions, we are currently unable to verify it against experiment at low energies. Finding new ways to tackle this problem will be the focus of this thesis.

## 1.2 Chiral Symmetries in QCD

### 1.2.1 Chiral Symmetry

In addition to the exact  $SU(3)$  colour symmetry, the quarks also possess an approximate global  $SU(2)$  flavour symmetry. This symmetry comes from unitary rotations of the u and d quarks. It is only an approximate symmetry as the u and d quarks have only approximately the same mass. In the limit that the quarks become massless, the quark action is invariant under an  $SU(2) \otimes SU(2)$  symmetry as we will now demonstrate. Note that we are ignoring the s quark in this discussion which is slightly heavier (relative to  $\Lambda_{QCD}$ ) than the u and d quarks. The following analysis can be extended in an obvious way to include the s quark.

The fermionic part of the QCD action can be written as

$$\mathcal{L} = \bar{Q}i\gamma^\mu D_\mu Q - \bar{Q}M Q, \quad (1.10)$$

where

$$Q \equiv \begin{pmatrix} u \\ d \end{pmatrix}, \quad M \equiv \begin{pmatrix} m_u & 0 \\ 0 & m_d \end{pmatrix} \quad (1.11)$$

If all of the masses are equal ( $M = mI$ ) then this action is invariant under

$$Q \rightarrow UQ, \quad (1.12)$$

where  $U$  is any constant unitary matrix mixing the u and d quark states. It is useful

to separate out the  $SU(2)$  and the  $U(1)$  parts of this transformation:

$$\begin{aligned} SU(2) : Q &\rightarrow e^{i\theta^a \mathbf{T}^a} Q, \\ U(1) : Q &\rightarrow e^{i\theta} Q, \end{aligned} \quad (1.13)$$

where  $\mathbf{T}^a$  are generators of  $SU(2)$ . The currents associated with these symmetries are

$$j^{a\mu} = \bar{Q} \gamma^\mu \mathbf{T}^a Q, \quad j^\mu = \bar{Q} \gamma^\mu Q \quad (1.14)$$

and the associated conserved quantities are isospin and baryon number.

We can re-write the Lagrangian (1.10) in terms of its chiral components. Let

$$Q_L \equiv \frac{1}{2} (1 - \gamma^5) Q, \quad Q_R \equiv \frac{1}{2} (1 + \gamma^5) Q. \quad (1.15)$$

In terms of these fields, the Lagrangian is

$$\mathcal{L} = \bar{Q}_L i \gamma^\mu D_\mu Q_L + \bar{Q}_R i \gamma^\mu D_\mu Q_R + m(\bar{Q}_R Q_L + \bar{Q}_L Q_R). \quad (1.16)$$

In the limit that  $m = m_u = m_d \rightarrow 0$  this is invariant under separate unitary transformations

$$Q_L \rightarrow U_L Q_L, \quad Q_R \rightarrow U_R Q_R \quad (1.17)$$

and the overall symmetry is enhanced to  $SU(2)_L \otimes SU(2)_R \otimes U(1)_L \otimes U(1)_R$ . The currents associated with these symmetries are

$$\begin{aligned} j_L^{a\mu} &= \bar{Q}_L \gamma^\mu \mathbf{T}^a Q_L, \quad j_R^{a\mu} = \bar{Q}_R \gamma^\mu \mathbf{T}^a Q_R, \\ j_L^\mu &= \bar{Q}_L \gamma^\mu Q_L, \quad j_R^\mu = \bar{Q}_R \gamma^\mu Q_R \end{aligned} \quad (1.18)$$

The sum of left-handed and right-handed currents give the vector currents

$$j_V^{a\mu} = \bar{Q} \gamma^\mu \mathbf{T}^a Q, \quad j_V^\mu = \bar{Q} \gamma^\mu Q \quad (1.19)$$

which are the isospin and baryon number currents (1.14). The difference between the left and right handed currents give the axial vector currents

$$j_A^{a\mu} = \bar{Q}\gamma^\mu\gamma^5\mathbf{T}^a Q, \quad j_A^\mu = \bar{Q}\gamma^\mu\gamma^5 Q. \quad (1.20)$$

These are new currents exclusive to the massless theory, however, they do not appear to be associated with any conserved quantity of the strong interactions. It was proposed in 1960 by Nambu and Jona-Lasinio [18] that the axial symmetries are spontaneously broken. This idea has led to a very good theory for the pions.

### 1.2.2 Chiral Symmetry Breaking

Before we address the consequences of chiral symmetry breaking in QCD, let us first discuss why chiral symmetry might be broken. The attractive force between quarks at low energies is strong, so the cost of creating a quark/anti-quark pair from the vacuum is small. We therefore expect the QCD vacuum to contain a condensate of quark/anti-quark pairs. These pairs must consist of one left-handed and one right-handed quark in order to preserve angular momentum. We therefore expect to find a non-zero condensate of the form

$$\langle \bar{Q}_L Q_R + \bar{Q}_R Q_L \rangle. \quad (1.21)$$

The presence of this expectation value means that quarks moving through the vacuum will appear to have an effective mass. Recall that the  $SU(2)_A$  axial symmetry was only a good symmetry in the limit  $m_u = m_d \rightarrow 0$ . The condensate therefore spontaneously

breaks the  $SU(2)_A$  symmetry group<sup>1</sup>. Goldstone's theorem [15] states that for every spontaneously broken continuous symmetry, the theory must contain a massless particle, known as a Goldstone boson. There are three independent generators of the group  $SU(2)$ , so we therefore expect there to be three massless particles associated with its breaking. Nambu and Jona-Lasinio [18] proposed that the Goldstone bosons of the breaking of the  $SU(2)_A$  are the pions  $(\pi^0, \pi^+, \pi^-)$ . Since the symmetry was not an exact symmetry due to  $m_u$  and  $m_d$  not being exactly equal, the pions are not exactly massless. This picture nicely explains why the pions are so light <sup>2</sup>

Notice that we did not include the  $U(1)_A$  symmetry in the above analysis, which corresponds to transformations

$$Q \rightarrow e^{i\gamma_5 \theta} Q. \quad (1.22)$$

This is because the  $U(1)_A$  is only a symmetry of the classical theory, not the quantum theory - the path integral measure is not invariant. The action of the  $U(1)_A$  symmetry on the measure can be shown [19] to change the Lagrangian by

$$\Delta \mathcal{L} = -\frac{\alpha_s N_f}{16\pi^2} \tilde{F}_{\mu\nu} F^{\mu\nu}, \quad (1.23)$$

where  $\tilde{F}^{\mu\nu} = \epsilon^{\mu\nu\rho\sigma} F_{\rho\sigma}$ . In the limit  $N_f/N \rightarrow 0$  this term goes to zero and the  $U(1)_A$  symmetry is restored. This will be important later on in this thesis when we will take this large  $N$  limit. The Goldstone boson associated with the breaking of this symmetry

---

<sup>1</sup>This is a heuristic argument that is widely believed, however, a formal proof that QCD dynamically breaks its chiral symmetry is yet to be found

<sup>2</sup>If we include the strange quark in this model, there are eight Goldstone bosons. The additional light states are the kaons. These are heavier than the pions as  $m_s$  is substantially heavier than  $m_u$  and  $m_d$

is known as the  $\eta'$  and, predictably, it is rather heavy since the symmetry only exists in the limit  $N_f/N \rightarrow \infty$  and yet in reality  $N_f/N = 1$ .

### 1.3 The 't Hooft Expansion

The main calculational tool for quantum field theories has been perturbation theory. The expansion parameter that is usually used is the coupling constant. Perturbative techniques have proven to be extremely successful when the value of the coupling is small. In fact, perturbative predictions from QED are some of the most accurately verified results in all of physics. However, in QCD, unlike QED, the value of the coupling becomes large in the low energy regime and perturbative techniques break down.

The difficulty for QCD is finding an expansion parameter that remains small for low energies. In [20] 't Hooft proposed that the inverse of the number of colours  $1/N$  could be used as such a parameter and he noticed that some remarkable simplifications occur as  $N \rightarrow \infty$ . The trouble is that  $1/N$  is not a particularly small parameter in which to expand when  $N = 3$ . The hope is that predictions made in the large  $N$  limit will be close to the actual values for  $N = 3$  and that such calculations will at least give some insight into the strong coupling limit of QCD. In fact, corrections to large  $N$  calculations are typically of order  $1/N^2 \sim 10\%$ .

The basis of 't Hooft's method is as follows: The pure gauge part of the QCD  $\beta$  function is given by

$$\mu \frac{dg}{d\mu} = -\frac{11}{3} \frac{g^3}{(4\pi)^2} N + \mathcal{O}(g^5). \quad (1.24)$$

Integrating this equation gives

$$\ln \mu = \frac{24\pi^2}{11} \frac{1}{g^2 N} + \dots \quad (1.25)$$

In order for the strong coupling scale to remain fixed for large  $N$ , the parameter  $\lambda \equiv g^2 N$  must remain fixed. This parameter is known as the 't Hooft coupling and the limit  $N \rightarrow \infty, g^2 \rightarrow 0$  with  $\lambda$  fixed is known as the 't Hooft limit.

The gauge part of the QCD action is

$$\begin{aligned} \mathcal{L} &= -\frac{1}{4} \text{Tr} F_{\mu\nu} F^{\mu\nu} \\ &= \text{Tr} \left[ -\frac{1}{2} \partial_\mu A_\nu^a (\partial^\mu A^{a\nu} - \partial^\nu A^{a\mu}) + g f_{abc} (\partial_\mu A_\nu^a) A^{b\mu} A^{c\nu} \right. \\ &\quad \left. - \frac{1}{4} g^2 f_{abc} f_{de}^a A_\mu^b A_\nu^c A^{d\mu} A^{e\nu} \right]. \end{aligned} \quad (1.26)$$

Notice that if we re-scale  $A \rightarrow A/g$  both of the interaction terms will have the same power of  $g$  and we can bring a factor of  $1/g^2$  outside of the bracket

$$\mathcal{L} = -\frac{1}{4g^2} \text{Tr} F_{\mu\nu} F^{\mu\nu}. \quad (1.27)$$

Now, letting  $g^2 = \lambda/N$

$$\mathcal{L} = -\frac{N}{4\lambda} \text{Tr} F_{\mu\nu} F^{\mu\nu} \quad (1.28)$$

Calculating amplitudes from this action amounts to adding up Feynman diagrams. The components of these diagrams come with the following powers of  $\lambda$  and  $N$

$$\begin{aligned} \text{Propagator} &: \frac{\lambda}{N} \\ \text{Vertex} &: \frac{N}{\lambda} \\ \text{Loop} &: N \end{aligned} \quad (1.29)$$

Considering the diagrams from a topological point of view, a propagator corresponds to an edge, a loop to a face and a vertex to a vertex. A diagram with  $E$  propagators,  $V$  vertices and  $F$  loops will contain a factor

$$N^{V+F-E} \lambda^{E-V} = N^\chi \lambda^{E-V}, \quad (1.30)$$

where  $\chi$  is the Euler characteristic of the surface. The scaling of the diagrams with  $N$  is entirely dependant on the Euler characteristic of the surface, which is topologically invariant. In this case  $\chi = 2 - 2g$ , where  $g$  is the genus of the diagram. The large  $N$  limit is therefore dominated by planar diagrams for which  $g = 0$ . This expansion in terms of  $\chi$  has parallels in string theory, where the surface in question is the string world-sheet. This hints at a possible link between non-Abelian gauge theory and string theory, which will be expanded upon in the next chapter.

## Chapter 2

# Superstring Theory

### 2.1 Superstring Theory

In this thesis we will mainly be concerned with the low energy limit of superstring theory, namely supergravity, and its relationship to strongly coupled gauge theories through the AdS/CFT correspondence. It will be useful, however, to briefly review the fundamentals of superstring theory. For a comprehensive introduction to the subject see for example [9, 10].

The simplest approach to string theory is the so-called *first quantized* approach whereby one formulates the action of a string on its world-sheet (the area swept out by a string as it propagates through spacetime) and then quantizes this action. The alternative *second quantized* approach more commonly used for quantum field theories is known as string field theory and is less well understood.

For simplicity, we will start with the action for a bosonic string

$$S = -\frac{1}{2\pi\alpha'} \int d\tau d\sigma [-\det(\partial_a X^\mu \partial_b X_\mu)]^{1/2}, \quad (2.1)$$

where  $(\tau, \sigma)$  are world-sheet coordinates, and  $X^\mu(\tau, \sigma)$ ,  $\mu = 0, \dots, D-1$  are spacetime coordinates.  $1/(2\pi\alpha')$  is equal to the string tension  $T$ . This action is (up to an overall scaling) nothing more than the area of the two-dimensional world-sheet when embedded in a  $D$  dimensional spacetime, with  $\partial_a X^\mu \partial_b X_\mu$  being the induced metric on the world-sheet. When one minimises this action, one is minimising the area of the world-sheet. This action is a direct extension of the action for a relativistic point particle. In that case, the action is proportional to the length of the particle's world-line and one minimises the length of the world-line in order to obtain the classical path.

The action (2.1) is known as the Nambu-Goto string action. We can simplify this action by introducing an independent *world-sheet* metric  $g_{ab}(\tau, \sigma)$ .

$$S = -\frac{1}{4\pi\alpha'} \int d\tau d\sigma \sqrt{-g} g^{ab} \partial_a X^\mu \partial_b X_\mu. \quad (2.2)$$

This is known as the Polyakov action. This action has the following symmetries:

- D-dimensional Poincaré invariance:

$$\begin{aligned} X^\mu(\tau, \sigma) &\rightarrow X'^\mu(\tau, \sigma) = \Lambda^\mu_\nu X^\nu(\tau, \sigma) + a^\mu, \\ g_{ab}(\tau, \sigma) &\rightarrow g'_{ab}(\tau, \sigma) = g_{ab}(\tau, \sigma). \end{aligned} \quad (2.3)$$

- Diffeomorphism (coordinate) invariance:

$$\begin{aligned} X^\mu(\tau, \sigma) &\rightarrow X'^\mu(\tau', \sigma') = X^\mu(\tau, \sigma), \\ g_{ab}(\tau, \sigma) &\rightarrow g'_{ab}(\tau', \sigma') = \frac{\partial \sigma^c}{\partial \sigma'^a} \frac{\partial \sigma^d}{\partial \sigma'^b} g_{cd}(\tau, \sigma), \end{aligned} \quad (2.4)$$

for new coordinates  $\sigma'^a(\tau, \sigma)$ .

- Two-dimensional Weyl (conformal) invariance:

$$X^\mu(\tau, \sigma) \rightarrow X'^\mu(\tau, \sigma) = X^\mu(\tau, \sigma),$$

$$g_{ab}(\tau, \sigma) \rightarrow g'_{ab}(\tau, \sigma) = \omega(\tau, \sigma)g_{ab}(\tau, \sigma), \quad (2.5)$$

for some general function  $\omega(\tau, \sigma)$ .

In fact, the Weyl symmetry is anomalous. It turns out that in order to cancel the Weyl anomaly the number of spacetime dimensions must be equal to 26. The existence of extra dimensions is a startling prediction of string theory that does not seem to be borne out by experiment. The popular view of string theorists is that the extra dimensions are small and thus beyond the reach of current experimental probes.

We can use these symmetries to gauge fix our action. We can use diffeomorphism invariance to choose the world-sheet metric to be of the form

$$g_{ab} = e^{\phi(\tau, \sigma)}\eta_{ab}, \quad (2.6)$$

where  $\eta_{ab}$  has a signature (-1,1). This is called the conformal gauge. Weyl invariance means that the function decouples from the action and we are left with the very simple action

$$S = \frac{1}{4\pi\alpha'} \int d\tau d\sigma \partial_a X^\mu \partial^a X_\mu, \quad (2.7)$$

Variation of this action with respect to  $X^\mu$  gives

$$\delta_X S = -\frac{1}{2\pi\alpha'} \int d\tau d\sigma (\partial_a \partial^a X_\mu) \delta X^\mu - \frac{1}{2\pi\alpha'} \int d\tau [\delta X^\mu \partial_\sigma X_\mu]_0^l, \quad (2.8)$$

where  $l$  is the length of the string. The first term results in a massless two-dimensional Klein-Gordon equation with independent left and right moving solutions  $X_L(\tau+\sigma)$ ,  $X_R(\tau-\sigma)$ . In addition to this, there is a boundary term due to the finite extent of the string. In order for this to vanish, we require that

$$\delta X^\mu(\tau, 0)\partial_\sigma X_\mu(\tau, 0) = \delta X^\mu(\tau, l)\partial_\sigma X_\mu(\tau, l) = 0. \quad (2.9)$$

We are free to choose either Neumann or Dirichlet boundary conditions at either end of the string. For example, at  $\sigma = l$ :

$$\begin{aligned} \partial_\sigma X^\mu(\tau, l) &= 0, & \text{Neumann} \\ X^\mu(\tau, l) &= c^\mu, & \text{Dirichlet} \end{aligned} \quad (2.10)$$

where  $c^\mu$  is an arbitrary constant. These open strings come in three varieties according to the boundary conditions that they satisfy - Neumann-Neumann (NN), Dirichlet-Dirichlet (DD) or Neumann-Dirichlet (ND).

In addition to open strings, we may also have closed strings where the endpoints of the string meet. These strings must satisfy the periodicity requirement that  $X^\mu(\tau, \sigma + l) = X^\mu(\tau, \sigma)$ . Since the strings are closed, left and right moving modes can exist on the string independently - for open strings a wave travelling one way hits the end and gets reflected back.

The theory of the bosonic string is a rich one with many interesting properties, however, ultimately it cannot describe nature because it does not result in any fermionic spacetime fields. To rectify this, we introduce Majorana world-sheet fermions  $\psi_\alpha^\mu(\tau, \sigma)$ , where  $\alpha = 1, 2$  is a spinor index on the world-sheet. Note that these world-sheet

fermions are *not* spacetime fermions. We would like to have world-sheet supersymmetry between  $X^\mu(\tau, \sigma)$  and  $\psi^\mu_\alpha(\tau, \sigma)$ . Since there is also the field  $g_{ab}$  present in the action we will need to introduce its fermionic superpartner  $\chi_{a\alpha}$ , which can be thought of as a world-sheet gravitino. The supersymmetric action is

$$S = -\frac{1}{4\pi\alpha'} \int d\tau d\sigma \sqrt{-g} \left[ g^{ab} \partial_a X^\mu \partial_b X_\mu - ig^{ab} \psi^\mu \rho_a \partial_b \psi_\mu + 2g^{ab} g^{cd} \bar{\chi}_a \rho_c \rho_b \psi^\mu \partial_d X_\mu + \frac{1}{2} g^{ab} g^{cd} \bar{\psi}_\mu \psi^\mu \bar{\chi}_a \rho_c \rho_b \chi_d \right], \quad (2.11)$$

where  $\rho^a$  are  $2 \times 2$  gamma matrices

$$\rho^0 = \begin{pmatrix} 0 & -i \\ i & 0 \end{pmatrix}, \quad \rho^1 = \begin{pmatrix} 0 & i \\ i & 0 \end{pmatrix} \quad (2.12)$$

As in the bosonic case, things simplify in the (super)conformal gauge:

$$S = -\frac{1}{4\pi\alpha'} \int d\tau d\sigma [\partial_a X^\mu \partial^a X_\mu - i\psi^\mu \rho_a \partial^a \psi_\mu]. \quad (2.13)$$

This gauge-fixed action has a world-sheet supersymmetry

$$\delta X^\mu = \bar{\epsilon} \psi^\mu, \quad \delta \psi^\mu = -i\rho^a \partial_a X^\mu \epsilon, \quad (2.14)$$

and, in addition to the Klein-Gordon equation for the bosonic fields, there is a two-dimensional Dirac equation for the fermions

$$\partial_a \partial^a X^\mu = 0, \quad \rho^a \partial_a \psi^\mu = 0. \quad (2.15)$$

In order for superstring theory to be consistent, it turns out that, instead of the 26 dimensions required by bosonic string theory, the required number of spacetime dimensions is 10.

For the fermionic fields in the closed string theory, there is an additional possibility when imposing periodicity requirements. It is equally valid for the fields to be anti-periodic in  $\sigma$ :

$$\begin{aligned}\psi^\mu(\tau, \sigma + l) &= \psi^\mu(\tau, \sigma), & \text{Ramond (R)} \\ \psi^\mu(\tau, \sigma + l) &= -\psi^\mu(\tau, \sigma), & \text{Neveu-Schwarz (NS).}\end{aligned}\tag{2.16}$$

It can be shown that the NS states are all spacetime bosons, and the R states are all spacetime fermions. It can also be shown that the NS sector contains a tachyon. In order to get a physically satisfying theory, we must somehow combine both the R and the NS sectors and remove the tachyonic state in a way that leaves a *spacetime* supersymmetry. This can be achieved in what is known as the GSO projection.

The full spectrum of the closed superstring is obtained by combining both the left moving and the right moving modes. We thus have four distinct sectors

$$\text{NS-NS, R-R, NS-R, R-NS}$$

The NS-NS and R-R sectors will consist of bosonic fields, and the NS-R, R-NS sectors will consist of fermionic fields.

We can split the massless states of the NS-NS sector into a symmetric, traceless part, an anti-symmetric part and a trace part. These are massless fields propagating in ten-dimensional space:

$$G_{\mu\nu}(x), \quad B_{\mu\nu}(x), \quad \Phi(x)$$

$G_{\mu\nu}(x)$  is the familiar metric tensor,  $\Phi(x)$  is the dilaton, and  $B_{\mu\nu}(x)$  is a 2-form.

In the R-R sector we have an additional choice to make, namely the chirality of the R modes. There are two inequivalent choices: Opposite chirality for the left and right movers, or the same chirality for both. Opposite chirality leads to the fields

$$C_{(1)\mu}, \quad C_{(3)\mu\nu\lambda}$$

The same chirality leads to

$$C_{(0)\mu}, \quad C_{(2)\mu\nu}, \quad C_{(4)\mu\nu\lambda\rho}$$

If we include the NS-R and the R-NS sectors, then each theory has  $\mathcal{N} = 2$  local spacetime supersymmetries. This is, in fact, the highest number of supersymmetries in ten dimensions consistent with a compactification to four dimensions. Remarkably, the massless content of these theories is exactly the same as that of the two classical theories of type IIA and type IIB supergravity, with opposite chirality  $\Rightarrow$  type IIA and same chirality  $\Rightarrow$  type IIB. Because of this, the string theories are known as type IIA and type IIB string theory. We will explore this connection in the next section.

Type IIA	bosons:	$G_{\mu\nu}, B_{\mu\nu}, \Phi, C_{(1)\mu}, C_{(3)\mu\nu\lambda}$
	fermions:	$\chi_{\mu,\alpha}^L, \chi_{\mu,\alpha}^R, \lambda_{\alpha}^L, \lambda_{\alpha}^R$
Type IIB	bosons:	$G_{\mu\nu}, B_{\mu\nu}, \Phi, C_{(0)\mu}, C_{(2)\mu\nu}, C_{(4)\mu\nu\lambda\rho}$
	fermions:	$\chi_{\mu,\alpha}^L, \chi_{\mu,\alpha}^R, \lambda_{\alpha}^L, \lambda_{\alpha}^R$

Table 2.1: Summary of the massless states in type IIA and type IIB string theory

We have so far considered non-interacting strings propagating in a flat background. Consider now adding a constant dilaton background  $\Phi(x) = \Phi_0$ . The string action will

acquire an extra term

$$\frac{\Phi_0}{4\pi} \int d\tau d\sigma \sqrt{-g} R. \quad (2.17)$$

In two dimensions, this factor is purely topological and is equal to  $2\Phi_0(1-h)$ , where  $h$  is the genus of the surface - the string world-sheet. In the string equivalent of Feynman diagrams adding a loop corresponds to increasing the genus of the surface by one. In a functional integral the addition of the dilaton will give

$$e^{-S} \rightarrow e^{-2\Phi_0(1-h)} e^{-S}. \quad (2.18)$$

If we define the string coupling as

$$g_s = e^{\Phi_0} \quad (2.19)$$

then

$$e^{-S} \rightarrow (g_s^2)^{h-1} e^{-S} \quad (2.20)$$

Adding a closed string loop will give an additional weighting of  $g_s^2$ . The coupling in string theory is given by the vacuum expectation value of the dilaton. Different values of  $g_s$  do not correspond to different theories, but rather different backgrounds of the same theory.

## 2.2 Supergravity

Before superstring theory was formulated, an alternative approach to quantum gravity, known as supergravity, was developed. Supergravity is a supersymmetric formulation of general relativity, where the supersymmetry is promoted to a local symmetry. The theory of supergravity is not a renormalisable quantum theory (due to the negative

dimension of Newton's constant  $G_N$ ), and its action is purely classical. However, it is entirely possible that it is the low energy effective action of some quantum theory. In fact, we will see that it emerges as the low energy limit of superstring theory.

The largest possible supersymmetry algebra in four dimensions is  $\mathcal{N} = 8$ . Any larger algebras would require massless states with helicities greater than 2, which is believed to be impossible. This theory has  $4\mathcal{N} = 32$  supercharges. This bound on the number of supercharges will also hold for higher dimensional theories, since one can reduce higher dimensional theories to four dimensions through some compactification. This puts an upper bound on the dimension of a consistent supersymmetric theory. In fact, the highest dimensional supersymmetric theory has  $\mathcal{N} = 1$  supersymmetry in 11 dimensions, since the smallest representation in 11 dimensions has 32 supercharges. If we restrict ourselves to an action with two or fewer derivatives, as one does with standard general relativity, there is a unique supersymmetric action in 11 dimensions

$$S_{11} = \frac{1}{2\kappa^2} \int d^{11}x \sqrt{-G} \left( R - \frac{1}{2} |F_4|^2 \right) - \frac{1}{12\kappa^2} \int A_3 \wedge F_4 \wedge F_4, \quad (2.21)$$

where  $A_3$  is a 3-form potential and  $F_4$  is its 4-form field strength. We can dimensionally reduce this theory to 10 dimensions by compactifying on a circle and keeping only the massless states. The smallest spinor representation in 10 dimensions has 16 supercharges. We therefore obtain a theory with  $\mathcal{N} = 2$  supersymmetry and two spinor representations. If we choose these to have the opposite chirality  $(\mathbf{16}, \overline{\mathbf{16}})$ , the theory is known as type IIA supergravity. The theory where the spinors have the same chirality  $(\mathbf{16}, \mathbf{16})$  is known as type IIB supergravity. The bosonic sector of the action (excluding

Chern-Simons terms) for these two theories is

$$S_{IIA} = \frac{1}{4\kappa^2} \int d^{10}x \sqrt{-G} e^{-2\Phi} (2R + 8(\partial\Phi)^2 - |dB|^2 - |F_2|^2 - |F_4|^2),$$

$$S_{IIB} = \frac{1}{4\kappa^2} \int d^{10}x \sqrt{-G} e^{-2\Phi} (2R + 8(\partial\Phi)^2 - |dB|^2 - |F_1|^2 - |F_3|^2 - |F_5|^2), \quad (2.22)$$

where  $F_n$  are n-form field strength tensors. Remarkably, this is precisely the low energy action for type IIA and type IIB string theory after integrating out heavy modes <sup>1</sup>.

The constant  $\kappa$  appearing in (2.22) is physically irrelevant due to the factor  $e^{-2\Phi}$ . If  $\Phi$  acquires a vacuum expectation value  $\Phi_0$ , we can scale this out of the action to get a pre-factor of  $e^{-2\Phi_0}$ . This confirms the role of the  $e^{\Phi_0}$  as the string coupling constant.

We have so far restricted the action to include terms with two or less derivatives. However, since there is no renormalisability requirement, terms with more derivatives can be added which are consistent with the symmetries of the theory. Such terms will come with a dimensional constant. In string theory this is  $\alpha'$ , which is proportional to the square of the string length  $l_s \sim \sqrt{\alpha'}$ . Allowing terms proportional to  $\alpha'$  will give *stringy* corrections to the supergravity action. However, in this thesis we will work in the limit that  $\alpha' \rightarrow 0$ .

The presence of the dilaton factor in (2.22) means that the supergravity action does not look like the usual Einstein-Hilbert action plus the action for fields in curved

---

<sup>1</sup>It was shown by Witten [21] that in the strong coupling limit an eleventh dimension emerges from IIA string theory, and the low energy limit of this 11-dimensional theory is 11-dimensional supergravity. This 11-dimensional theory is believed to unite all consistent string theories into a single model known as M-Theory. The low energy limit of this is believed to be 11-dimensional supergravity.

spacetime. This can be rectified by performing a Weyl rescaling of the metric

$$G_{\mu\nu} = e^{\frac{1}{2}\Phi} g_{\mu\nu}. \quad (2.23)$$

The metric  $G_{\mu\nu}$  is known as the *string frame* metric, and  $g_{\mu\nu}$  is known as the *Einstein frame* metric. In the Einstein frame the action (2.22) becomes

$$\begin{aligned} S_{IIA} &= \frac{1}{4\kappa^2} \int d^{10}x \sqrt{-g} \left( 2R - (\partial\Phi)^2 - e^{\frac{3}{2}\Phi} |dB|^2 - e^{\frac{3}{2}\Phi} |F_2|^2 - e^{\frac{1}{2}\Phi} |F_4|^2 \right), \\ S_{IIB} &= \frac{1}{4\kappa^2} \int d^{10}x \sqrt{-g} \left( 2R - (\partial\Phi)^2 - e^{\frac{3}{2}\Phi} |dB|^2 - e^{2\Phi} |F_1|^2 - e^{\Phi} |F_3|^2 - |F_5|^2 \right), \end{aligned} \quad (2.24)$$

### 2.3 D-Branes

We have already seen that open strings can obey either Neumann or Dirichlet boundary conditions at either end independently in each direction. Consider an open string with  $p$  Neumann and  $9 - p$  Dirichlet boundary conditions at one end. Such strings ends will be restricted to a  $p$ -dimensional hypersurface. This is known as a Dp-brane [22]. Open strings living on the brane mean that it is truly a dynamical object. Consider Figure 2.1 showing an open string with both ends on a single Dp-brane. If the two ends meet, the string can become closed and leave the surface of the Dp-brane. The Dp-brane is acting as a source for closed strings. The time reversed process is of course also possible whereby a closed string touches a Dp-brane and the endpoints open up to form an open string whose end points are free to move along the surface of the Dp-brane. In fact, it can be shown that Dp-branes are solitonic solutions of the closed string theory [23].

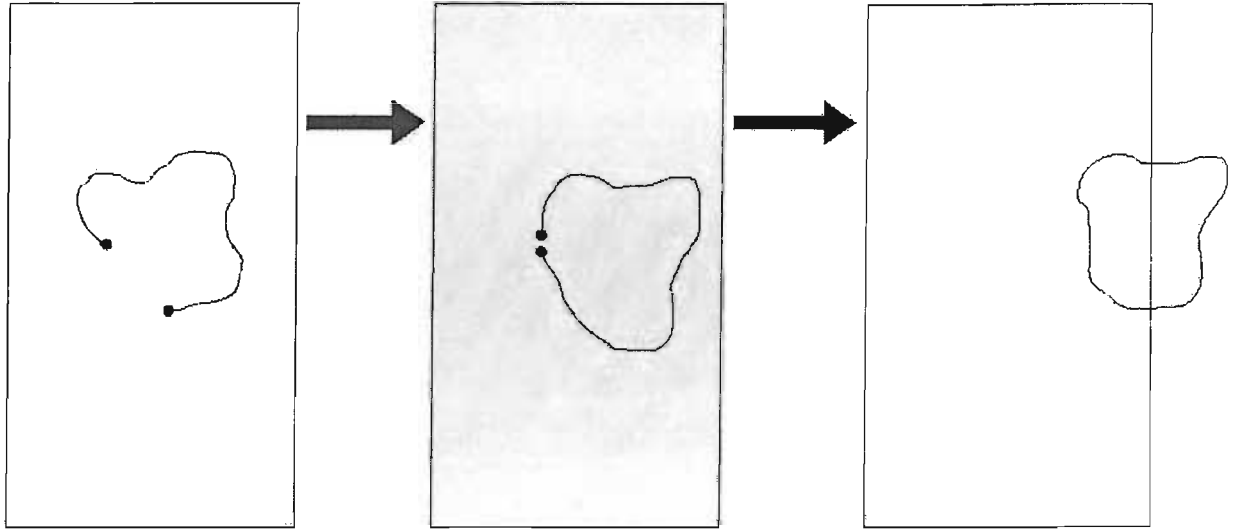


Figure 2.1: Dp-brane emitting a closed string

The simplest form of action for a Dp-brane is given by

$$S_p = -\mu_p \int d^{p+1}\xi e^{-\Phi} [-\det(\mathbf{P}[G]_{ab})]^{1/2}, \quad (2.25)$$

where  $\xi^a, a = 0, \dots, p$  are coordinates on the brane and  $\mu_p$  is proportional to the tension of the D-brane.  $\mathbf{P}[G]_{ab}$  is the metric induced on the D-brane when it is embedded in the space with metric  $G_{\mu\nu}$ , otherwise known as the *pullback* of the metric

$$\mathbf{P}[G]_{ab} = \frac{\partial X^\mu}{\partial \xi^a} \frac{\partial X^\nu}{\partial \xi^b} G_{\mu\nu}, \quad (2.26)$$

where  $X^\mu(\xi^a)$  are the embedding coordinate functions. The form of the action (2.25) is a direct extension of the string action (2.1) to higher dimensions. The action is proportional to the *world-volume* of the Dp-brane.

We have included in the action (2.25) the coupling to the dilaton. We can also include coupling to other spacetime fields. The Dp-brane can couple to the NS-NS

2-form  $B_{\mu\nu}$ . As with the metric, the action will contain the pullback of this field. The brane can also couple to a RR  $(p+1)$ -form since we can include in the action a term

$$i\mu_p \int_{p+1} C_{(p+1)}$$

which obeys all of the relevant symmetries.

Since the Dp-branes have open strings with their end points fixed to the surface, we expect to find in the action a  $U(1)$  gauge theory describing these strings. We can include this as a field strength  $F_{ab}$  living on the surface of the brane. The full bosonic action for the Dp-brane is

$$S_p = -\mu_p \int d^{p+1}\xi e^{-\Phi} \left[ -\det(G_{ab} + B_{ab} + 2\pi\alpha' F_{ab}) \right]^{1/2} + i\mu_p \int_{p+1} \exp(2\pi\alpha' F_{ab} + B_{ab}) \wedge \sum_q C_{(q)}. \quad (2.27)$$

Note that the integral of the expansion in the Chern-Simons-like term will pick out only those terms of the correct dimensionality. Also note that we have dropped the pullback notation for simplicity. All bulk fields appearing in this action are the pullbacks of the full dimensional fields onto the Dp-brane. The precise form of this action can be deduced by requiring gauge invariance and by using *T-Duality*, a topic not discussed here, see for example [9].

## Chapter 3

# The AdS/CFT Correspondence

The Maldacena conjecture [14] or AdS/CFT correspondence is a conjecture concerning certain string theories on backgrounds of the form  $\text{AdS}_d \times M_{D-d}$ , where  $\text{AdS}_d$  is  $d$ -dimensional anti de-Sitter space and  $M_{D-d}$  is some compactified space in  $D - d$  dimensions. The conjecture states that string theory on these backgrounds are mathematically equivalent to certain conformal gauge theories in spacetimes of dimension  $d - 1$ , interpreted as the boundary of  $\text{AdS}_d$ . By mathematically equivalent we mean that any quantity that can be calculated in one theory can, in principle, be calculated in the other theory. A more precise formulation of the conjecture was subsequently presented in [33, 34]. A number of checks have been performed in order to test the conjecture, see for example [24, 25], although a proof has yet to be found. The idea of a higher dimensional theory being determined entirely by a lower dimensional theory is known as *holography*. For a discussion of this concept see for example [26].

One of the exciting things about the AdS/CFT correspondence is that it relates

weakly coupled string theories to strongly coupled gauge theories and vice-versa. This means that both the gauge theories and the string theories can be studied in the non-perturbative strong coupling limit by switching to the dual description. In this thesis, we will be using the correspondence to investigate non-perturbative physics in the boundary gauge theory.

An important extension to the original correspondence was made in [27]. In this paper, the author demonstrated that the correspondence could be extended to non-conformal gauge theories by modifying the background spacetime of the string theory. Subsequently, a number of papers have been published demonstrating dualities between various non-conformal gauge theories and string theories on certain backgrounds, see for example [28, 29, 30].

Another important breakthrough came in [31], where the authors demonstrated a technique for introducing quarks into the gauge theory through the use of probe D7-branes. These developments will be discussed later in this chapter. First, however, we will review the origins of the AdS/CFT correspondence. This involves considering two different descriptions of a stack of parallel Dp-branes.

There are many reviews of the AdS/CFT correspondence available. Some of the better ones are [58, 32].

### 3.1 Maldacena’s Conjecture

Before stating Maldacena’s conjecture, we will first give two different descriptions for a stack of  $N$  D3-branes.

## *D-Branes and Non-Abelian Gauge Theory*

D-branes can be used to construct a non-Abelian gauge theory. Consider a stack of  $N$  coincident D-branes as shown in Figure 3.1. Open strings can have either both endpoints on a single D-brane or different endpoints on different D-branes. Now associate a particular (colour) charge with all of the string endpoints ending on a particular D-brane - a so-called *Chan-Paton* factor. The massless modes of the  $N^2$  different species of open strings will lead to a  $U(N)$  gauge theory of gauge bosons in the adjoint representation.

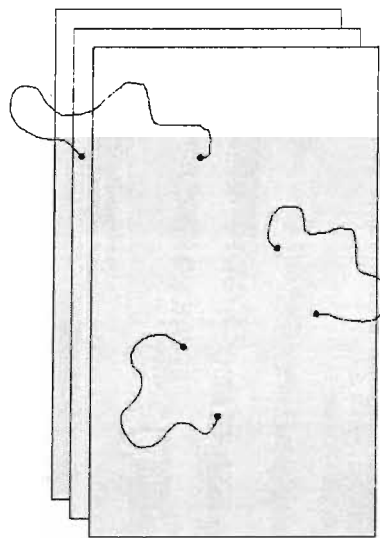


Figure 3.1: Constructing a non-Abelian gauge theory from open strings attached to a stack of D-branes

The presence of the Dp-branes in string theory will break the 10-dimensional Lorentz invariance

$$SO(1, 9) \rightarrow SO(1, p) \times SO(9 - p)$$

The remaining symmetry is a  $(p+1)$ -dimensional Lorentz symmetry on the world-volume of the  $D_p$ -branes and an  $SO(9 - p)$  symmetry in the remaining directions. From the point of view of the  $U(N)$  field theory on the world-volume, this can be regarded as an internal symmetry group. We will be most interested in the case  $p = 3$ , where the field theory is four-dimensional. The internal symmetry group for  $p = 3$  is  $SO(6)$  which is locally isomorphic to  $SU(4)$ , and this symmetry is regarded as the R-symmetry part of the  $\mathcal{N} = 4$  supersymmetry. Therefore, the theory of massless open strings on  $N$  coincident  $D3$ -branes is  $\mathcal{N} = 4$   $U(N)$  supersymmetric Yang-Mills theory.

The field content of this theory consists of a vector gauge boson  $A^\mu, \mu = 0, \dots, 3$ , six scalars  $\phi^a, a = 1, \dots, 6$  and four fermions  $\psi^i, i = 1 \dots, 4$ . In  $\mathcal{N} = 1$  language, these can be grouped into a vector multiplet  $(A^\mu, \psi^4)$  and three gauge multiplets  $(\psi^i, \lambda^i)$ , where we have grouped the six real scalars into three complex scalars  $\lambda^i$ . It must also be noted that this theory is finite.

In total, there are three parts to the effective action of the massless modes: The four dimensional action of open strings on the world-volume of the branes, the closed string modes in the bulk and interactions between the two

$$S = S_{\text{brane}} + S_{\text{bulk}} + S_{\text{int}} \quad (3.1)$$

The interaction terms will all involve derivatives, each coming with a power of  $\sqrt{\alpha'}$ . Therefore, if we take the low energy, supergravity limit  $\alpha' \rightarrow 0$  the two theories on the branes and in the bulk will decouple.

*Multiple  $D3$ -branes in Supergravity*

Any string theory with closed strings will contain gravity. A stack of  $N$  Dp-branes in such a theory will be heavy and will naturally warp the space into which they are embedded. This may be described by some classical metric along with some other background fields including the dilaton and the RR  $(p+1)$ -form potential for which the Dp-branes act as a source. A solution for a stack of  $N$  D3-branes in type IIB supergravity can be found which takes the form

$$ds^2 = H^{-1/2}(r) \left[ -dt^2 + \sum_{i=1}^3 dx_i^2 \right] + H^{1/2}(r) [dr^2 + r^2 d\Omega_5^2], \quad (3.2)$$

where

$$H(r) = 1 + \left( \frac{R}{r} \right)^4 \quad (3.3)$$

and  $d\Omega_5^2$  is the metric of a unit 5-sphere.  $R$  is an overall length scale of the metric

$$R^2 = \sum_{i=4}^9 dy_i^2$$

The form of  $H$  can be understood as  $H$  is a solution of the Laplace equation over the transverse 5-sphere

$$\partial_r (\sqrt{-g} g^{\mu\nu} \partial_r H(r)) = 0 \quad (3.4)$$

$\Rightarrow$

$$\partial_r (r^5 \partial_r H(r)) = 0. \quad (3.5)$$

which gives the result quoted in (3.2).

The only RR field allowed by the symmetries is  $A_{(4)\mu\nu\rho\sigma}$ . The equation of motion for this field yields

$$R^4 = \frac{4}{\Omega_5} \int_{S^5} *F_5, \quad (3.6)$$

where  $F_5 = dA_{(4)}$  and  $\star$  denotes the Hodge dual. From this it is clear that the value of  $R$  is determined by the flux of  $F_5$  through the transverse 5-sphere. For  $N$  D3-branes this flux evaluates to [32]

$$R^4 = 4\pi N g_s l_s^4, \quad (3.7)$$

where  $g_s$  is the string coupling and  $l_s$  is the string length.

The metric (3.2) implies that the energy  $E$  of an object measured by an observer at a position  $r$  will be related to the energy  $E_\infty$  of the same object measured by an observer at infinity by

$$E_\infty = H^{-1/4} E. \quad (3.8)$$

In the low energy limit an observer at infinity will measure two distinct types of low energy excitations: Massless bulk closed string excitations and any excitations in the near horizon  $r \rightarrow 0$  region of the geometry. In the low energy limit these two types of excitations will decouple and we will be left with two contributions to the total action

$$S = S_{\text{near-horizon}} + S_{\text{bulk}} \quad (3.9)$$

In the near-horizon limit the geometry (3.2) becomes

$$ds^2 = \frac{r^2}{R^2} \left[ -dt^2 + \sum_{i=1}^3 dx_i^2 \right] + \frac{R^2}{r^2} dr^2 + d\Omega_5^2. \quad (3.10)$$

This is just  $\text{AdS}_5 \times \text{S}^5$  with both an AdS radius and a 5-sphere radius of  $R$ .

Equations (3.1) and (3.9) must be equated since they describe the same physics. In the low energy limit we then have

$$S_{\text{near-horizon}} = S_{\text{brane}} \quad (3.11)$$

This is the essence of the AdS/CFT correspondence.

“ $\mathcal{N} = 4$  super-Yang-Mills theory in 3+1 dimensions is the same as (dual to) type IIB superstring theory on  $AdS_5 \times S^5$ ”[14, 58].

We must be careful when taking the low energy limit. Consider moving one of the D3-branes away from rest of the stack by a distance  $r$ . A string stretched between this brane and one in the stack will have a minimum energy  $E \sim r/\alpha'$  (since the string tension is  $T \sim 1/\alpha'$ ). When we take the limit  $\alpha' \rightarrow 0$  we would like to keep this “W-boson” mass fixed, so we require that  $U \equiv r/\alpha'$  is fixed as  $\alpha', r \rightarrow 0$ .

In order for the supergravity approximation to be valid the radius of curvature  $R$  must be much greater than the string length  $l_s$ . From (3.7) this implies that

$$\frac{R^4}{l_s^4} \sim g_s N \gg 1. \quad (3.12)$$

The string coupling  $g_s$  is related to the Yang-Mills coupling  $g_{YM}$  by  $g_s = g_{YM}^2$ <sup>1</sup>, so the supergravity approximation is valid for  $g_{YM}^2 N \gg 1$ . This is the t’Hooft coupling of Section 1.3. This is important as it is telling us that the correspondence only holds in the non-perturbative limit of the SYM field theory. This is one of the reasons why the AdS/CFT correspondence is so powerful. Non-perturbative four-dimensional field theory calculations can be transformed into perturbative ten-dimensional supergravity problems. We would also like the string coupling  $g_s$  to be small so that we can ignore higher order string interactions. We must therefore take  $N \rightarrow \infty$ .

As a check on this correspondence we can look at the symmetries of each theory. The SYM field theory is invariant under the superconformal group  $C(1, 3)$  and an  $SU(4)_R$

---

<sup>1</sup>This can be seen by expanding the DBI action (2.27) for a D3-brane

R-symmetry. The supergravity theory is invariant under the isometry group  $SO(2, 4)$  corresponding to the  $AdS_5$  space, and  $SO(6)$  rotations on the 5-sphere. We can see that there is indeed a local isomorphism between the symmetry groups on both sides:  $C(1, 3) \simeq SO(2, 4)$  and  $SU(4) \simeq SO(6)$ .

### 3.2 Deformations and Renormalisation Group Flow

Fixed values of  $r$  in  $AdS_5$  correspond to slices of four-dimensional Minkowski space. In the standard AdS/CFT correspondence, the Minkowski slice is defined at  $r = \infty$ . This means that the CFT has a cut-off energy scale set at infinity. We can look at CFTs with a finite energy cut-off by taking the Minkowski slice to be at some finite value of  $r$ . A picture of this is shown in Figure 3.2. The radial AdS coordinate  $r$ , therefore, corresponds to a (renormalisation group) energy scale in the field theory. To demonstrate this assertion consider a dilatation transformation on the field theory coordinates

$$x^\mu \rightarrow \lambda x^\mu, \quad E \rightarrow \lambda^{-1} E. \quad (3.13)$$

Now consider the same scaling on the AdS metric

$$ds^2 = \frac{r^2}{R^2} dx_\mu dx^\mu + \frac{R^2}{r^2} dr^2. \quad (3.14)$$

$x^\mu \rightarrow \lambda x^\mu$  is only a symmetry if  $r$  scales like an energy,  $r \rightarrow \lambda^{-1}r$ . Large  $r$  corresponds to large energies and small  $r$  to small energies. Throughout the thesis, as is common in works involving the AdS/CFT correspondence, we will refer to large  $r$  regions as the “UV” of the supergravity dual and small  $r$  as the “IR”, remembering that these terms

refer to the energy scale of the dual field theory.

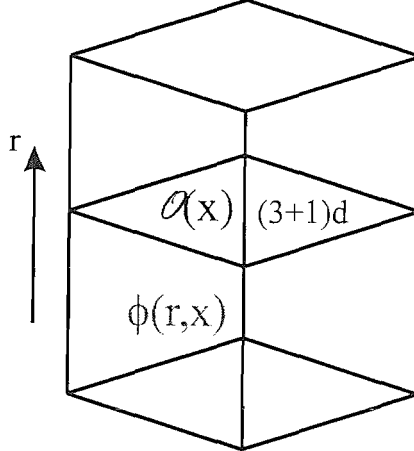


Figure 3.2: Minkowski space as a radial slice of  $\text{AdS}_5$ .

This idea is important as it allows us to construct dual supergravity theories to other four-dimensional field theories besides  $\mathcal{N} = 4$  supersymmetric Yang-Mills. Field theories can be studied that are  $\mathcal{N} = 4$  SYM in the UV but flow to different theories in the IR through the introduction of extra symmetry breaking operators. The gravity dual of such operators can be found by considering perturbations about the  $\mathcal{N} = 4$  theory in the UV. By adding the appropriate fields on the supergravity side of the duality one can in theory construct a supergravity theory which matches the field theory at all points during the renormalisation group flow. The supergravity theory may be modified by deforming the metric and/or adding extra fields. It is important that any deformations or extra fields must go to zero for large  $r$  (the UV) and the geometry return to  $\text{AdS}_5 \times \text{S}^5$ .

In the next chapter we will describe in some detail an example of a deformed

AdS/CFT correspondence and show the explicit matching of the two theories at different points along the renormalisation group flow.

### 3.3 Operator Matching

We have stated that ten-dimensional type IIB supergravity on  $\text{AdS}_5 \times \text{S}^5$  and four-dimensional  $\mathcal{N} = 4$  supersymmetric Yang-Mills are different descriptions of the same theory. What is not yet clear is precisely how states on either side of the correspondence are related. This matter was greatly clarified in [33, 34].

The explicit correspondence states that

$$\langle \exp \int d^4x \phi_0 \mathcal{O} \rangle_{\text{CFT}} = \mathcal{Z}_{\text{SUGRA}}(\phi_0). \quad (3.15)$$

Here  $\mathcal{O}$  is some four dimensional field theory operator,  $\mathcal{Z}_{\text{SUGRA}}$  is the generating functional of the supergravity theory, and  $\phi_0$  is some “dual” bulk supergravity field evaluated on the  $r \rightarrow \infty$  boundary of AdS space which acts as a source for the operator  $\mathcal{O}$ . We can use this relationship to calculate arbitrary correlation functions in the CFT purely in terms of supergravity fields, e.g.

$$\langle \mathcal{O}(x_1) \dots \mathcal{O}(x_n) \rangle = \frac{\delta}{\delta \phi_0(x_1)} \dots \frac{\delta}{\delta \phi_0(x_n)} \mathcal{Z}_{\text{SUGRA}}(\phi_0). \quad (3.16)$$

In order to determine correlation functions for CFT operators  $\mathcal{O}(x)$ , we must first discover the correct dual supergravity field  $\phi(x, r)$ . A simple check is to look at the dimension and symmetry properties of  $\phi$  at the boundary  $r \rightarrow \infty$  ( $\phi_0(x) \equiv \phi(x, \infty)$ ). We know that the product  $\phi_0 \mathcal{O}$  must have mass dimension four and be invariant under all symmetries associated with the CFT.

As an example of operator matching consider the problem of finding the supergravity dual to the bilinear quark operator  $\bar{q}q$ . This is a Lorentz scalar of dimension three, we are therefore looking for a scalar supergravity field of dimension one. The  $\bar{q}q$  operator does not transform under the  $SU(4)$  R-symmetry, so we will also require that the dual field has no indices on the 5-sphere. The action for a massive scalar  $\phi(r)$  in  $\text{AdS}_5$  is

$$S = \int dr \sqrt{g} \left[ (\partial_r \phi)^2 + M^2 \phi^2 \right]. \quad (3.17)$$

The equation of motion

$$\partial_r (\sqrt{g} g^{rr} \partial_r \phi) = M^2 \sqrt{g} \phi \quad (3.18)$$

has the general solution

$$\phi(r) = Ar^{-(4-\Delta)} + Br^{-\Delta}, \quad (3.19)$$

where  $\Delta \equiv 2 \pm \sqrt{4 + M^2}$  and  $A$  and  $B$  are arbitrary constants. If we take<sup>2</sup>  $M^2 = -3$  the solution is

$$\phi(r) = \frac{m}{r} + \frac{c}{r^3}. \quad (3.20)$$

Again  $m, c$  are constants. Because supergravity fields do not scale under four-dimensional conformal transformations,  $m$  must have dimension one. It therefore corresponds to a mass parameter, being a source for  $\bar{q}q$ . For the other solution,  $c$  must have mass dimension three corresponding to the vacuum expectation value (vev) of the quark bilinear  $\langle \bar{q}q \rangle$ .

---

<sup>2</sup>The fact that AdS space has negative curvature means that we can have fields with  $M^2 < 0$  and still have a positive overall energy density.

### 3.4 Introducing Fundamental Matter

Quarks can be added to the dual supergravity theory through the addition of D7-branes [31]. More properly, fields in the fundamental representation of the  $SU(N)$  group can be included. Gauge fields living on the stack of D3-branes are in the adjoint of the  $SU(N)$  colour group since both endpoints have an associated colour charge which depends on the brane that they are attached to - these types of strings transform as an  $(\bar{N}, N)$ . In order for strings to transform in the fundamental representation, they must have only one end attached to a D3-brane. The other is attached to a D7 brane. The mass of the string is determined by the distance of the D7 from the D3 stack at the origin - see Figure 3.4.

D7-branes are used for a number of reasons: Firstly, the dimension is different to three, so they can be distinguished from the D3-branes and have a different associated charge - a flavour charge. Secondly, the degrees of freedom of the system are such that the supergravity Lagrangian gives a dual theory of mesons. This will be explored in Chapter 5. Lastly, the D3-D7 system is stable due to the D7 wrapping a 3-cycle of the 5-sphere. For more on the stability of this system see [31].

One may worry that the introduction of extra D7-branes will distort the geometry. In general this will be the case but, if the number of D7-branes  $N_f$  is small compared to the number of D3-branes  $N$ , the correction to the geometry will be small and can be ignored in the first approximation. This is known as the probe approximation. It is usually valid to use the probe approximation as we take the number to D3-branes to approach infinity.

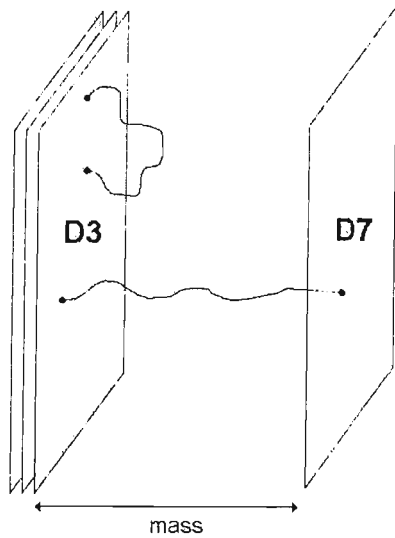


Figure 3.3: Fundamental and adjoint fields in a D3-D7 system.

Adding quarks through probe D7 branes, coupled to deformations of the geometry in the IR means that we can begin to construct supergravity duals of field theories remarkably similar to QCD. The main focus of this thesis will be to describe efforts towards the construction of a supergravity dual of QCD. The aim of finding such a dual theory is to shed some light on low energy phenomena such as hadrons which are currently inaccessible to conventional perturbation theory.

## Chapter 4

# Leigh-Strassler Off Moduli Space

In this chapter, we will be investigating the geometry of Leigh and Strassler [35]. This geometry describes a renormalisation group (RG) flow from  $\mathcal{N} = 4$  supersymmetric Yang-Mills in the UV down to an  $\mathcal{N} = 1$  theory in the IR. The supersymmetry breaking is achieved through the addition of a mass term. Specifically, we will be looking at the RG flow of this theory off of its moduli space and explicitly matching the field theory with its gravity dual at the conformal fixed points. First we must introduce the technique of brane probing and define the moduli space.

### 4.0.1 Brane Probing

A useful tool in investigating supergravity duals is brane probing. This technique involves introducing a single D3-brane in the background geometry and looking at the induced field theory on the brane. In the limit of an infinite number of branes the addition of one more will not disturb the geometry.

The action for the theory on the world-volume of the D3-brane will be the DBI action<sup>1</sup> (2.27):

$$S_3 = -\mu_3 \int d^4\xi e^{-\Phi} [-\det(G_{ab})]^{1/2} + i\mu_3 \int C_{(4)}, \quad (4.1)$$

where

$$G_{ab} = \frac{\partial X^\mu}{\partial \xi^a} \frac{\partial X^\nu}{\partial \xi^b} G_{\mu\nu}, \quad \mu, \nu = 0, \dots, 9, \quad a, b = 0, \dots, 3. \quad (4.2)$$

A sensible gauge to use is the *static gauge* whereby space-time coordinates and world-volume coordinates are aligned so that

$$\xi^0 = t, \quad \xi^i = x^i, i = 1, \dots, 3. \quad (4.3)$$

The remaining space-time directions  $y^m, m = 0, \dots, 9$  will appear as scalar fields on the world-volume. It is typical to assume that the brane is rigid and that these fields are functions of  $t$  only. It is also typical to assume that the brane is moving slowly so that  $dy^m/d\xi^0$  is small and the square root in the DBI action can be expanded.

D3-probes are particularly useful in the study of holographic renormalisation group flows. By moving the probe along the radial coordinate one can study the gauge theory dual to the background supergravity theory at different points along the RG flow.

Directions for which the probe brane feels no potential define a *moduli space* of inequivalent vacua of the gauge theory. For example, the  $\mathcal{N} = 4$  SYM theory has six scalars and is invariant under six-dimensional rotations of these scalars. These six scalars will correspond to directions  $y^m(t)$  in the background space-time. The D3-probe should therefore feel no potential in these directions.

---

<sup>1</sup>Note that we are assuming for simplicity that  $B_{ab}$  and  $F_{ab}$  are zero.

#### 4.0.2 The Calculation

The dual geometry we will be investigating is the  $\mathcal{N} = 1$  Leigh-Strassler geometry [35].

$$ds^2 = \Omega^2 e^{2A} \sum_{i=0}^3 dx_i^2 + \Omega^2 dr^2 + L^2 \frac{\Omega^2}{\rho^2 \cosh^2 \chi} \left[ d\theta^2 + \rho^6 \cos^2 \theta \left( \frac{\cosh \chi}{\bar{X}_2} \sigma_3^2 + \frac{\sigma_1^2 + \sigma_2^2}{\bar{X}_1} \right) + \frac{\bar{X}_2 \cosh \chi \sin^2 \theta}{\bar{X}_1^2} \left( d\phi + \frac{\rho^6 \sinh \chi \tanh \chi \cos^2 \theta}{\bar{X}_2} \sigma_3 \right)^2 \right], \quad (4.4)$$

$$C_{(4)} = -\frac{4}{g_s} w(r, \theta) dx_0 \wedge dx_1 \wedge dx_2 \wedge dx_3, \quad (4.5)$$

where

$$\Omega^2 = \frac{\sqrt{\bar{X}_1} \cosh \chi}{\rho},$$

$$\bar{X}_1 = \cos^2 \theta + \rho^6 \sin^2 \theta,$$

$$\bar{X}_2 = \operatorname{sech} \chi \cos^2 \theta + \rho^6 \cosh \chi \sin^2 \theta \quad (4.6)$$

and

$$w(r, \theta) = \frac{e^{4A}}{8\rho^2} [\rho^6 \sin^2 \theta (\cosh 2\chi - 3) - \cos^2 \theta (\cosh 2\chi + 1)]. \quad (4.7)$$

The  $\sigma_i$  coordinates parametrise a (squashed) 3-sphere:

$$\sigma_1 = \frac{1}{2} (\cos \alpha \, d\psi + \sin \alpha \sin \psi \, d\beta),$$

$$\sigma_2 = \frac{1}{2} (-\sin \alpha \, d\psi + \cos \alpha \sin \psi \, d\beta),$$

$$\sigma_3 = \frac{1}{2} (d\alpha + \cos \psi \, d\beta). \quad (4.8)$$

Note that we are only showing the relevant part of  $C_{(4)}$ , i.e. the part whose pullback onto the D3-brane will be non-zero. There is also a non-zero  $C_{(2)}$  and NS-NS field  $B_{(2)}$ ,

but we will align the probe brane in such a way that their pullback onto the brane is exactly zero.

The supergravity superpotential for this theory is

$$W = \frac{1}{4\rho^2} [(\rho^6 - 2) \cosh 2\chi - (3\rho^6 + 2)] \quad (4.9)$$

and the fields  $\rho(r)$ ,  $\chi(r)$  and  $A(r)$  obey the first order set of equations

$$\begin{aligned} \frac{d\rho}{dr} &= \frac{1}{6L} \rho^2 \frac{\partial W}{\partial \rho} = \frac{1}{6L} \frac{\rho^6(\cosh 2\chi - 3) + 2 \cosh^2 \chi}{\rho}, \\ \frac{d\chi}{dr} &= \frac{1}{L} \frac{\partial W}{\partial \chi} = \frac{1}{2L} \frac{(\rho^6 - 2)}{\rho^2} \sinh 2\chi, \\ \frac{dA}{dr} &= -\frac{2}{3L} W = -\frac{1}{6L\rho^2} [(\rho^6 - 2) \cosh 2\chi - (3\rho^6 + 2)]. \end{aligned} \quad (4.10)$$

This geometry describes a deformation of the  $\mathcal{N} = 4$  super Yang-Mills theory in the UV down to an  $\mathcal{N} = 1$  theory in the IR. In  $\mathcal{N} = 1$  supersymmetry language there are three chiral supermultiplets in the dual gauge theory  $\Phi_k = (\lambda_k, \phi_k)$ ,  $k = 1, \dots, 3$  consisting of a fermion  $\lambda_k$  and a complex scalar  $\phi_k$ , and a single vector multiplet  $(A_\mu, \lambda_4)$ . The  $SU(4)_R$  symmetry is broken by giving a mass to one of the chiral multiplets

$$\mathcal{L} \rightarrow \mathcal{L} + \int d^2\theta \frac{1}{2} m \Phi_3^2 + \text{h.c.} \quad (4.11)$$

The theory then flows to an  $\mathcal{N} = 1$  theory in the IR with a symmetry group  $SU(2)_F \times U(1)_R$ , where the  $SU(2)_F$  symmetry comes from rotations of the two massless flavours.

This RG flow corresponds to turning on scalar supergravity fields whose values asymptotes to zero in the ( $r = +\infty$ ) UV limit. In the IR, below the scale set by the mass  $m$ , these fields give a significant contribution to the geometry. The geometry will return back to  $\text{AdS}_5$  in the IR as the dual theory has a conformal fixed point there, but

the transverse space will change from an  $S^5$  to a deformed space with an  $SU(2) \times U(1)$  isometry group.

This background has been probed in [36], where the correspondence was tested on the moduli space of the theory. We will be investigating a region off of the moduli space. The Kähler structure has also been investigated in [37].

We will use a D3-brane probe to investigate the properties of this geometry (see the previous section). We will use a static gauge and assume that the brane is moving slowly ( $\dot{y} \equiv dy/dt \ll 1$ ). Expanding the square root up to  $\mathcal{O}(\dot{y}^2)$  yields a Lagrangian

$$\mathcal{L} = T - V = \frac{1}{2} \tau_3 \Omega^2 e^{2A} G_{mn} \dot{y}^m \dot{y}^n - \tau_3 \sin^2 \theta e^{4A} \rho^4 (\cosh 2\chi - 1). \quad (4.12)$$

It was shown in [36] that in the large  $r$  UV limit the potential takes the form

$$V \sim e^{2r/L} \sin^2 \theta. \quad (4.13)$$

In that paper, they looked at the moduli space given by  $\theta = 0$  and found that the metric was topologically  $\mathbb{R}^4$  corresponding to the parameter space of the vevs of the two complex massless scalars. They also found that the metric had an  $SU(2) \times U(1)$  symmetry in the IR as required by the duality.

Here we wish to look at a particular flow off of this moduli space. For convenience we will set  $\theta = \pi/2$ . For this choice, the kinetic and potential terms of the probe D3-brane Lagrangian are

$$T = \frac{1}{2} \tau_3 \rho^4 \cosh^2 \chi e^{2A} \left( \dot{r}^2 + \frac{L^2}{\rho^8} \dot{\phi}^2 \right),$$

$$V = \tau_3 \rho^4 e^{4A} (\cosh 2\chi - 1). \quad (4.14)$$

We are interested in the geometry at the two fixed points. Consider the equations for  $\rho$  and  $\chi$  (4.10)

$$\begin{aligned}\frac{d\rho}{dr} &= \frac{1}{6L} \frac{\rho^6(\cosh 2\chi - 3) + 2\cosh^2 \chi}{\rho}, \\ \frac{d\chi}{dr} &= \frac{1}{2L} \frac{(\rho^6 - 2)}{\rho^2} \sinh 2\chi.\end{aligned}\quad (4.15)$$

We can simplify these by making a change of variables

$$\varphi(r) \equiv \cosh^2 \chi(r). \quad (4.16)$$

Then

$$\begin{aligned}\frac{d\rho}{dr} &= \frac{1}{3L} \frac{\rho^6(\varphi - 2) + \varphi}{\rho}, \\ \frac{d\varphi}{dr} &= \frac{2}{L} \frac{(\rho^6 - 2)}{\rho^2} \varphi(\varphi - 1).\end{aligned}\quad (4.17)$$

The fixed points in the flow will be given by  $\frac{d\rho}{dr} = \frac{d\varphi}{dr} = 0$ . The solutions are

$$\begin{aligned}(\rho, \varphi) &= (1, 1) & (\text{UV}) \\ (\rho, \varphi) &= (2^{1/6}, 4/3) & (\text{IR})\end{aligned}\quad (4.18)$$

A direction field showing these fixed points is shown in Figure 4.1.

We are interested in the mapping between the supergravity theory and the dual field theory at the fixed points. Let us combine  $r$  and  $\phi$  into a single complex scalar field

$$A = v(r)e^{i\phi}. \quad (4.19)$$

We expect that if our Lagrangian derives from a Kähler potential  $K(A, A^\dagger)$ , then the kinetic term should be of the form

$$T = (K' + K''v^2) \dot{A}\dot{A}^*, \quad (4.20)$$

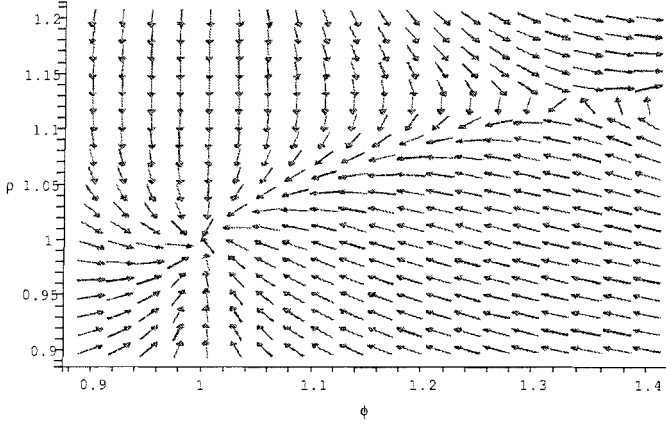


Figure 4.1: Direction field for the supergravity fields  $\rho(r)$  and  $\varphi(r) = \cosh^2 \chi(r)$  showing UV and IR fixed points

where

$$K' \equiv \frac{\partial K(|A|^2)}{\partial |A|^2}.$$

This can be derived from the standard result found in many textbooks on supersymmetry that

$$T = g_{AA^*} |\partial A|^2, \quad (4.21)$$

where  $g_{AA^*}$  is the Kähler metric

$$g_{AA^*} = \frac{\delta^2 K(|A|^2)}{\delta A \delta A^*} \quad (4.22)$$

(see for example [7]). This gives

$$\begin{aligned}
g_{AA^*} &= \frac{\partial}{\partial A} (K' A) \\
&= K' + K'' |A|^2 \\
&= K' + K'' v^2.
\end{aligned} \tag{4.23}$$

We also expect that, if there is a mass term in the supersymmetric action

$$\int d^2\theta \frac{1}{2} m \Phi_3^2 + \text{h.c.},$$

then the potential should be given by

$$V = \frac{m^2 |A|^2}{(g_{AA^*})^2}. \tag{4.24}$$

This can be derived as follows: Let the superfield  $\Phi = A + \theta\bar{\theta}F$ , where  $F$  is the standard “F term”. Then  $\Phi^2|_{\theta\bar{\theta}} = AF$  and the supersymmetric Lagrangian is

$$\mathcal{L} = g_{AA^*} (|\partial A|^2 + |F|^2) + m(AF + A^*F). \tag{4.25}$$

The equations of motion for  $F$  and  $F^*$  give

$$\begin{aligned}
\frac{\partial \mathcal{L}}{\partial F^*} = 0 &\Rightarrow F = -\frac{mA^*}{g_{AA^*}}, \\
\frac{\partial \mathcal{L}}{\partial F} = 0 &\Rightarrow F^* = -\frac{mA}{g_{AA^*}}
\end{aligned} \tag{4.26}$$

and the result follows.

Letting  $f(v^2) \equiv K' + K''v^2$  we expect that

$$f(v^2) \left( \frac{dv}{dr} \right)^2 \dot{r}^2 + f(v^2)v^2 \dot{\phi}^2 \tag{4.27}$$

and at the IR fixed point, where the dual theory has a mass term for one of the multiplets,

$$V = \frac{v^2}{f(v^2)}, \quad (4.28)$$

with  $V = 0$  at the UV fixed point. Matching (4.27) to (4.14) we find that

$$\frac{1}{v} \frac{dv}{dr} = \pm \frac{\rho^4}{L} \quad (4.29)$$

so

$$v(r) = \exp \left[ -\frac{1}{L} \int dr \rho(r)^4 \right]. \quad (4.30)$$

Note that we have taken the negative solution to ensure that  $v(\infty) = 0$ .  $v(r)$  can also be derived by matching the potential (4.28) to (4.14) using the flow equations (4.10).

We find

$$\frac{1}{v} \frac{dv}{dr} \frac{v^2}{4L\rho^2} [(\rho^6 - 2) \cosh 2\chi + 3\rho^6 + 2]. \quad (4.31)$$

Note that this is only valid away from the UV fixed point. At the UV fixed point  $\cosh^2 \chi = 1$  and the potential is zero as required. Equating these two derivations gives

$$0 = (\rho^6 - 2)(\cosh^2 \chi - 1). \quad (4.32)$$

At the IR fixed point  $\rho^6 = 2$  and the matching works.

We have successfully matched the supergravity theory to a dual supersymmetric theory with a non-trivial Kähler metric at the UV fixed point, and a supersymmetric theory with a non-trivial Kähler metric and a mass term at the IR fixed point.

What happens at points in the flow away from the two fixed points? As an example, we expand around the IR fixed point and solve the linearized flow equations for  $\rho$  and

$\chi$ . The results are

$$\begin{aligned}\rho(r) &= 2^{1/6} \left( 1 - \frac{\sqrt{7}-1}{6} b_0 e^{\lambda r/L} \right) + \dots, \\ \phi(r) &= \frac{4}{3} \left( 1 - \sqrt{7} \frac{\sqrt{7}-1}{6} b_0 e^{\lambda r/L} \right).\end{aligned}\quad (4.33)$$

The matching to the dual supersymmetric theory no longer works as the right hand side of (4.32) is no longer equal to zero (it goes to zero in the  $r = -\infty$  IR limit). This is to be expected as in the dual supersymmetric theory we expect renormalisation of our fields as we move away from the conformal fixed points. This would have to be included in the four-dimensional theory in order for our analysis to work. The trouble is that in order to determine the exact form of the dual theory away from the fixed points we would have to be able to solve the full non-perturbative renormalisation group flow. The difficulty of this problem is in fact one of the reasons why people turn to the dual supergravity theory. Without being able to solve both the supergravity theory and the dual gauge theory at arbitrary energies, it is not possible to verify the correspondence between the two theories at points away from the conformal fixed points. Recently, however, a supergravity theory including D-branes and ghost D-branes was found which is dual to an  $SU(N|N)$  gauge theory [38]. The interesting thing about this set-up is that it may be possible to solve the dual gauge theory at arbitrary energies and therefore test the AdS/CFT correspondence at all points along the renormalisation group flow.

## Chapter 5

# Gravitational Dual Theories of Chiral Symmetry Breaking

One of the major aspects of QCD that we would like to learn more about is its chiral symmetry breaking. The AdS/CFT correspondence is an extremely useful tool in investigating this problem. In the first section of this chapter we will show how the AdS/CFT correspondence can be used to provide a geometric picture of chiral symmetry breaking in a QCD-like theory. In the second section we will provide a simple test to determine whether this phenomenon is exhibited by various supergravity geometries.

### 5.1 A Geometric Picture of Chiral Symmetry Breaking

The basic tool we will be using to study chiral symmetry in this section is a D7-brane probe. Through studying the field theory induced on the world-volume of such a D-

brane in a deformed AdS geometry we are able to examine chiral symmetry breaking from in a geometric way.

The induced action on the world-volume is the DBI action (2.27):

$$S_7 = -\mu_7 \int d^8\xi [-\det(\mathbf{P}[G]_{ab})]^{1/2}, \quad (5.1)$$

where

$$\mathbf{P}[G]_{ab} = \frac{\partial X^\mu}{\partial \xi^a} \frac{\partial X^\nu}{\partial \xi^b} G_{\mu\nu}, \quad \mu, \nu = 0, \dots, 9, \quad a, b = 0, \dots, 7. \quad (5.2)$$

Note that, for simplicity, we are only including the graviton contribution to this action.

Let us assume that we can align the brane so that the two directions transverse to the brane ( $x^8, x^9$ ) have an associated diagonal metric  $G_{ij} = G\delta_{ij}, i, j = 8, 9$  and all other bulk coordinates are aligned with brane world-volume coordinates. The pullback metric can then be written as

$$\mathbf{P}[G]_{ab} = G_{ab} + G\partial_a X \partial_b X^\dagger, \quad (5.3)$$

where  $X = x^8 + ix^9$ . Without loss of generality<sup>1</sup>, we can re-write this complex scalar field as

$$X(r, x) = \sigma(r) e^{i\theta(r, x)}. \quad (5.4)$$

Let us try to interpret the field  $\sigma(r)$ . For now we will set  $\theta = 0$ . All deformed geometries must go to AdS for large  $r$ . In this limit the Lagrangian on the world-volume takes the form

$$\mathcal{L} \sim r^3 \sqrt{1 + \left(\frac{d\sigma}{dr}\right)^2}. \quad (5.5)$$

---

<sup>1</sup>We are not letting the fields have components on the 5-sphere as we are interested in studying non-supersymmetric theories.

Note that here  $\sigma$  must have mass dimension one. The equation of motion for  $\sigma$  is

$$3\frac{d\sigma}{dr} + r\frac{d^2\sigma}{dr^2} \sim 0, \quad (5.6)$$

whose asymptotic solution is

$$\sigma(r) \sim m + \frac{c}{r^2}. \quad (5.7)$$

The constant  $m$  must have mass dimension one, and  $c$  must have mass dimension three.

Since  $\sigma(r)$  is a dimension one scalar with this asymptotic form, we interpret it as the supergravity dual of the quark bilinear operator  $\bar{q}q$ .  $m$  corresponds to the quark mass and  $c$  to the quark condensate.

From the point of view of the geometry,  $\sqrt{\sigma(r)^2 + r^2}$  is the distance of the D7-brane from the origin. This suggests that the position in which the D7-brane lies will determine the value of  $\sigma$  and hence the value of the quark mass and condensate in the dual field theory.

A picture of a D7-brane lying in some hypothetical background geometry is shown in Figure 5.1. At  $r = \infty$  the D7-brane is lying at  $\sigma(r) = 0$ . As the geometry moves into the small  $r$  IR region there is some potential which causes the brane to be deflected away from the origin.  $\sigma(r)$  becomes non-zero and a dynamical mass for the quarks is generated. Dynamical quark masses break chiral symmetry and so this picture shows the gravity dual of a chiral symmetry breaking renormalisation group flow.

At  $r = \infty$  with the brane at  $\sigma(r) = 0$  there is a  $U(1)$  symmetry in the geometry. As the brane is deflected, that symmetry is broken. Goldstone's theorem says that breaking a continuous global symmetry will result in a massless Goldstone boson and

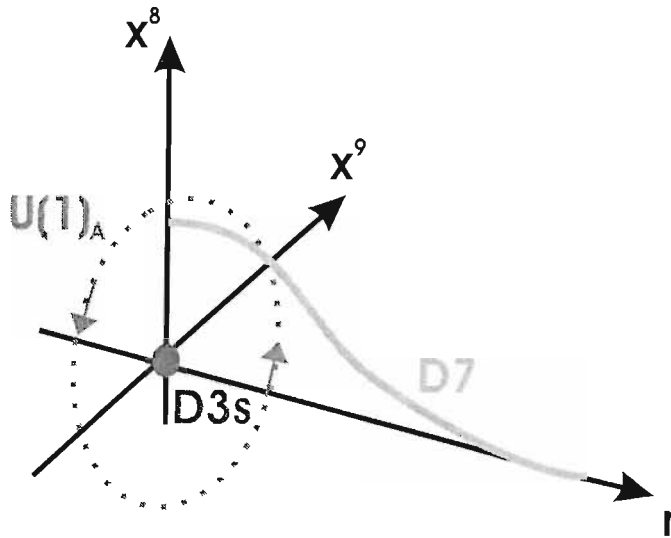


Figure 5.1: Geometric chiral symmetry breaking in a D3-D7 system.

indeed it does. When  $\sigma$  is non-zero, the field  $\theta(r, x)$  appears in the Lagrangian. Since there are only derivative terms for this field, it is massless. The field  $\theta$  is the pion generated by the breaking of the  $U(1)$  chiral symmetry<sup>2</sup>.

## 5.2 A Test for Chiral Symmetry Breaking

It would be nice to have a wider understanding of how generic the phenomena of chiral symmetry breaking is in gravitational duals - naively one might expect any non-supersymmetric, strongly coupled gauge background to induce chiral symmetry breaking. In this section we will pursue this goal by studying D7 brane embeddings

---

<sup>2</sup>Actually the symmetry is the axial  $U(1)$  symmetry so technically the Goldstone boson is the  $\eta'$ . In the limit  $N \rightarrow \infty$  this has the same contributions to its mass as the regular pions. Throughout the thesis we will use the term pion loosely as a Goldstone boson of chiral symmetry breaking.

in a range of deformations of  $AdS_5 \times S^5$ . In general, such geometries are considerably more complicated and the embedding profile depends on many of the coordinates on the brane. This turns finding the solutions into an extended and complicated numerical problem. Instead we propose a simple spherical embedding of a D7 brane that can be performed analytically and tests the repulsion of the core of the geometry. We believe this is a good indication of whether chiral symmetry would be induced. Further, in the case of a known dilaton induced flow, it provides an analytic estimate of the dynamical quark mass at zero energy which matches the numerical results well.

We begin by looking at a deformed geometry of Freedman, Gubser, Pilch and Warner [30]. In fact, this geometry is a coordinate transformation of an  $\mathcal{N} = 4$  preserving multi-centre solution in which chiral symmetry breaking can not occur. Study of it, though, highlights the pitfalls of interpreting the numerical embedding solutions too glibly. In one coordinate system we find solutions for the D7 brane embedding that appear to give a non-zero value for the quark condensate in the ultra-violet (UV) when in fact there is none. We learn that for there to be chiral symmetry breaking there must be a spatial gap between the embedded D7 brane and the core singularity for the case of a massless quark in the UV.

We next quickly review the dilaton induced flow results [48, 49] and introduce our spherical D7 embedding showing how the full solutions corresponding to the usual D7 embedding match on to these solutions in the infra-red. The spherical embedding illustrates the repulsion of the core of the geometry and provides the analytic result for the induced mass gap in the theory.

As a first new non-supersymmetric geometry we look at an extension of the FGPW solution [39] which allows for the inclusion of non-zero masses for the adjoint scalars of the  $\mathcal{N} = 4$  gauge theory as well as a vacuum expectation value. The gauge theory here has an unbounded scalar potential but the supersymmetry breaking could induce chiral symmetry breaking for the probe. We find that this is a case where chiral symmetry breaking is not present.

Pilch and Warner have constructed a number of geometries describing the  $\mathcal{N} = 2^*$  gauge theory [40, 41, 42]. We study a D7 embedding that preserves the  $\mathcal{N} = 2$  symmetry. The spherical D7 embedding allows us to check that there is no repulsion in this case and hence no chiral symmetry breaking as one expects in a supersymmetric theory.

Finally we look at the non-supersymmetric Yang Mills\* geometry [43]. Here the deformation is instigated by a mass and/or condensate for the adjoint fermions of the  $\mathcal{N} = 4$  theory (one would expect these parameters to be linked, but the supergravity geometry provides inconclusive evidence for what this link is). This supersymmetry breaking induces a mass for the adjoint scalars too, leaving just the Yang Mills field to survive to the IR. One would expect this theory to break chiral symmetries. We find using the spherical embedding that generically the core is repulsive (although there is a line of flows in the adjoint mass vs condensate plane where chiral symmetry breaking is absent).

### 5.2.1 D7 Branes and $\mathcal{N} = 4$ Geometries

The large  $N_c$   $\mathcal{N} = 4$  gauge theory at the origin of its moduli space is dual, via the AdS/CFT Correspondence to supergravity on  $AdS_5 \times S^5$  with radius  $R$

$$ds^2 = \frac{u^2}{R^2} dx_{//}^2 + \frac{R^2}{u^2} \sum_{i=1}^6 du_i^2, \quad (5.8)$$

where  $x_{//}$  is the 3+1d plane parallel to the D3 world volume and  $u^2 = \sum_i u_i^2$ . Quark fields may be introduced (see Section 3.4) and  $\mathcal{N} = 2$  supersymmetry preserved by placing a D7 probe in the  $x_{//}$  and  $u_1 - u_4$  directions (we write the metric on these four directions as  $d\rho^2 + \rho^2 d\Omega_3^2$ ). The  $U(1)$  symmetry in the  $u_5 - u_6$  plane is the geometric realisation of the  $U(1)_A$  axial symmetry of the quark fields on the probe. The Dirac Born Infeld action for the probe, with tension  $T_7$ , is

$$S = -T_7 \int d^8\xi \sqrt{-\det G_{ab}} = -T_7 \int d^4x d\rho d\Omega_3 \rho^3 \sqrt{1 + u_5'^2 + u_6'^2}, \quad (5.9)$$

where the prime indicates a derivative with respect to  $\rho$ ,  $G_{ab}$  is the pullback of the metric onto the probe, and we generically use  $d^8\xi$  to indicate integration over the world volume. The resulting equation of motion for the profile in, for example, the  $u_6$  direction is:

$$\frac{d}{d\rho} \left[ \frac{\rho^3 u_6'}{\sqrt{1 + u_6'^2}} \right] = 0. \quad (5.10)$$

The regular solution is  $u_6 = m$  with the separation of the D7 from the  $\rho$  axis,  $m$ , representing the hypermultiplet's mass. Asymptotically at large  $u$  there is a second

solution

$$u_6 = m + \frac{c}{\rho^2} + \dots \quad (5.11)$$

The parameter  $c$  represents the magnitude of the fermionic quark bilinear  $\bar{\psi}\psi$ . In pure AdS this solution is singular in the interior and unphysical [48, 49].

Now as a first example of embedding a D7 brane in a deformed geometry we consider the geometry of Gubser, Freedman, Pilch and Warner [30]. This geometry was constructed in the 5d truncation of IIB supergravity on AdS [44]-[45] then lifted to 10d. A scalar field,  $\chi$ , in the 20-dimensional representation of  $SU(4)_R$  has a non trivial radial profile corresponding to the scalar operator  $\text{Tr}\phi^2$  having a vev of the form  $\text{diag}(1, 1, 1, 1, -2, -2)$ . This vev preserves the supersymmetry of the  $\mathcal{N} = 4/2$  theory and we would expect to be able to introduce quarks of any mass via a D7 brane and find no chiral symmetry breaking. This is indeed the case, as we will show, but there are some interesting subtleties.

The 10d geometry is given by:

$$ds^2 = \frac{X^{1/2}}{\chi} e^{2A} dx_{IJ}^2 - \frac{X^{1/2}}{\chi} \left( du^2 + \frac{R^2}{\chi^2} \left[ d\theta^2 + \frac{\sin^2 \theta}{X} d\phi^2 + \frac{\chi^6 \cos^2 \theta}{X} d\Omega_3^2 \right] \right). \quad (5.12)$$

Here  $d\Omega_3^2$  is the metric of a three sphere,  $R$  is the asymptotic (large  $u$ ) AdS radius, and

$$X = \cos^2 \theta + \chi^6 \sin^2 \theta. \quad (5.13)$$

The fields  $\chi$  and  $A$  satisfy the differential equations

$$\frac{d\chi}{du} = \frac{1}{3R} \left( \frac{1}{\chi} - \chi^5 \right), \quad \frac{dA}{du} = \frac{2}{3R} \left( \frac{1}{\chi^2} + \frac{\chi^4}{2} \right), \quad (5.14)$$

with solution

$$e^{2A} = \frac{l^2}{R^2} \frac{\chi^4}{\chi^6 - 1}, \quad (5.15)$$

where  $l$  is an integration constant. The solution also has a non-zero four-form potential

$$C_{(4)} = \frac{e^{4A} X}{g_s \chi^2} dx^0 \wedge dx^1 \wedge dx^2 \wedge dx^3. \quad (5.16)$$

Note that this solution is singular at the point where  $\chi = 1$  - we will see the physical interpretation of this shortly.

It is natural to embed the D7 brane in this geometry to lie in the  $x_{//}, u, \Omega_3$  directions and look at the profile of the D7 brane  $\theta(u)$  at fixed  $\phi$  ( $\phi$  provides the  $U(1)$  symmetry of the embedding which is the chiral symmetry of the theory with quarks). The DBI action is

$$S_{DBI} = -T_7 \int d^8 \xi e^{4A(u)} R^3 |\cos^3 \theta(u)| \sqrt{X} \chi(u)^2 \sqrt{1 + \frac{\theta'(u)^2 R^2}{\chi(u)^2}}. \quad (5.17)$$

To place the solutions in a Cartesian-like plane instead we can make a change of coordinates from the circular coordinates  $(u, \theta)$  into the set  $(r, v)$ :

$$\begin{aligned} r^2 + v^2 &= e^{2u}, \\ \frac{v}{r} &= \tan \theta. \end{aligned} \quad (5.18)$$

Using this coordinate transformation, the metric becomes:

$$\begin{aligned} ds^2 = \frac{\sqrt{X}}{\chi} e^{2A} dx_{//}^2 &- \frac{\sqrt{X}}{\chi (v^2 + r^2)^2} \left( dv^2 \left( v^2 + \frac{R^2 r^2}{\chi^2} \right) + dr^2 \left( r^2 + \frac{R^2 v^2}{\chi^2} \right) + 2rv dv dr \left( 1 - \frac{1}{\chi^2} \right) \right. \\ &\left. + \frac{R^2 (v^2 + r^2)^2}{X} \left( \frac{1}{\chi^2 \left( \frac{r^2}{v^2} + 1 \right)} d\phi^2 + \frac{\chi^4}{\left( 1 + \frac{v^2}{r^2} \right)} d\Omega_3^2 \right) \right). \end{aligned} \quad (5.19)$$

Note that in these coordinates  $v$  and  $r$  are not perpendicular. In the AdS limit  $r, v$  become  $\rho, u_6$  above though, and hence the embedding results will be easier to interpret in these coordinates where we can compare them to the AdS  $u_6 = m$  result.

From the metric we can calculate the action when we embed with  $v$  and  $\phi$  as the perpendicular directions. Again we choose  $\phi = \text{const}$  and now our variable is  $v(r)$ .

$$S_{DBI} = -T_7 \int d^8\xi \frac{e^{4A} R^3 \chi^2 \sqrt{X}}{v^2 + r^2} \frac{1}{\left(1 + \frac{v^2}{r^2}\right)^{\frac{3}{2}}} \sqrt{r^2 + \frac{R^2 v^2}{\chi^2} + 2rv(1 - \frac{R^2}{\chi^2})v' + (v^2 + \frac{R^2 r^2}{\chi^2})v'^2},$$

where

$$\chi = \chi(\frac{1}{2} \log(v(r)^2 + r^2)), \quad A = A(\frac{1}{2} \log(v(r)^2 + r^2)). \quad (5.20)$$

We can solve the equations of motion resulting from this action numerically and the solutions are shown in Figure 5.2. Note that the D7 appears to deform around the singularity and there is a non-zero gradient at large  $r$ . Naively, therefore, our embedding solutions suggest that there is a quark condensate present for some values of the quark mass - we plot the value extracted asymptotically also in Figure 5.3. If there were a quark condensate for any value of the mass, supersymmetry would be broken, which would be a surprise!

In fact, this result is an artefact of being in the wrong coordinates for the duality to the field theory to be manifest. In general, finding the appropriate coordinates is rather hard, but in this highly supersymmetric theory the “correct” coordinates have been identified in [30, 47]. If we change the coordinates  $u, \theta$  for  $\hat{u}, \alpha$  so

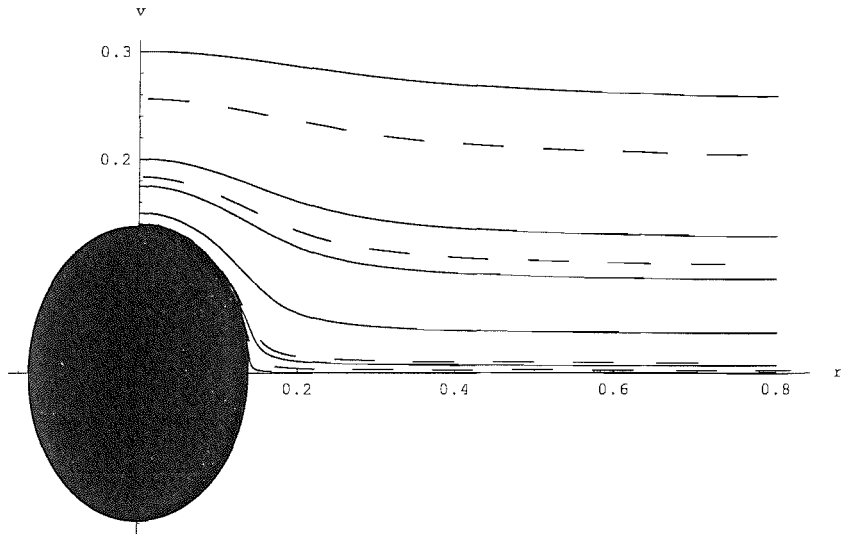


Figure 5.2: D7 brane flow in the FGPW geometry. The solid lines are the numerical solutions and the dashed lines the coordinate transform of the full analytic solutions. The singularity of the geometry is shown as a black circle.

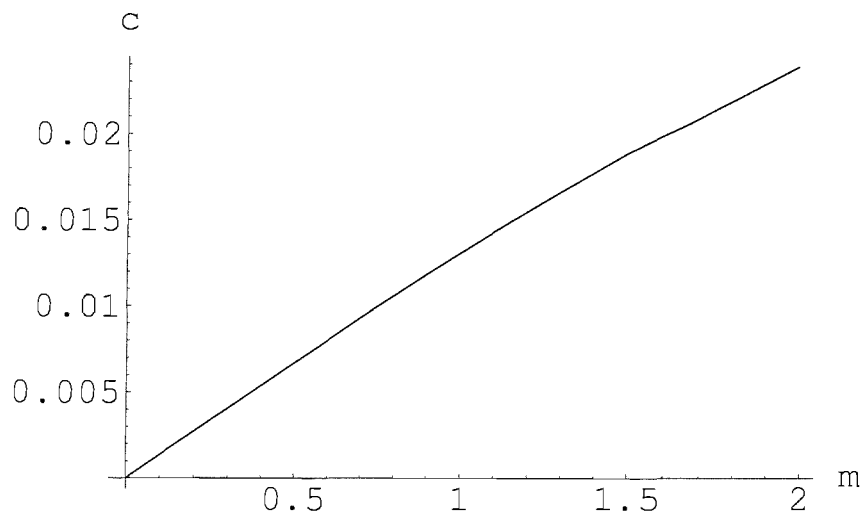


Figure 5.3: Apparent values of the quark mass and condensate extracted asymptotically from the flows in Figure 5.2.

$$\hat{u}^2 \cos^2 \alpha = R^2 e^{2A} \rho^2 \cos^2 \theta, \quad \hat{u}^2 \sin^2 \alpha = R^2 \frac{e^{2A}}{\rho^4} \sin^2 \theta, \quad (5.21)$$

then the metric takes the form of a standard multi-centre D3 brane solution:

$$ds^2 = H^{-1/2} dx_{//}^2 + H^{1/2} \sum_{i=1}^6 d\hat{u}_i^2, \quad C_{(4)} = \frac{1}{H g_s} dx^0 \wedge dx^1 \wedge dx^2 \wedge dx^3, \quad (5.22)$$

with

$$H = \frac{\chi^2}{X e^{4A}}. \quad (5.23)$$

The singular region of the space is transformed from a sphere to a disc by this transformation. The disc lies at the origin in the  $v, r$  space. The singularity is now understood to be caused by the presence of a disc of D3 branes and the solution is a perfectly good geometry.

Embedding the D7 brane in the  $x_{//}$  and four of the  $\hat{u}_i$  directions leaves the standard DBI action (eq. (5.9)) for the D7 in AdS space - the factors of  $H$  cancel and play no part. There are as usual solutions with  $\hat{u}_5, \hat{u}_6$  constant as in AdS. We interpret this as quark fields with a non-renormalized mass and no quark condensate.

Using the change of coordinates in eq. (5.21) we can map these simple  $\hat{u}_6 = \text{constant}$  solutions onto the solutions shown in Figure 5.2. These are given by the dashed lines showing that the numerical solutions to the equations of motion do match with those acquired from the analytic functions of  $\chi$  and  $A$ . There are a number of lessons we can learn from this example. Firstly, it is not straightforward to interpret the D7

embedding solutions in terms of the field theory because of the potential ambiguity in the identification of the coordinate system. We can see, though, that there were two signals of the absence of chiral symmetry breaking in this system even in the wrong coordinates. Firstly, the value of the parameter  $c$  in the solutions fell to zero as  $m$  fell to zero. Secondly, the embedding solutions filled the full space down to the singularity - that is there was no clear radial gap between the embedding solutions and the singularity. The result of this is that, as we have seen, the singularity can be transformed to a branch cut by a coordinate transformation and the solution for a massless quark then lies along the  $\hat{u}_6 = 0$  axis. A true signal of chiral symmetry breaking, as we'll see shortly, is if there is a radial gap between the  $m = 0$  embedding and the singularity - such an energy scale gap can never be removed by a coordinate transformation.

### 5.2.2 Quarks in a Dilaton Flow Geometry

Chiral symmetry breaking was first observed with a D7 embedding [48, 49] in the non-supersymmetric geometry of Constable and Myers [53]. This geometry in *Einstein frame* is given by

$$ds^2 = H^{-1/2} \left( \frac{w^4 + b^4}{w^4 - b^4} \right)^{\delta/4} dx_4^2 + H^{1/2} \left( \frac{w^4 + b^4}{w^4 - b^4} \right)^{(2-\delta)/4} \frac{w^4 - b^4}{w^4} \sum_{i=1}^6 dw_i^2, \quad (5.24)$$

where

$$H = \left( \frac{w^4 + b^4}{w^4 - b^4} \right)^\delta - 1, \quad (5.25)$$

and the dilaton and four-form are

$$e^{2\Phi} = e^{2\Phi_0} \left( \frac{w^4 + b^4}{w^4 - b^4} \right)^{\Delta}, \quad C_{(4)} = -\frac{1}{4} H^{-1} dt \wedge dx \wedge dy \wedge dz. \quad (5.26)$$

There are formally two free parameters,  $R$  and  $b$ , since

$$\delta = \frac{R^4}{2b^4}, \quad \Delta^2 = 10 - \delta^2. \quad (5.27)$$

It is convenient to write  $w$  and  $b$  in units of  $R$  which removes  $R$  from the definition of  $\delta$  and puts a factor of  $R^2$  into  $g_{ww}$ . The parameter  $b$  has no R-charge and dimension four so is interpreted as the vev of the operator  $\text{Tr}F^2$ . The  $\mathcal{N} = 4$  gauge theory is not expected to have a vev for this operator and hence this geometry probably does not describe a physical gauge theory vacuum. Nevertheless, it is an interesting geometry to study chiral symmetry breaking in because it does describe a non-supersymmetric, strongly coupled gauge background.

This geometry is particularly simple to study because it has a flat six plane transverse to the D3s. We parameterize this six plane as

$$\sum_{i=1}^6 dw_i^2 = d\rho^2 + \rho^2 d\Omega_3^2 + dw_5^2 + dw_6^2, \quad (5.28)$$

where we will embed the D7 brane on the directions  $x_{//}$ ,  $\rho$  and  $\Omega_3$ . The  $U(1)$  symmetry in the transverse  $w_5 - w_6$  plane is the geometric realisation of the  $U(1)_A$  symmetry of the quark fields. The DBI action for the D7 is

$$S = -T_7 \int d^8\xi \rho^3 \left( \frac{(\rho^2 + w_6^2)^4 - b^8}{(\rho^2 + w_6^2)^4} \right) \left( \frac{(\rho^2 + w_6^2)^2 + b^4}{(\rho^2 + w_6^2)^2 - b^4} \right)^{\frac{\Delta}{2}} \sqrt{1 + (\partial_\rho w_6)^2}, \quad (5.29)$$

and we look for solutions where  $w_5 = 0$  and  $w_6$  is a function of  $\rho$ . The equation of motion is

$$\frac{d}{d\rho} \left[ \frac{e^\Phi \mathcal{G}(\rho, w_6)}{\sqrt{1 + \partial_\rho w_6^2}} (\partial_\rho w_6) \right] - \sqrt{1 + \partial_\rho w_6^2} \frac{d}{dw_6} [e^\Phi \mathcal{G}(\rho, w_6)] = 0, \quad (5.30)$$

where

$$\mathcal{G}(\rho, w_6) = \rho^3 \frac{((\rho^2 + w_6^2)^2 + b^4)((\rho^2 + w_6^2)^2 - b^4)}{(\rho^2 + w_6^2)^4}. \quad (5.31)$$

The final terms in the equation of motion is a “potential” like term that is evaluated to be

$$\frac{d}{dw_6} [e^\Phi \mathcal{G}(\rho, w_6)] = \frac{4\rho^3 w_6 b^4}{(\rho^2 + w_6^2)^5} \left( \frac{((\rho^2 + w_6^2)^2 + b^4)}{((\rho^2 + w_6^2)^2 - b^4)} \right)^{\Delta/2} (2b^4 - \Delta(\rho^2 + w_6^2)^2). \quad (5.32)$$

Asymptotically at large radius these equations are just those in AdS with solution

$$w_6 = m + \frac{c}{\rho^2} + \dots, \quad (5.33)$$

where  $m$  corresponds to the quark mass and  $c$  the condensate.

Numerical solutions for the regular embedding solutions are shown in Figure 5.4 as well as a plot of the parameter  $c$  vs  $m$ . We take  $b = 1$  for these plots. The  $m = 0$  solution breaks the symmetry in the  $w_5 - w_6$  plane which is present asymptotically at large  $w$  where the D7 lies at the origin of the space - this is the geometric breaking of  $U(1)_A$ .

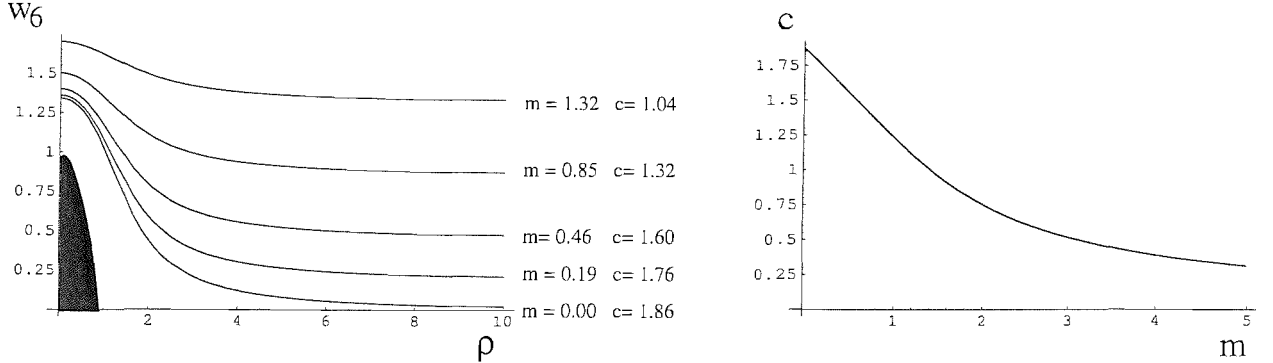


Figure 5.4: Numerical solutions for D7 embeddings in the Constable-Myers geometry with  $b = 1$ . The shaded area corresponds to the singularity in the metric. Also plotted is the value of the quark condensate vs the mass extracted asymptotically from those flows.

Let us compare this case to that of the previous section where we showed that in the  $\mathcal{N} = 4$  theory with scalar vev there was no chiral symmetry breaking. Here there is a non-zero value of  $c$  as  $m$  goes to zero. There is also a radial gap between the  $m = 0$  embedding and the singularity. Whatever coordinate transformation we might make on the geometry this gap will remain and the  $U(1)$  symmetry in the  $w_5 - w_6$  plane will be broken - this solution therefore definitely breaks chiral symmetry.

### 5.2.3 Spherical D7 Embedding

The above solutions in Figure 5.4 are calculated numerically, but it would be nice to be able to extract the chiral symmetry breaking behaviour and some dynamical information analytically. To do this we will look for minimum action solutions in the

form of a circle in the  $\rho - w_6$  plane plotted in Figure 5.4. The chiral symmetry breaking solutions naively look to match on to such a solution close to the singularity. Whether such an embedding falls into the singularity or is stabilized away from it will test whether the core of the geometry is repulsive to D7s and hence will be our test for chiral symmetry breaking. The distance it rests from the singularity will provide an estimate of the radial gap of the full embedding above. This gap corresponds to the dynamically generated quark mass at zero energy or the mass gap of the theory.

Concretely, we write the metric in the six  $w$  directions as

$$\sum_{i=1}^6 dw_i^2 = dr^2 + r^2(d\alpha^2 + \cos^2 \alpha d\phi^2 + \sin^2 \alpha d\Omega_3^2), \quad (5.34)$$

and embed the D7 brane on the  $\Omega_3$  and in  $\alpha$  at constant  $r = r_0$ . The action of the D7 brane is

$$S_{\text{wrapped D7}} = -T_7 \int d^8\xi r^4 e^{\Phi(r)} g_{xx}^2(r) g_{ww}^2(r) \sqrt{1 + \frac{1}{r^2} \left( \frac{dr}{d\alpha} \right)^2}. \quad (5.35)$$

Note that in pure AdS or a multi-centre solution  $g_{xx}^2 g_{ww}^2 = 1$ , the dilaton is a constant,  $dr/d\alpha$  is zero if  $r$  is fixed to some  $r_0$  and so the action is simply  $r_0^4$ . In the supersymmetric case the circle collapses to the origin ( $r_0 \rightarrow 0$ ) so here the core of the geometry is not repulsive which we take as evidence of the lack of chiral symmetry breaking.

In the Constable-Myers geometry, though, we have

$$S_{\text{wrapped D7}} = -T_7 \int d^8\xi r^4 \left( \frac{r^4 + b^4}{r^4 - b^4} \right)^{1+\Delta/2} \left( \frac{r^4 - b^4}{r^4} \right)^2 \sqrt{1 + \frac{1}{r^2} \left( \frac{dr}{d\alpha} \right)^2}. \quad (5.36)$$

Taking the equation of motion for  $r(\alpha)$  we see that there is indeed a solution with  $\frac{dr}{d\alpha} = 0$ . The action is then minimised by the constant value of  $r = r_0$  which is the root of

$$r_0^8 - b^4 \Delta r_0^4 + b^8 = 0 \quad (5.37)$$

which is real and greater than  $b$ . For  $b = 1$  there is a minimum of this action away from the singularity showing that the singularity is repulsive to such a configuration. For  $b = 1$  this gives  $r_0 = 1.29$ . In Figure 5.5 we plot this solution and the massless quark solutions above. Comparison shows that the circular embedding provides a good approximation to the gap value for the D7 brane solutions we are interested in above. Generically, how good this match is will depend on the form of the repulsive potential induced by the geometry. In this case the potential sets in steeply and the two solutions do match well.

It's clear that the full embedding comes close to matching to the spherical case in the infra-red. In fact, there is a small gap between these solutions. In [48] solutions were identified that lay closer to the singularity; these correspond to a second, higher action solution for each asymptotic value of the mass up to some critical mass. These solutions were identified with the chiral vacuum with  $-\langle \bar{\psi} \psi \rangle$  whose energy is raised by the quark mass. If the quark mass were too big, this vacuum is not even metastable and there is no solution describing it. In Figure 5.6 we plot this critical flow and the minimum action circular embedding showing that they overlap almost exactly. Overall, though, we conclude that the spherical embedding provides a good measure of the quark

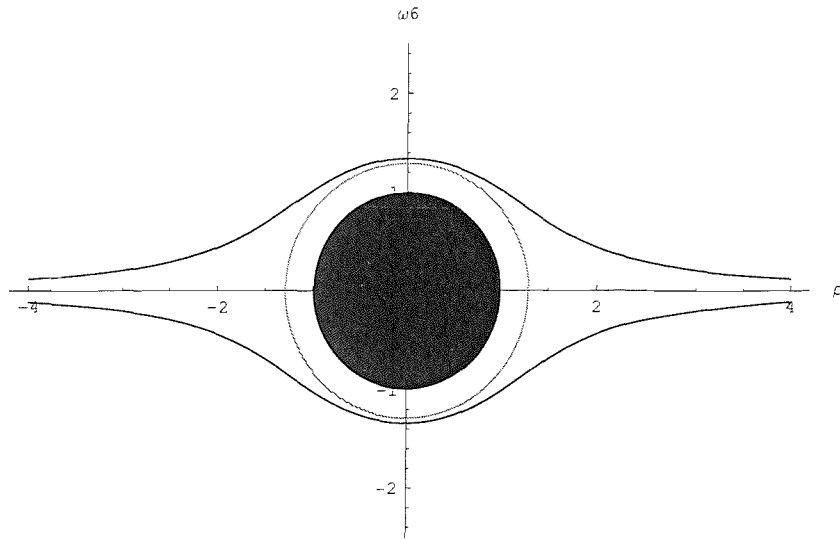


Figure 5.5: Plot of the minimum action spherical D7 embedding and the massless quark embeddings in the Constable Myers Geometry. The black circle represents the singularity in the geometry.

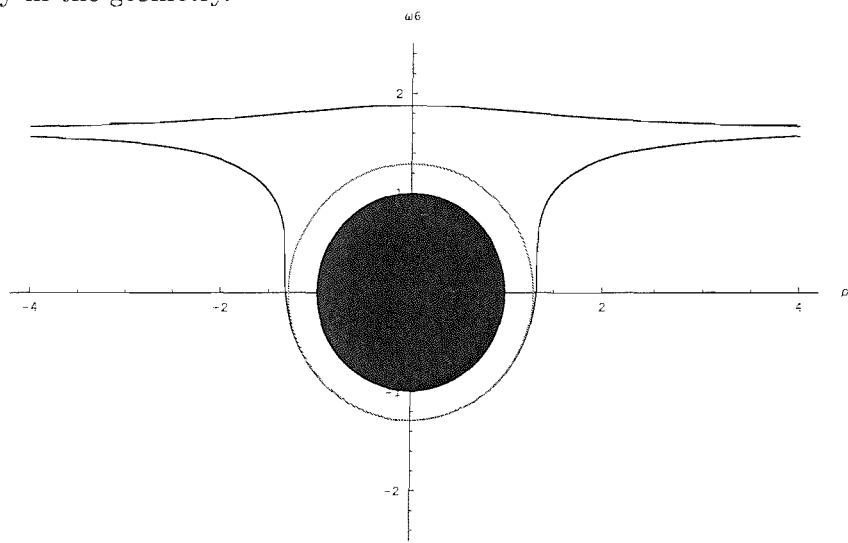


Figure 5.6: Plot of the minimum action spherical D7 embedding and a local minimum embedding action for a massive quark in the Constable Myers Geometry.

mass gap.

There is also some structure as  $b$  is changed. Writing  $w$  in powers of  $b$  removes  $b$  from everywhere in the metric except the expression for  $\Delta$  in the dilaton. For  $\Delta$  to be real requires

$$b \geq \left(\frac{1}{40}\right)^{\frac{1}{8}} R. \quad (5.38)$$

Now the quadratic equation (5.37) has a solution for the position of the minimum action, spherically embedded D7 which lies outside the radius  $b$  where the geometry is singular only if

$$b > \left(\frac{1}{24}\right)^{\frac{1}{8}} R. \quad (5.39)$$

There is therefore a small range of  $b$  that we can study where the spherical D7 falls into the singularity. For these values we expect the full D7 embedding corresponding to the quark fields to fall in too. Numerically this is what we find. In fact there is a few percent discrepancy between where a chiral symmetry breaking solution is lost and where the spherical embedded D7 enters the singularity corresponding to the slight mismatch seen above for the gap value in the exact method and the spherical embedding approximation. For these cases where the singularity is crossed we can come to no further understanding without more knowledge of the singularity.

### 5.2.4 A Non-supersymmetric Scalar Deformation

Let us now turn to our first example of a non-supersymmetric gravity dual [39] that has not been previously studied in this context. The background we will look at is related to the  $\mathcal{N} = 4$  [30] embedding introduced in Section 5.2.2. It was generated from a five-dimensional supergravity flow which was lifted to ten dimensions in [39]. A five-dimensional scalar field,  $\lambda$ , in the 20 representation of  $\text{SO}(6)$  is switched on and has the potential

$$V = -e^{-\frac{4\lambda(r)}{\sqrt{6}}} - 2e^{\frac{2\lambda(r)}{\sqrt{6}}}. \quad (5.40)$$

The scalar field  $\lambda$  acts as the source and vev of the field theory operator  $\text{Tr}(\phi_1^2 + \phi_2^2 + \phi_3^2 + \phi_4^2 - 2\phi_5^2 - 2\phi_6^2)$ . Switching on a mass term will give rise to unbounded directions in the scalar potential and so, as with the Constable-Myers case, this is not a realistic dual. Nevertheless, it is an interesting case to see if the breaking of supersymmetry generates chiral symmetry breaking - we will see that in this case it does not.

The relevant equations of motion for the scalar field are given by the usual five-dimensional field equations [46]:

$$\begin{aligned} \lambda''(r) + 4\lambda'(r)\sqrt{\frac{1}{6}(\lambda'(r)^2 - 2V)} &= \frac{\partial V}{\partial \lambda(r)}, \\ A'(r) &= \sqrt{\frac{1}{6}(\lambda'(r)^2 - 2V)}. \end{aligned} \quad (5.41)$$

The large  $r$  limit of this field is given by

$$\lambda = \mathcal{A}re^{-2r} + \mathcal{B}e^{-2r}, \quad (5.42)$$

where  $\mathcal{A}$  is interpreted as a source for our operator and  $\mathcal{B}$  is the vev. The  $\mathcal{N} = 4$  deformation described earlier is the special case where only the vev is non-zero. Now, we are interested in the case where there is both a mass and condensate present. We plot numerical solutions of the five-dimensional field equations in Figure 5.7. Generically, the flows either diverge in the IR with  $\lambda \rightarrow \pm\infty$ . There is a boundary in the  $\mathcal{A}$ - $\mathcal{B}$  plane between these two behaviours. In Figure 5.7 we show examples of each of these two behaviours  $\lambda_3, \lambda_4$  and the unique flows that lie on the boundary between these two regimes.  $\lambda_1$  describes this boundary in the positive  $\mathcal{A}$  positive  $\mathcal{B}$  quadrant whilst  $\lambda_2$  describes the boundary in the quadrant where they are both negative. We will provide analytic forms for the IR of these flows below.

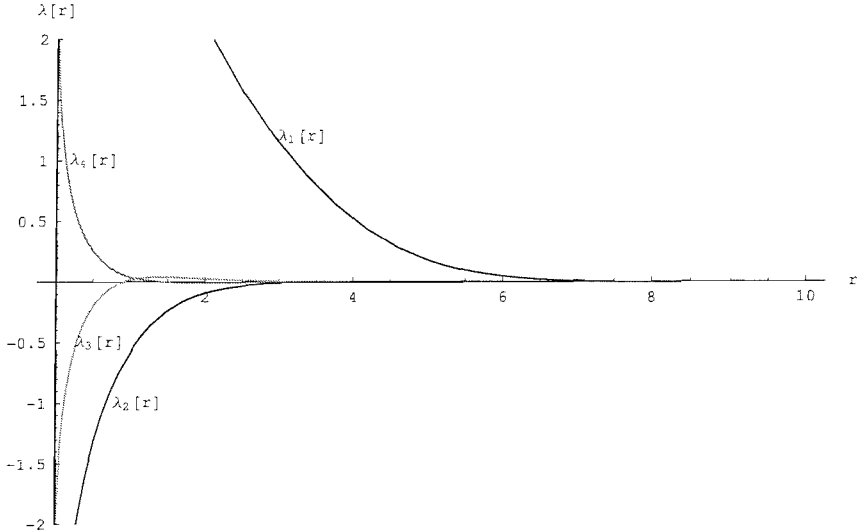


Figure 5.7: 4 different flows of the SUGRA field  $\lambda(r)$  all of which become singular at  $r=0$ .  $\lambda_1$  and  $\lambda_2$  are the turning point flows between the flows of the form  $\lambda_3$  and  $\lambda_4$ .

The ten dimensional lift of the full set of five dimensional solutions shares the form

of the metric with the supersymmetric geometry so

$$ds^2 = \frac{\sqrt{X}}{\chi} e^{2A} dx_{//}^2 + \frac{\sqrt{X}}{\chi} \left( du^2 + \frac{R^2}{\chi^2} \left[ d\theta^2 + \frac{\sin^2 \theta}{X} d\phi^2 + \frac{\chi^6 \cos^2 \theta}{X} d\Omega_3^2 \right] \right), \quad (5.43)$$

where the parameters are defined in exactly the same way as in the supersymmetric case (see eqn. (5.13)) and

$$\chi = e^{\frac{\lambda(r)}{\sqrt{6}}}. \quad (5.44)$$

Of course the solutions for  $\chi$  and  $A$  differ from the supersymmetric case. The four-form potential of the lift does not match that in the supersymmetric case but in neither case does it enter the DBI action of our D7 brane.

We can look for chiral symmetry breaking using both of the techniques we have seen in previous examples. The first method is more direct but a little less enlightening; we probe with a D7 brane by embedding in the  $x_{//}, r, \Omega_3$  directions (the angle  $\phi$  again provides the  $U(1)_A$  symmetry). The D7 action is given by eq. (5.17) and we will solve for flows in from the IR towards the UV with the symmetric boundary condition  $v = const$  and calculate numerically the geometry of the brane. We saw in the supersymmetric example that we are not in the “correct” coordinate system to make the gauge theory living on the brane manifest and therefore to find the quark mass and condensate. In that case, we were helped by the first order equations and could find the correct coordinate system. In this more general case, where  $\chi$  and  $A$  are solutions of second order equations, we have no hint as to how to find the correct coordinates.

We can perform the embedding by calculating  $\theta$  as a function of  $r$ , or we can change to the cartesian like set of coordinates,  $(v, r)$ , given by the same change of variables as

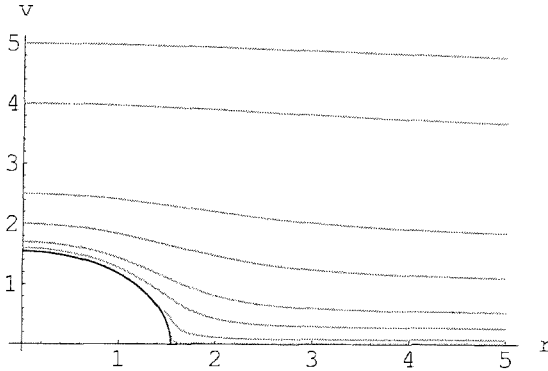


Figure 5.8: Sample solutions for a D7 brane embedding in the non-supersymmetric scalar deformation geometry showing the absence of a gap between the solutions and the singularity.

in the supersymmetric calculation eq. (5.18) and calculate the flow of  $v(r)$ . The action is then given in eq. (5.20). We solve for the D7 embedding with IR boundary condition  $v(r) = \text{constant}$ . We plot some representative solutions in Figure 5.8, which are in a background with positive  $\mathcal{A}$  and  $\mathcal{B}$  in eq. (5.42).

We find generically that for geometries with D7 embeddings that correspond to small quark masses the flow wraps onto the surface of the singularity. As far as we can tell numerically, there is a solution that hugs the  $v$  axis down to the singularity and then follows the singularity to  $r = 0$ . For this flow, both the mass and condensate asymptote to zero. We conclude that the geometry does not break chiral symmetries. Note that, as with the supersymmetric flows, naively a flow that hugs the singularity breaks the  $U(1)$  symmetry due to  $\phi$  translations. However, it seems likely that there

is a coordinate transformation that presses the singularity to the  $v = 0$  axis as in the supersymmetric case. The absence of a gap between the D7 brane embedding and the singularity, which could not be removed by such a transformation, implies no clear signal of chiral symmetry breaking.

The numerical studies above are somewhat messy and it would be nice to have an analytic understanding of the results. Such results are provided by our spherical embedding method developed in Section 5.2.3. We study the action of a circular D7 brane wrapped on  $x_{//}, \Omega_3, \theta$  at constant  $r$  as it gets nearer to the singular region. We expect the full solutions above to match onto these solutions in the IR. If the spherical embedding collapses into the singularity then there will be D7 embeddings that flow in from infinite radius that also touch the singularity. This can be calculated from the numerical flows of the scalar field  $\lambda$ , but it is more satisfactory to be able to get an analytic form for the potential. It turns out that we can do this for the IR limit of the scalar flow equations. We find four different solutions for the scalar fields  $\chi$  and  $A$ . These numbered solutions to  $\chi$  are related to the four types of behaviour in Figure 5.7 by  $\chi = e^{\frac{\lambda}{\sqrt{6}}}$ :

$$\begin{aligned}
\chi_1(r) &= \sqrt{\frac{45}{2}} \frac{1}{(r-r_s)}, & A_1(r) &= 4 \log(c(r-r_s)), \\
\chi_2(r) &= (\frac{2}{3}(r-r_s))^{\frac{1}{2}}, & A_2(r) &= \log(c(r-r_s)), \\
\chi_3(r) &= (b(r-r_s))^{\frac{1}{4}}, & A_3(r) &= \frac{1}{4} \log(c(r-r_s)), \\
\chi_4(r) &= (b(r-r_s))^{-\frac{1}{4}}, & A_4(r) &= \frac{1}{4} \log(c(r-r_s)),
\end{aligned} \tag{5.45}$$

where  $r_s$  is the singular radius and  $b$  and  $c$  are free parameters <sup>3</sup>. We have checked that these are all of the possible solutions by numerically solving the flow equations with these as the IR conditions. We flow out to the UV with these boundary conditions and calculate the mass and condensate in this limit. As best we can tell, these are indeed all the IR solutions of the SUGRA field equations.

Having found the analytic IR solutions, we can look at the action for the circular brane wrapping. We calculate the pullback for a brane with  $r$  and  $\phi$  as the perpendicular directions with  $r(\theta)$  and  $\phi$  constant which gives:

$$S_{DBI} = -T_7 \int d^8 \xi R^4 \sqrt{\cos(\theta)^2 + \chi(r(\theta)) \sin^2(\theta)} e^{4A(r(\theta))} \chi(r(\theta)) \cos^3(\theta) \sqrt{1 + \left(\frac{dr(\theta)}{d\theta}\right)^2 \frac{\chi(r(\theta))^2}{R^2}} \tag{5.46}$$

---

<sup>3</sup>We have found this asymptotic behaviour by looking for solutions of the form  $\lambda(r) = a \log(b(r-r_s))$  as  $r \rightarrow r_s$ . In fact, the last two solutions are valid for any potential  $V$  which asymptotically smaller than  $\frac{1}{(r-r_s)^2}$  as  $r \rightarrow r_s$ . In this case the supergravity equation reduces to the first order equation:

$$\lambda''(r) + 4\lambda'(r) \sqrt{\frac{1}{6}(\lambda'(r)^2)} \sim 0$$

There are solutions where  $r(\theta) = r_0$  and using the above IR solutions we can write down the action for each of these which gives

$$\begin{aligned}
S_{DBI1} &\sim - \int d^8\xi (r_0 - r_s)^{12} |\sin(\theta)| |\cos^3(\theta)|, \\
S_{DBI2} &\sim - \int d^8\xi (r_0 - r_s)^{\frac{9}{2}} \cos^4(\theta), \\
S_{DBI3} &\sim - \int d^8\xi (r_0 - r_s)^{\frac{5}{4}} \cos^4(\theta), \\
S_{DBI4} &\sim - \int d^8\xi |\sin(\theta)| |\cos^3(\theta)|.
\end{aligned} \tag{5.47}$$

We can see that for the first three there is obviously a minimising solution for which  $r_0 = r_s$ , meaning that the circular brane will fall into the singularity. This strongly suggests from our earlier studies that there will not be any chiral symmetry breaking induced by this geometry. Indeed we saw above that numerical studies of the D7 embedding appropriate for the addition of quarks also suggest there is not chiral symmetry breaking here. It is not immediately apparent that the brane will collapse in the fourth solution, but we note that this solution interpolates from the UV for which the potential goes like  $e^{4r}$ . By performing this calculation numerically we find a monotonically decreasing potential indicating that the flat behaviour seen in the equation interpolates smoothly into the exponential behaviour meaning that the brane collapses with this solution as well.

We conclude that this non-supersymmetric geometry does not induce chiral symmetry breaking. The unrealistic nature of the geometry, having as it does an unbounded scalar potential, does not make this result overly concerning but it is interesting that supersymmetry breaking and chiral symmetry breaking do not appear to be necessarily

directly linked.

### 5.2.5 $\mathcal{N}=2^*$ Geometry

We now turn to a more complicated supersymmetric geometry describing the  $\mathcal{N} = 2^*$  gauge theory [40][54]. This theory is the  $\mathcal{N} = 4$  theory with mass terms for two adjoint chiral matter fields. It has the massless fields of  $\mathcal{N} = 2$  super Yang Mills and thus a two-dimensional scalar moduli space. The supergravity description has a field corresponding to the fermionic mass and another which describes both the scalar masses and vev. The lift of the original 5d background to 10d has been made [40] and the solution in the Einstein frame is given by

$$ds^2 = \Omega^2 \left( e^{2A} dx_{//}^2 + dr^2 \right) + \frac{R^2 \Omega^2}{\chi^2} \left( \frac{d\theta^2}{c} + \chi^6 \cos^2 \theta \left( \frac{\sigma_1^2}{c X_2} + \frac{\sigma_2^2 + \sigma_3^2}{X_1} \right) + \frac{\sin^2 \theta}{X_2} d\phi^2 \right), \quad (5.48)$$

where

$$\begin{aligned} \Omega^2 &= \frac{(c X_1 X_2)^{\frac{1}{4}}}{\chi}, \\ c &= \cosh 2\zeta, \\ X_1 &= \cos^2 \theta + \chi^6 c \sin^2 \theta, \\ X_2 &= c \cos^2 \theta + \chi^6 \sin^2 \theta, \\ C_{(4)} &= \frac{e^{4A} X_1}{4g_s \chi^2} dx^0 \wedge dx^1 \wedge dx^2 \wedge dx^3, \end{aligned} \quad (5.49)$$

and the axion/dilaton is given by:

$$\lambda = i \left( \frac{1 - B}{1 + B} \right) = C_{(0)} + i e^{-\Phi}, \quad B = e^{2i\phi} \left( \frac{b^{\frac{1}{4}} - b^{-\frac{1}{4}}}{b^{\frac{1}{4}} + b^{-\frac{1}{4}}} \right), \quad b = \frac{X_1}{X_2} \cosh 2\zeta. \quad (5.50)$$

In addition, there is the anti-symmetric two form, whose NSNS and RR parts are given respectively by

$$\begin{aligned} B_{(2)} &= a_3 \cos \phi \sigma_1 \wedge d\phi + a_1 \sin \phi d\theta \wedge \sigma_1 - a_2 \sin \phi \sigma_2 \wedge \sigma_3, \\ C_{(2)} &= -a_1 \cos \phi d\theta \wedge \sigma_1 + a_2 \cos \phi \sigma_2 \wedge \sigma_3 + a_3 \sin \phi \sigma_1 \wedge d\phi, \end{aligned} \quad (5.51)$$

where

$$\begin{aligned} a_1 &= R^2 \tanh 2\zeta \cos \theta, \\ a_2 &= R^2 \frac{\chi^6 \sinh 2\zeta}{X_1} \sin \theta \cos^2 \theta, \\ a_3 &= R^2 \frac{\sinh 2\zeta}{X_2} \sin \theta \cos^2 \theta. \end{aligned} \quad (5.52)$$

The SUGRA fields  $\zeta$ ,  $A$  and  $\chi = e^\alpha$  satisfy the equations of motion

$$\begin{aligned} \frac{d\alpha}{dr} &= \frac{1}{3R} \left( \frac{1}{\chi^2} - \chi^4 \cosh(2\zeta) \right), \\ \frac{dA}{dr} &= \frac{2}{3R} \left( \frac{1}{\chi^2} + \frac{1}{2} \chi^4 \cosh(2\zeta) \right), \\ \frac{d\zeta}{dr} &= -\frac{1}{2R} \chi^4 \sinh(2\zeta). \end{aligned} \quad (5.53)$$

These have partial solutions:

$$\begin{aligned} e^A &= k \frac{\chi^2}{\sinh(2\zeta)}, \\ \chi^6 &= \cosh(\zeta) + \sinh^2(2\zeta) (\gamma + \log(\tanh \zeta)), \end{aligned} \quad (5.54)$$

The solutions with large  $\gamma$  deform into  $\mathcal{N} = 4$  solutions of the form seen in section 5.2.2 - here the scalar vev is so much larger than the supersymmetry breaking mass that the theory is effectively the  $\mathcal{N} = 4$  theory. The smallest possible vev in the theory corresponds to the background with  $\gamma = 0$  and we will concentrate on this case since

it is the vacuum most distinct from the  $\mathcal{N} = 4$  theory. Probing the geometry with a D3 brane [41, 42] shows that the  $\theta = \pi/2$  plane corresponds to the moduli space. Further in [42] a set of coordinates were found on that moduli space that correspond to the physical coordinates for computing the  $\beta$ -function of the field theory. In these coordinates the singularity is again transformed to a branch cut.

As we have done in previous cases, we can analytically study the asymptotic solutions to the flow equations in the IR limit. The results are<sup>4</sup>

$$\begin{aligned}\zeta(r) &= -\frac{3}{2} \log \left( \left( \frac{2}{3^5} \right)^{\frac{1}{3}} \frac{(r - r_s)}{R} \right), \\ \chi(r) &= \frac{\sqrt{2}}{3} \sqrt{\frac{(r - r_s)}{R}}, \\ A(r) &= 4 \log \frac{(r - r_s)}{R} + b.\end{aligned}\tag{5.55}$$

These are a one parameter family of solutions as expected due to the fact that the flow equations in this case are first order. The parameter  $b$  is related to  $k$  by  $b = \log k + \log \left( \frac{8}{2187} \right)$ . This is not a free parameter, but is fixed by requiring that this flows to a solution which is asymptotically  $A(r) \rightarrow r$  in the UV.

Now consider including quark fields via a D7 brane probe in this geometry. The quark superfields have a superpotential coupling to the  $\mathcal{N} = 4$  adjoint scalars of the form  $\tilde{Q}AQ$ , where the adjoint field  $A$  is represented in the geometry by the two transverse directions to the D7 brane. Therefore, in this geometry, where the  $\mathcal{N} = 4$  fields have

---

<sup>4</sup>We find these by looking for real solutions to the flow equations which behave asymptotically like  $\zeta(r) \sim a \log(b(r - r_s)/R)$ ,  $\chi(r) \sim c((r - r_s)/R)^d$  as  $r \rightarrow r_s$ . It can be shown that these solutions correspond to  $\gamma = 0$  as, for  $\gamma = 0$ , we know from (5.54) that, for large  $\zeta$ ,  $\chi \sim \left(\frac{4}{3}\right)^{\frac{1}{6}} e^{-\frac{\zeta}{3}}$ , as can be checked for our solution.

already been broken into  $\mathcal{N} = 2$  multiplets, we must be careful to embed in such a way that we do not further break supersymmetry. The probe must lie perpendicular to the  $\theta = \pi/2$  plane since that plane corresponds to the massless scalar fields. Were the probe at some angle to that plane the superpotential term would be with fields in a mix of superfields in terms of the breaking intrinsic in the geometry. In this configuration, though, we expect that we should be able to include arbitrary mass quarks and maintain supersymmetry.

If we were attempting to find the flow of the brane in from the UV, we would want to embed it in the  $x_{\parallel}, r, \alpha, \beta, \psi$  directions and the DBI action of this embedding can be calculated easily. However, it can be seen that the two perpendicular directions  $\theta$  and  $\phi$  will be dependent on both  $r$  and  $\psi$ , which will make the equations of motion for the brane computationally very difficult to solve. Instead, we will fall back on our wrapping technique. We write the DBI action of the brane in terms of an embedding where the perpendicular directions  $r$  and  $\phi$  are functions of  $\theta$  and  $\psi$  and we take a constant value of  $\phi$ . This time by looking at the symmetries of the metric we know that the minimum action solution will not be spherical, however we can find out if there is a repulsive potential on the brane stopping it falling in on the singularity.

To calculate the potential of a D7 brane in this background we first rewrite the 3 differentials  $\sigma_{1,2,3}$  in terms of the spherical coordinates  $\alpha, \beta, \psi$  using  $\sigma_1 = \frac{1}{2}(d\alpha + \cos \psi d\beta)$ ,  $\sigma_2 = \frac{1}{2}(\cos \alpha d\psi + \sin \alpha \sin \psi d\beta)$ ,  $\sigma_3 = \frac{1}{2}(-\sin \alpha d\psi + \cos \alpha \sin \psi d\beta)$ . This gives

a metric of the form

$$ds^2 = \Omega^2(e^{2A}dx_{//}^2 + dr^2) + \frac{R^2\Omega^2}{\chi^2} \left( \frac{1}{c}d\theta^2 + \frac{\sin^2\theta}{X_2}d\phi^2 + \frac{\chi^6\cos^2\theta}{4} \left( \frac{d\psi^2}{X_1} + \frac{d\alpha^2}{cX_2} + d\beta^2 \left( \frac{\sin^2\psi}{X_1} + \frac{\cos^2\psi}{cX_2} \right) + \frac{2d\alpha d\beta \cos\psi}{cX_2} \right) \right) \quad (5.56)$$

In fact even this configuration is hard to study because of the forms present in the geometry. For simplicity we will place the D7 probe at  $\phi = n\pi$  where the axion vanishes, and the dilation is given by

$$e^\Phi = \sqrt{\frac{cX_1}{X_2}}. \quad (5.57)$$

In addition, the NSNS two form is zero.

The DBI action for this configuration is given by

$$S_{DBI} = -T_7 \int d^8\xi \frac{R^4}{4} e^{4A} cX_1 \cos^2\theta |\sin\psi| \sqrt{\left( \frac{\chi^2 \cos^2\theta}{4cX_1} + \frac{\chi^4 \cos^2\theta}{4R^2X_1} \left( \frac{\partial r}{\partial\theta} \right)^2 + \frac{1}{cR^2\chi^2} \left( \frac{\partial r}{\partial\psi} \right)^2 \right)}. \quad (5.58)$$

We also have to consider the Wess-Zumino part of the action for the D7 brane. As there are no gauge fields living on the brane, this is given by

$$S_{WZ} = \mu_7 \int_{\mathcal{M}_8} (C_{(8)} + C_{(6)} \wedge B_{(2)}). \quad (5.59)$$

For  $\phi = n\pi$  this will be zero as the dual of  $C_{(8)}$  (the axion) is zero and  $B_{(2)}$  is also zero.

As before, we are only interested in the IR behaviour of the potential felt by the brane so we can use our analytic solution in the above equation. Ignoring proportionality factors, we find that for a constant  $r_0$  solution

$$V_{IR} \sim (r_0 - r_s)^{15} |\cos^3\theta| |\sin\psi| \sqrt{5 + \cos 2\theta}. \quad (5.60)$$

We can see clearly that, as expected, this supersymmetric background, when probed in this particular way, does not have the signature of chiral symmetry breaking. There is no potential stopping the spherical D7 brane falling onto the singularity and the situation is analogous to that found in the  $\mathcal{N} = 4$  geometries.

### 5.2.6 The Yang Mills\* Geometry

Finally we will turn our spherical D7 embedding technique on a geometry where physically one might expect chiral symmetry breaking. The  $YM^*$  geometry [43] was developed as a model of non-supersymmetric Yang Mills theory. The UV of the theory is the  $\mathcal{N} = 4$  gauge theory but then at a scale  $\mathcal{M}$  a mass term is introduced for the four adjoint fermions,  $\lambda_i$ . It is also possible to include in the solutions a vev for the operator  $\sum_i \lambda_i \lambda_i$ . One would expect some dynamical determination of this condensate in terms of  $\mathcal{M}$  but the supergravity solution does not clearly provide this link - we will investigate this whole space of geometries therefore.

The  $YM^*$  geometry was originally constructed as a 5d supergravity solution but then lifted to a full 10d solution. In 10d D3 brane probe analysis indicates that the six adjoint scalars of the  $\mathcal{N} = 4$  theory acquire masses radiatively as one would expect since supersymmetry is broken. In [55] the glueball spectrum and string tension properties were analysed. For the geometries with a fermion mass and small or vanishing condensate, a discrete glueball spectrum was found though probe strings fell onto the singularity. The interior of the geometry is therefore still ill understood, and possibly is also incomplete since the restricted 5d solution on which the geometry is built may not

have sufficient freedom to describe the full non-supersymmetric theory. Nevertheless, this is a prime candidate geometry to examine for chiral symmetry breaking, since it describes a model that shows some very QCD-like qualities.

In the SUGRA theory the fermion mass terms correspond to turning on a scalar in the 10 of  $SO(6)$ . As in the other examples, we can solve the 5d SUGRA equations numerically using the relevant field equations.

$$\begin{aligned}\lambda''(r) + 4A'(r)\lambda'(r) &= \frac{\partial V}{\partial \lambda}, \\ A'(r) &= \sqrt{\frac{1}{6}(\lambda'(r)^2 - 2V)},\end{aligned}\tag{5.61}$$

with

$$V = -\frac{3}{2}(1 + \cosh(\lambda(r))^2).\tag{5.62}$$

The AdS limit of this field has solutions

$$\lambda(r) = \mathcal{M}e^{-r} + \mathcal{C}e^{-3r},\tag{5.63}$$

with  $\mathcal{M}$  and  $\mathcal{C}$ , the mass and condensate of the operator  $\sum_i \lambda_i \lambda_i$  respectively. We will be particularly interested in the large negative  $r$  limit of the space corresponding to the IR of the gauge theory. We can try to find analytic solutions in this limit as we did in the previous section. The solutions we have found are

$$\begin{aligned}\lambda_{IR,1}(r) &= -\log \left( \sqrt{\frac{9}{20}}(r - r_s) \right), & A(r) &= \frac{2}{3} \log(r - r_s), \\ \lambda_{IR,2}(r) &= \log \left( \sqrt{\frac{9}{20}}(r - r_s) \right), & A(r) &= \frac{2}{3} \log(r - r_s),\end{aligned}\tag{5.64}$$

$$\lambda_{IR,3}(r) = -\frac{\sqrt{6}}{4} \log(a(r - r_s)), \quad A(r) = \frac{1}{4} \log(r - r_s),$$

$$\lambda_{IR,4}(r) = +\frac{\sqrt{6}}{4} \log(a(r - r_s)), \quad A(r) = \frac{1}{4} \log(r - r_s),$$

where  $r_s$  is the radius where the flow becomes singular in the IR. In the  $\mathcal{C}$  vs  $\mathcal{M}$  plane there are regions where the  $\lambda$  flows diverge positively and negatively described by the second two solutions. There is then a unique flow on the boundary which in the positive quadrant is described by  $\lambda_1$  and in the negative quadrant by  $\lambda_2$ . Numerically the unique flow lies at least close to the boundary condition  $\mathcal{C} = 0$ .

The 10d lift of the  $YM^*$  background is given by

$$\begin{aligned}
ds_{10}^2 &= \xi^{\frac{1}{2}}(e^{2A}dx^2 + dr^2) + \xi^{-\frac{3}{2}}(\xi^2 d\alpha^2 + \sin^2 \alpha F_+ d\Omega_+^2 + \cos^2 \alpha F_- d\Omega_-^2), \\
d\Omega_\pm^2 &= d\theta_\pm^2 + \sin^2 \theta_\pm d\phi_\pm^2, \\
\xi^2 &= \cosh^4 \lambda(r) + \sinh^4 \lambda(r) \cos^2 2\alpha, \\
F_\pm &= \cosh^2 \lambda(r) \pm \sinh^2 \lambda(r) \cos 2\alpha, \\
A_\pm &= \frac{\sinh 2\lambda(r)}{\cosh^2 \lambda(r) \pm \cos 2\alpha \sinh^2 \lambda(r)}, \\
B &= \frac{\sinh^2 \lambda(r) \cos 2\alpha}{\cosh^2 \lambda(r) + \xi}, \\
e^{-\Phi} &= \frac{1 - B}{1 + B}.
\end{aligned} \tag{5.65}$$

Now consider including quark fields via a D7 brane probe in this geometry. The probe would naturally lie in the  $x_{//}$  and  $r$  directions and then wrap a three sphere in the deformed five sphere. For example we could wrap one of the two spheres (e.g.  $\Omega_-$ ) and fill the angle  $\alpha$  leaving us to find the embedding  $\theta_+$ . The angle  $\phi_+$  provides the  $U(1)_A$  symmetry of the quarks. Clearly  $\theta_+$  will be a function of both  $r$  and  $\alpha$  on the D7 world volume. In this complicated geometry it is too difficult to find the full embedding<sup>5</sup>. It is more straightforward though to embed a D7 spherically on  $x_{//}, \Omega_-, \alpha$  and  $\theta_+$

---

<sup>5</sup>Note that the usual AdS geometry can be written in the same coordinate system as  $YM^*$  so the metric is

$$ds^2 = e^{2r} dx_{//}^2 + dr^2 + d\alpha^2 + \cos \alpha d\Omega_+^2 + \sin \alpha d\Omega_-^2 \tag{5.66}$$

The flat D7 embedding of section 2 in these coordinates is then given by

$$\theta_- = \arcsin \frac{me^{-r}}{\sin \alpha} \tag{5.67}$$

which is itself a complicated function. Even in this case sophisticated numerical techniques would be

at fixed  $\phi_+$ . We treat the radius of this sphere  $r$  as our embedding coordinate. The DBI action for this configuration is

$$S_{DBI} = -T_{D7} \int d^8\xi e^\Phi \sqrt{-M} \left( (\partial_{\theta_+} r)^2 + (1 + (\partial_\alpha r)^2) \frac{\sin^2 \alpha}{F_-} \right)^{\frac{1}{2}}, \quad (5.68)$$

where

$$\sqrt{-M} = e^{4A} \sqrt{\cos^4 \alpha F_-^2 \sin^2 \theta_- + \frac{A_-^2}{4} \sin^6 \alpha \cos^2 \theta_- \xi^3}. \quad (5.69)$$

The Wess-Zumino contribution eq.(5.59) of the action must also be studied. However, the integral over  $C_{(8)}$  is zero as its dual, the axion, is zero and the integral over  $C_{(6)} \wedge B_{(2)}$  will also be zero since  $C_{(6)}$  is dual to  $C_{(2)}$  ( $dC_{(6)} = *dC_{(2)}$ ) and  $C_{(2)}$  has a basis  $d\theta_+ \wedge d\phi_+$ , whereas  $B_{(2)}$  has a basis  $d\theta_- \wedge d\phi_-$ . This means that we will end up with a wedge product of identical basis one forms which will be zero. For this embedding we can therefore drop these terms.

The symmetries of our action imply that there are solutions where  $r$  is just a function of  $\alpha$  which is to be compared with the more complicated full embedding where  $\theta_+(r, \alpha)$ . Numerical analysis will therefore be simpler in this case.

As our variable is not dependent on  $\theta_-$ , we must integrate over this quantity in the action before we can try to find a solution. This integral gives

$$S_{DBI} = -T_7 \int d^7\xi e^\Phi e^{4A} 2F_- \cos^2 \alpha \text{EllipticE} \left( 1 - \frac{A_-^2 \sin^6 \alpha \zeta^3}{4F_-^2 \cos^4 \alpha} \right) \sqrt{(\partial_{\theta_+} r)^2 + (1 + (\partial_\alpha r)^2) \frac{\sin^2 \alpha}{F_-}}. \quad (5.70)$$

The simplest analysis we can perform is just to look at the potential felt by a brane of fixed radius  $r_0$ . This will not be a solution of the equations of motion but will show

---

needed to find this solution.

us whether there is a repulsion in the geometry to such a configuration collapsing. For our four analytic solutions, we find two sorts of behaviour in the IR. These are given by the potentials

$$V_{circle} = T_7 \int d^7 \xi (r_0 - r_s)^{\frac{2}{3}} \text{EllipticE} \left( 1 - \frac{18}{5} (r_0 - r_s)^2 |\cot \alpha| \right) \sqrt{|\cos^5 \alpha \sin^3 \alpha|}, \quad (5.71)$$

corresponding to  $\lambda_{IR,1}$  and  $\lambda_{IR,2}$  and

$$V_{circle} = T_7 \int d^7 \xi (b(r_0 - r_s))^{1 - \sqrt{\frac{3}{2}}} \text{EllipticE} \left( 1 - 8(b(r_0 - r_s)) \sqrt{\frac{3}{2}} |\cot \alpha| \right) \sqrt{|\cos^5 \alpha \sin^3 \alpha|}, \quad (5.72)$$

corresponding to  $\lambda_{IR,3}$  and  $\lambda_{IR,4}$ . For both of these solutions the elliptic integral tends to a constant in the IR so we can see explicitly the behaviour of the potential as a function of  $r_0 - r_s$ . In the first case, corresponding to a line of solutions in the  $\mathcal{M}$  vs  $\mathcal{C}$  plane the embedding collapses onto the singularity. For the remainder of the  $\mathcal{M}$  vs  $\mathcal{C}$  space the probe is repelled from the singularity in the IR. In the UV where the geometry returns to AdS the potential always pushes the field into the IR so there must be a stable configuration away from the singularity. This suggests that the majority of parameter space in the model will give rise to chiral symmetry breaking.

We know, however, from the  $\alpha$  dependence of the action that the solution of the wrapped brane will not have a circular symmetry. Therefore, although we know that there is a repulsive potential at least somewhere around the singularity, we don't yet know what form the brane embedding will take. To calculate this, we have used a numerical relaxation method. We discretise the points on the brane parameterised by the angle  $\alpha$  and write the action for  $r(\alpha)$  in the discretised form with a starting

guess for the solution. We then minimise the action with respect to all points on the lattice, giving us  $N$  coupled equations for  $N$  lattice points. Because we are looking at a wrapping solution, we also have a boundary condition that the first and last points in  $\alpha$  are at the same value of  $r$ . We performed this calculation using Mathematica. The resulting configuration of the brane is shown in Figure 5.9 for a generic flow of the type we have seen with a repulsive potential. We see that the repulsive potential is present away from  $\alpha = n\pi/2$  but vanishes at precisely  $n\pi/2$  at which points the brane can fall in on the singularity. This is obviously an added complication which muddies the result. Consider beginning with a flat D7 brane far from the singularity which would include a heavy quark field in the theory. As the brane is brought in towards the singularity the repulsion centred at  $\alpha = \pi/4$  will stop the brane moving to the origin of the space as sketched in Figure 5.10 implying a chiral symmetry breaking set of UV boundary conditions.

The outstanding question is whether the probe will touch the singularity at  $\alpha = \pi/2$ . We cannot address this completely within our analysis. Of course touching the singularity may not be a disaster if it is simply indicating the presence of a fuzzy configuration of D3s - some brane bound state may form there. We tentatively conclude that  $YM^*$  generically does break chiral symmetries although there are outstanding issues to be understood.

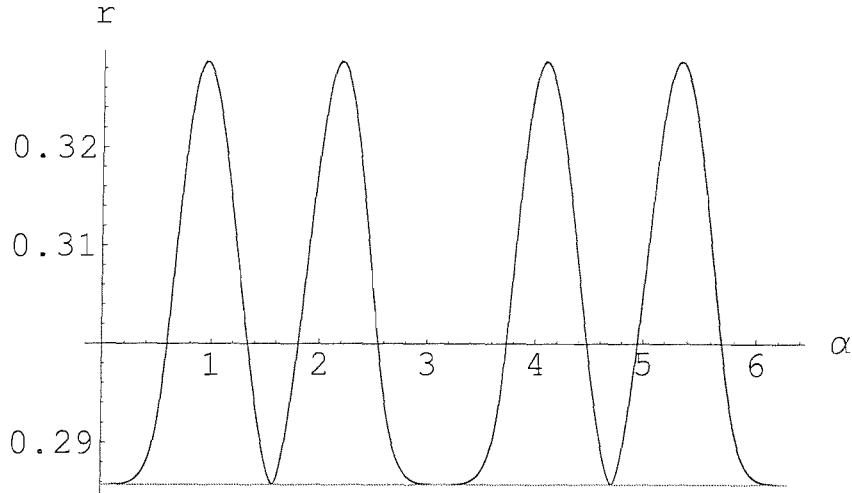


Figure 5.9: Sample result of a numerical solution for the determination of a spherical D7 brane embedding  $r$  vs  $\alpha$  that wraps the  $YM^*$  singularity shown by the lower straight line.

### 5.2.7 Summary

Quark fields can be introduced into the AdS/CFT Correspondence and its deformations via D7 brane probes. The mass and any chiral condensate induced can be read off from the asymptotic behaviour of the scalar in the D7 DBI action describing its embedding. We have shown that in fact this prescription must be tempered by the possibility of making coordinate transformations that alter the asymptotic behaviour of the field. In the FGPW geometry [30] that describes the  $\mathcal{N} = 4$  gauge theory on its moduli space we saw that the D7 embedding flows fill the whole space away from the central singularity of the geometry. A transformation that takes the singularity to a branch cut would then remove the signal for chiral symmetry breaking. In this case that is

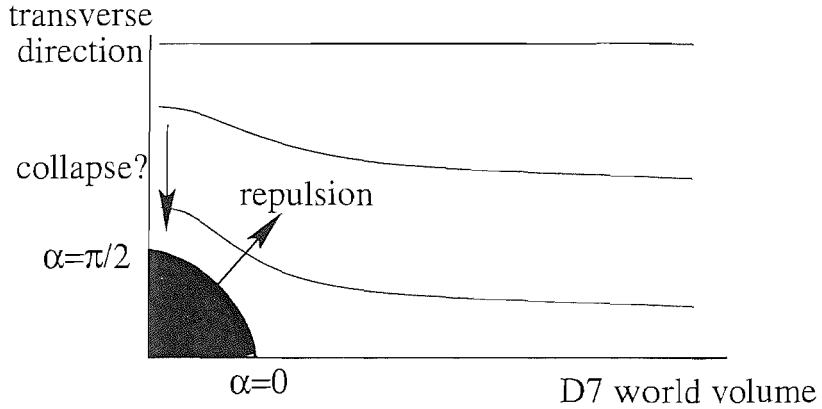


Figure 5.10: A sketch of how a flat D7 brane embedding is expected to behave in  $YM^*$  as the brane is brought close to the singularity. The repulsive potential away from  $\alpha = n\pi/2$  will induce a chiral symmetry breaking like configuration although the D7 may collapse into the singularity at  $\alpha = \pi/2$ .

precisely the coordinate transformation that has been previously identified as necessary in the literature. In contrast, in the non-supersymmetric dilaton flow [53] in which chiral symmetry breaking has previously been studied [48, 49], there are D7 embeddings for all possible quark masses that lie separated from the core singularity. Here no coordinate transformation can remove the symmetry breaking embedding.

To look at more complicated metrics where the full D7 embedding is numerically too involved to find, we developed a simple spherical D7 embedding in the dilaton driven flow. The full embedding appropriate for quark fields matches on to this spherical embedding in the IR. In the dilaton flow case, we could analytically find the potential

for the spherical embedding and use it to show that the core of the geometry is repulsive. This repulsion drives the D7 brane into a chiral symmetry breaking configuration. We could also compute an analytic estimate of the quark mass gap.

We then used this spherical embedding technique to test three new geometries for chiral symmetry breaking behaviour. The first is a non-supersymmetric version of the FGPW background [56] in which an unbounded scalar mass is included in the gauge theory. D7 branes in this geometry behaved precisely as those in the supersymmetric version of the FGPW geometry leaving no gap between the flows and the singularity. The spherical embedding technique showed there was no potential stopping the spherical D7 falling onto the singularity. We conclude that this geometry does not break chiral symmetries.

We next looked at a spherical D7 embedding in the  $\mathcal{N} = 2^*$  geometry [40] and found again that the D7 falls in on the singularity. This implies that for a supersymmetric embedding of a D7 for the inclusion of quarks in the geometry there would be no chiral symmetry breaking as we would expect.

Finally we studied a spherical D7 embedding in the non-supersymmetric Yang Mills\* geometry [43]. For most of the parameter space we found the central singularity of the geometry displayed a repulsive potential. This would imply chiral symmetry breaking embeddings for quark fields. There are special angles at which the repulsion vanishes but most probably this will not affect the conclusion.

Interestingly we have found chiral symmetry breaking in only those theories that are both non-supersymmetric and have a running dilaton. The former matches our

expectations but the generality of the latter point is unclear. We believe that our spherical embedding technique will provide a simple test for chiral symmetry breaking in the more complicated geometries that will be needed to describe QCD realistically.

## Chapter 6

# Improving the Glueball Spectrum in Finite Temperature QCD<sup>1</sup>

An interesting use of the AdS/CFT correspondence has been the calculation of glueball masses. These are inherently non-perturbative phenomena due to the strength of the strong interaction at low energies. Before the advent of the AdS/CFT correspondence the masses of the glueballs could only be calculated using lattice QCD techniques.

Naturally, there is not a discrete spectrum of glueballs in  $\mathcal{N} = 4$  supersymmetric Yang-Mills theory as this theory is conformal. A deformation of the correspondence was formulated by Witten [27] where a dual supergravity theory of finite temperature QCD was developed. This theory does have a discrete glueball spectrum which has been calculate using AdS/CFT techniques [60, 69, 70]. The results lie within 30%

---

<sup>1</sup>The finite temperature theory we are referring to is known in the literature as QCD<sub>4</sub>, which is QCD in  $\mathbb{R}^3 \otimes S^1$ .

or so of the QCD lattice results. In the first section of this chapter we review these calculations.

One of the problems with trying to find a dual gravitational picture of QCD is that all dual geometries go to  $\text{AdS}_5 \times \text{S}^5$  for large values of the radial coordinate where the operator matching takes place. On the field theory side, this corresponds to the theory flowing to the conformal  $\mathcal{N} = 4$  SYM at high energy. In QCD, the theory flows to a non-interacting fixed point as the energy goes to infinity. Even if properties of the dual theory are similar to QCD in the IR limit, the fact that the two theories differ in the UV will affect IR predictions through loop effects. In the second section of this chapter we show that, through adding a UV cutoff and tuning non-renormalisable operators, we can systematically remove these effects. We apply the technique to the calculation of glueball spectra in finite temperature QCD.

## 6.1 AdS-Schwarzschild Geometries and Finite Temperature QCD

An approach to studying finite temperature QCD was proposed by Witten in [27]. He proposed a theory which starts as a maximally supersymmetric gauge theory on the world-volume of  $N$  M5-branes<sup>1</sup>. One then compactifies this theory on a circle of radius  $R$ . Fermions are given anti-periodic boundary conditions around the circle which means that they will get a mass of order  $m \sim 1/R$ . This in turn breaks the supersymmetry of the theory.

---

<sup>1</sup>We are using M to denote branes in M-Theory.

The 11-dimensional supergravity description of a stack of M5-branes is given by the AdS/Schwarzschild solution[57].

$$ds_{11}^2 = h^{-\frac{1}{3}} \left[ \left( 1 - \frac{b^6}{\rho^3} \right) d\tau^2 + \sum_{i=1}^5 dx_i^2 \right] + h^{\frac{2}{3}} \left[ \left( 1 - \frac{b^6}{\rho^3} \right)^{-1} d\rho^2 + \rho^2 d\Omega_4^2 \right], \quad (6.1)$$

where  $h$  is the solution of the 5d Laplace equation and  $b$  corresponds to the inverse of the temperature of the dual field theory [27]. If we let  $\rho = \lambda^2$  and go to the non-extremal near horizon limit ( $b = 0, h = \rho^{-3}$ ) of this metric, we get:

$$ds_{11}^2 = \lambda^2 \left[ d\tau^2 + \sum_{i=1}^5 dx_i^2 \right] + \frac{4}{\lambda^2} d\lambda^2 + d\Omega_4^2, \quad (6.2)$$

ie.  $\text{AdS}_7 \times \text{S}^4$  after appropriate scaling of coordinates and a Wick rotation<sup>2</sup>. The AdS/CFT dual theory to this is six-dimensional superconformal Yang-Mills.

$\text{QCD}_4$  is dual to the low energy limit of IIA string theory on the AdS-Schwarzschild background [58, 59] on imposing anti-periodic boundary conditions for the fermions in the compact  $\tau$  direction<sup>3</sup>. We can obtain the type IIA metric from (6.1) by compactifying the 11<sup>th</sup> dimension and rescaling the metric by a factor  $e^{\frac{2\phi}{3}} = h^{-\frac{1}{6}}$ :

$$ds_{\text{IIA}}^2 = h^{-\frac{1}{2}} \left[ \left( 1 - \frac{b^6}{\rho^3} \right) d\tau^2 + \sum_{i=1}^4 dx_i^2 \right] + h^{\frac{1}{2}} \left[ \left( 1 - \frac{b^6}{\rho^3} \right)^{-1} d\rho^2 + \rho^2 d\Omega_4^2 \right]. \quad (6.3)$$

This solution also has a non-constant dilaton  $e^\phi = h^{-\frac{1}{4}}$ . Note that this metric is quoted in the *string frame*.

We now follow the analysis of [60] and calculate the glueball spectrum for this theory.

---

<sup>2</sup>From this we can see that  $\rho$  has mass dimension two.

<sup>3</sup>Imposing anti-periodic boundary conditions for the fermions gives them an effective mass. This has the additional effect of breaking supersymmetry as the mass of the bosons will be different.

### 6.1.1 The $0^{++}$ Mass Spectrum

Glueballs are labelled by their quantum numbers.  $J^{PC}$  denotes a glueball of spin  $J$ , parity  $P$  and charge  $C$ . In this section we will calculate the  $0^{++}$  glueball spectrum in finite temperature QCD<sub>4</sub> using the dual supergravity description.

The first step is to determine the dual field that acts as a source to the  $0^{++}$  glueball. The dominant contribution to the glueball mass will come from the term  $\frac{1}{g^2} \text{Tr} F^2$ . This is a scalar of dimension 6. The supergravity dual is a massless scalar whose equation of motion is

$$\partial_\mu \left[ \sqrt{g} g^{\mu\nu} e^{-2\phi} \partial_\nu \Phi \right] = 0. \quad (6.4)$$

In order to determine the glueball mass spectrum we must look for solutions to this equation of the form  $\Phi = f(\rho) e^{ikx}$ . These solutions are four-dimensional momentum eigenstates with some overall variation in  $\rho$ . The mass spectrum of the glueballs will then be  $m^2 = -k^2$ . Using this ansatz the equation of motion becomes<sup>4</sup>

$$\frac{1}{\rho} \frac{d}{d\rho} \left[ (\rho^4 - \rho) \frac{df}{d\rho} \right] = k^2 f(\rho). \quad (6.5)$$

The problem of finding the mass spectrum of the  $0^{++}$  glueballs has been reduced to finding the eigenvalues of this second order differential equation. This equation can be solved in many ways, for instance as a series expansion, by using the WKB method, or by numerical methods. We will describe a numerical method for finding the eigenvalues as this technique will be used in the next section with our modified geometry. The particular technique we use is known as the *shooting technique*:

---

<sup>4</sup>Note that we have set the dimensionful parameter  $b = 1$ . This means that all calculated masses will implicitly be in units of  $b$ . We use this freedom to fix the lightest  $0^{++}$  mass.

The large  $\rho$  asymptotic solution to (6.5) is easily seen to be

$$f(\rho) \sim \rho^{-3}. \quad (6.6)$$

We impose boundary conditions  $f(R) = R^{-3}$ ,  $f(R) = -3R^{-4}$  in the limit as  $R \rightarrow \infty$  and then numerically solve the equation of motion down to the black hole horizon at  $\rho = 1$ . This solution will be a function of  $k^2$ . We demand that our solutions be quantum mechanically normalisable, so reject solutions that go to  $\pm\infty$  at  $\rho = 1$ . Each value of  $-k^2$  that yields a normalisable solution is interpreted as a valid glueball  $m^2$ .

The results of this are shown in the next section in Table 6.1 ( $\alpha = 0$ ) where they are compared to results from our improved geometry.

We now consider the  $0^{-+}$  glueballs. We assume that the dominant contribution to their mass spectrum will come from the  $\text{Tr}F\tilde{F}$  operator as this is the lowest dimension operator with the correct quantum numbers. In order to find the supergravity dual of this field, consider the Chern-Simons term in the action of a probe D4-brane 10D type IIA background.

$$S_{CS} = -\mu_4 \int \text{Tr} \left[ \exp((2\pi\alpha')F) \wedge \sum_q C_{(q)} \right], \quad (6.7)$$

where  $C_{(q)}$  are R-R  $q$ -form fields,  $F = dC_{(1)}$ , and we have neglected the NS-NS fields. In IIA string theory, there are RR fields for odd  $q$ . Letting  $C_{(1)} = A_\mu$ , and expanding (6.7) gives

$$S_{CS} = -\mu_4 \int d^5x (2\pi\alpha')^2 \epsilon^{\alpha\beta\gamma\delta\rho} A_\rho \text{Tr}(F_{\alpha\beta} F_{\gamma\delta}), \quad (6.8)$$

which in turn gives

$$S_{CS} = -\mu_4 (2\pi\alpha')^2 \int d\tau A_\tau \int d^4x \text{Tr}\tilde{F}F. \quad (6.9)$$

Since  $\tau$  is periodic, we have

$$\int d\tau A_\tau = 2\pi A_\tau|_\infty. \quad (6.10)$$

The boundary value of the  $\tau$  component on a vector field  $A_\mu$  acts as a source for  $\text{Tr} \tilde{F}F$

and is thus its AdS dual. The equation of motion for a vector field  $A$  is

$$\partial_\nu \left[ \sqrt{g} g^{\mu\delta} g^{\nu\sigma} (\partial_\delta A_\sigma - \partial_\sigma A_\delta) \right] = 0. \quad (6.11)$$

As with the  $0^{++}$ , we look for solutions which are an eigenstate of 4d momentum on the boundary of the form  $A_\tau = f(\rho) e^{ik \cdot x}$  in the background (6.3). The result is the equation

$$\frac{1}{\rho^4} (\rho^3 - 1) \frac{d}{d\rho} \left[ \rho^4 \frac{df}{d\rho} \right] = k^2 f(\rho). \quad (6.12)$$

As with the  $0^{++}$  glueballs, we use the shooting technique to numerically find the eigenvalues of this equation. The results are shown in Table 6.2.

## 6.2 Improving the Ultra-Violet

Whilst deformed AdS geometries presumably do a good job of catching QCD-like physics in the IR below the mass of the superpartners, these theories all have additional massive states at strong coupling and evolve to a conformal strongly coupled theory in the UV. A priori this appears to leave very non QCD-like theories and any match with QCD states would appear to be telling us mainly about the universality of these masses across a range of gauge theories. In this section we want to begin addressing the issue of systematically removing this unwanted UV physics. We clearly do not want a large UV strongly coupled conformal interval so we will apply a hard UV

cutoff in the gravitational description, corresponding to roughly the scale where QCD would transition between perturbative and non-perturbative physics. In the theories developed to date there will be additional fields to those we want even at this scale (typically with masses of order this scale). The couplings of these fields will necessarily alter the physics of the fields we are interested in describing. Since the extra fields are massive we hope that their influence on the running of the gauge coupling will be small. Their main effect will be to distort the coefficients of higher dimension operators in the fields we wish to study. We want to assume that the physics above the cutoff scale is that of QCD rather than the  $\mathcal{N} = 4$  theory, but the higher dimensional operators will be the wrong ones for this case if we just impose a cutoff. The natural correction is to hand tune the higher dimension couplings to the values in QCD to reproduce the correct physics. This is what we begin to study here.

The idea of tuning higher dimension operators to remove the effects of “regulator” fields is similar to the idea of *perfect* or *improved* actions in lattice gauge theory [61, 62]. Ideally, one would like to take the lattice spacing to zero, but this is impossible computationally. Having a finite lattice spacing means that the field theory on the lattice will have a finite cutoff given by the inverse of the lattice spacing. We know that in a field theory with a cutoff, extra non-renormalisable operators will be generated. If working on too coarse a lattice, the effects of these operators will be significant. In practice, adjusting just one or a few of these higher dimension operators to correctly reproduce the physical data shows improvement across the whole predicted spectrum.

The picture of this is shown in Figure 6.1. We apply a hard UV cutoff at around

the scale where the theory becomes conformal. By tuning the coefficient of a higher dimensional operator, we aim to change the effective UV of the theory.

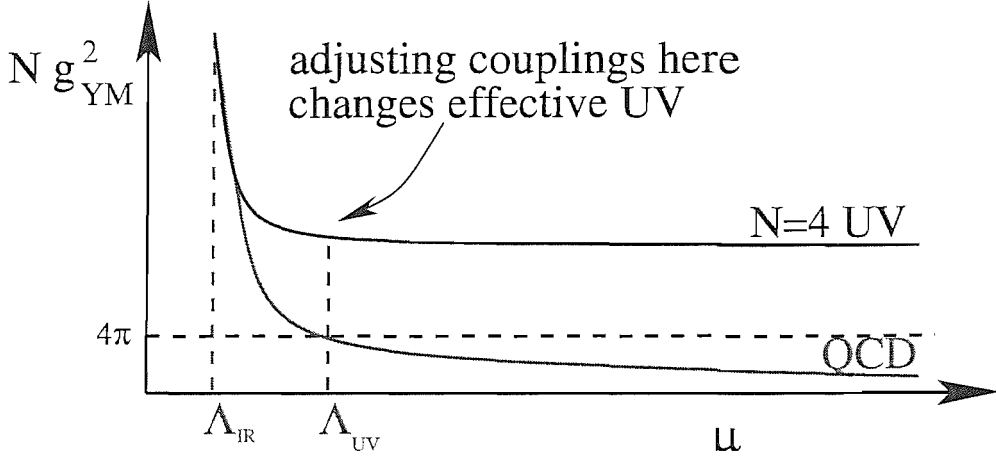


Figure 6.1: Direction field for the supergravity fields  $\rho(r)$  and  $\varphi(r) = \cosh^2 \chi(r)$  showing UV and IR fixed points

As a test of this idea, we will calculate the glueball mass spectrum in the  $\text{AdS}_7$  Schwarzschild black hole geometry of the previous section. We will introduce an explicit UV cutoff into this theory and then add the supergravity dual of the  $\text{Tr}F^4$  operator. We will then tune the coefficient of this operator to try to remove the incorrect UV physics (i.e. the effects of these extra fields) in the glue sector and hence improve the glueball results. To switch on this operator one simply allows the solution to revert to flat space asymptotically by undoing the near horizon limit. The resulting deformation has the correct dimension and symmetry properties to play the role of the  $\text{Tr}F^4$  coupling. Previous studies of this theory can be found in [50, 51, 52, 53]. We imagine that above our UV cutoff the theory is true Yang Mills theory. If we did not impose a cutoff the

higher dimension operator would grow into the UV and eventually come to dominate the physics. In this case the operator makes the potential that is responsible for the discrete glueball spectrum unbounded. We therefore take the scale where the potential instability sets in as the natural UV cutoff.

We will see that to match the lattice large  $N$   $0^{++}$  glueball mass data, we must make the operator  $\text{Tr}F^4$  large at a rather low scale. In fact, there turns out to be such a small interval between the UV and IR cutoffs that there is no AdS-like geometry left, and barely any gravity description at all! This is perhaps not surprising since QCD presumably moves into the strong coupling regime fairly quickly and then almost immediately generates a mass gap. We nevertheless look at the predictions of our short interval for the  $0^{-+}$  glueballs. Only  $N = 3$  lattice data exists but our improved geometry is a better match to the data than the unimproved geometry.

### 6.2.1 The Improved Geometry

We wish to modify the metric (6.3) to include the effect of adding  $\text{Tr}F^4$  to the dual field theory.

$$S_{FT} = \int d^6x \left[ \frac{1}{g^2} \text{Tr}F^2 + G \text{Tr}F^4 + \dots \right] \quad (6.13)$$

The coupling  $G$  has mass dimension -6. The gravitational dual of this can be included by adding a constant term in the solution for  $h$

$$h = \rho^{-3} \rightarrow \rho^{-3}(1 + \alpha\rho^3), \quad (6.14)$$

i.e. going away from the near horizon limit.  $\alpha$  has the right mass dimension -6 to be dual to  $G$ , plus correctly has no R-charge since it does not depend on angles on the

four sphere.

Note that the function  $h$ , being a solution of the five dimensional Laplace equation, can encode a more complicated function if we allow it to have angular dependence. Terms in  $h$  that fall off at large radius are associated with operators of the form  $\text{Tr}\phi^n$  in the field theory [63, 47], whilst those that grow correspond to R-charged higher dimension operator couplings. Since we are interested in the glue sector, we will not make use of these operators.

### 6.2.2 The $0^{++}$ Mass Spectrum

We must use our modified metric in the equation of motion (6.4). The result is

$$\frac{1}{\rho} \frac{d}{d\rho} \left[ (\rho^4 - \rho) \frac{df}{d\rho} \right] = k^2 (1 + \alpha\rho^3) f(\rho), \quad (6.15)$$

In order to change this equation of motion into a Schrödinger form we use the procedure outlined in Appendix A. We make a change of the dependant variable to  $z$  and re-scale

$$\frac{dz}{d\rho} = \sqrt{\frac{1 + \alpha\rho^3}{\rho^3 - 1}}, \quad f(z) \rightarrow f(z) e^{-\frac{1}{2} \int dz' p(z')}, \quad (6.16)$$

where

$$p(\rho) = \frac{5\rho^3 - 2 + \alpha\rho^3(8\rho^3 - 5)}{2\rho\sqrt{\rho^3 - 1}(1 + \alpha\rho^3)^{\frac{3}{2}}}. \quad (6.17)$$

We now have an equation in Schrödinger form with a Schrödinger potential

$$-g''(z) + Q(z)g(z) = m^2 g(z), \quad Q(z) = \frac{1}{2}p'(z) + \frac{1}{4}p(z)^2, \quad (6.18)$$

or, in terms of the radial coordinate  $\rho$

$$Q(\rho) = \frac{1}{2} \sqrt{\frac{\rho^3 - 1}{1 + \alpha\rho^3}} \frac{dp}{d\rho} + \frac{1}{4}p(\rho)^2. \quad (6.19)$$

We plot the potential as a function of  $\alpha$  in Figure 6.2 for different values of  $\alpha$ . For  $\alpha = 0$  the pure AdS geometry gives a well that is bounded into the UV and an infinite, discrete glueball spectrum. When  $\alpha$  is non-zero, the UV potential is modified and eventually falls to zero. In the field theory the higher dimension operator grows into the UV until it dominates the physics and removes the discrete spectrum. If we allow this to happen then we are not describing a QCD-like theory in the UV, so we will impose a hard UV cutoff,  $\Lambda$ . The natural scale to place the cutoff is at the turning point of the potential since that includes in the IR theory the highest possible tower of discrete states - we will adopt this value for the cutoff henceforth. Thus as we increase  $\alpha$  we will necessarily be working on a shorter radial interval.

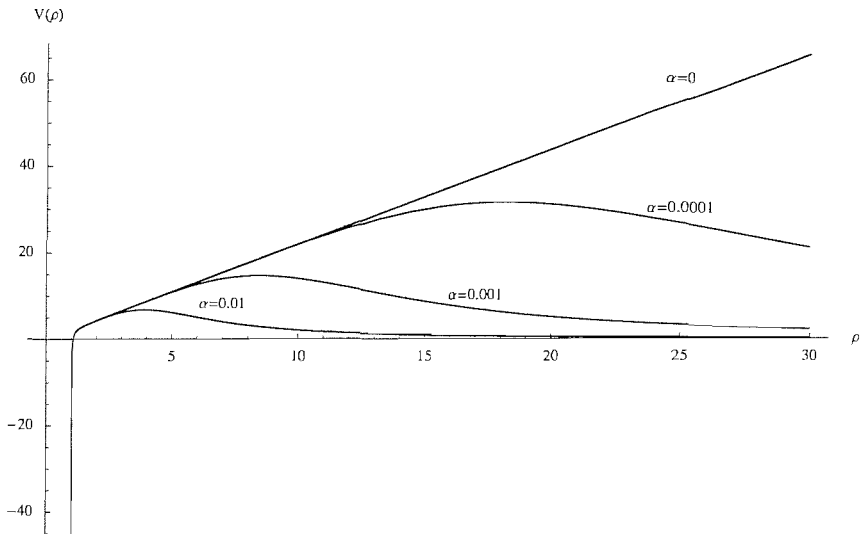


Figure 6.2: QCD<sub>4</sub> Schrödinger potential for the 0<sup>++</sup> glueballs  $\alpha = 0$  to  $\alpha = 0.01$ .

Again we calculate the eigenvalues using the shooting technique. The problem here is what to set as the appropriate boundary conditions. We know that for  $\alpha = 0$

taking  $\rho \rightarrow \infty$ , the metric goes to AdS space and the normalisable solution to the wave equation (6.15) goes like  $\rho^{-3}$ . We will use the naive boundary conditions  $f(\Lambda) = \Lambda^{-3}$ ,  $f'(\Lambda) = -3\Lambda^{-4}$  in all cases below. As  $\alpha$  grows and the cutoff falls, this boundary condition, which represents the effective dimension of  $\text{Tr}F^2$ , should presumably change - it is essentially a matching condition on the dimension that should come from the UV theory. We have checked that if we instead use the boundary conditions  $f(\Lambda) = \Lambda^{-(3+\epsilon)}$ ,  $f'(\Lambda) = -(3+\epsilon)\Lambda^{-(4+\epsilon)}$  with  $-1 < \epsilon < 1$  the ratio of the lightest two glueballs masses only changes by 6%. This indicates that the mass spectrum is largely insensitive to the precise values of the boundary conditions. Note that this range includes  $\text{Tr}F^2$  having dimension four as one might expect in real QCD.

Using this shooting technique, we tune  $\alpha$  to get a glueball spectrum that agrees best with the available large  $N$  lattice data [64, 65]. Figure 6.3 shows the ratio  $m(0^{++*})/m(0^{++})$  for different values of  $\alpha$ . We can see that setting  $\alpha = 0.0855$  gives the correct value for the second glueball mass (the first is fixed by normalisation). This implies that  $\Lambda = 1.99$  - we will refer to this case as the “improved geometry”. For this value of  $\alpha$  we get the spectrum of masses shown in Table 6.1. The glueball masses rise in the theory although we have no more lattice data to compare to for this state.

The result, that to correctly reproduce the lattice data we must raise  $\alpha$  so that the theory only provides a description between an IR scale of  $b = 1$  and a UV scale of  $\sqrt{\Lambda} = 1.41$  (note  $\sqrt{\Lambda}$  has mass dimension 1), is important. Although the original AdS black hole produced results that match the QCD data reasonably we find that to move to a phenomenological model of QCD we must actually distort the AdS space

considerably. Indeed, the gravitational theory's interval is worryingly small and non-AdS like. This is not so surprising in terms of real QCD where the regime between the QCD coupling becoming non-perturbative and the scale of the mass gap of the theory is quite small. This result may have important ramifications for attempts to turn toy models of the sort in [66, 67, 68] into true phenomenological tools.

<i>Glueball State</i>	<i>Improved Geometry</i>	$\alpha = 0$	$N = 3$ <i>Lattice</i>	$N = \infty$ <i>Lattice</i>
$0^{++}$	1.00	1.00	1.00	1.00
$0^{++*}$	1.90	1.58	1.74	1.90
$0^{++**}$	3.05	2.15	-	-
$0^{++***}$	4.27	2.72	-	-
$0^{++****}$	5.52	3.33	-	-

Table 6.1:  $\text{QCD}_4$   $0^{++}$  glueball masses from AdS ( $\alpha = 0$ ) and Improved ( $\alpha = 0.0855$ ) geometries along with lattice data [64, 65]. Normalisation is such that the ground state mass is set to one.

### 6.2.3 The $0^{-+}$ Mass Spectrum

The result of using our improved metric in the equation of motion (6.11) is

$$\frac{1}{\rho^4}(\rho^3 - 1)\frac{d}{d\rho}\left[\rho^4\frac{df}{d\rho}\right] = k^2(1 + \alpha\rho^3)f(\rho). \quad (6.20)$$

If we set  $\alpha = 0.0855$  and  $\Lambda = 1.99$ , which were their optimum values for the  $0^{++}$ , we get the spectrum shown in Table 6.2. We have normalised all masses to the  $0^{++}$  ground state. The lightest state does not match well to the  $N=3$  lattice data - this state was

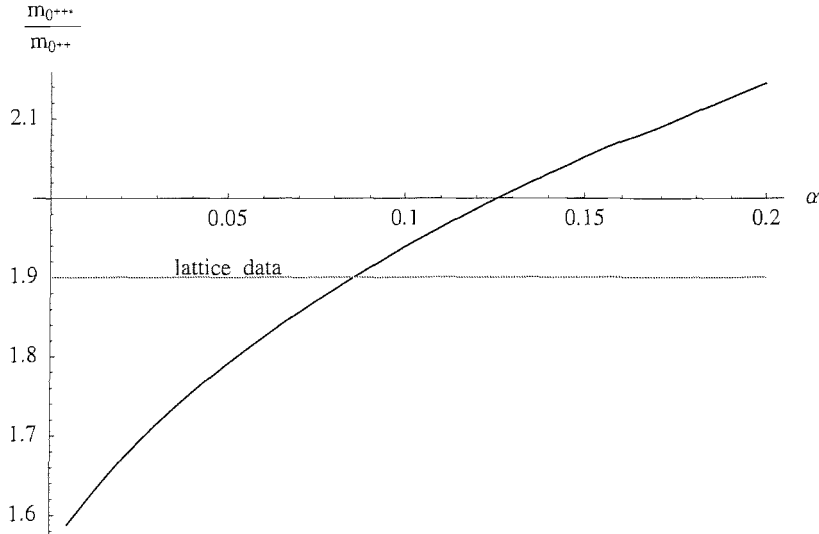


Figure 6.3:  $m_{0+++}/m_{0++}$  for different values of  $\alpha$

omitted from the spectrum in [69, 70] which then improves the fit considerably! The effect of our improved geometry is to make the states more massive, which improves the fit to the data whether the first state is omitted or left in. To truly match these states to the data would presumably require a higher dimension operator with  $P = -1, C = +1$  quantum numbers to be tuned - it is not clear how to include such an operator though.

### 6.3 Conclusions

We have shown that by including the gravitational dual of a higher dimensional field theory operator to the usual AdS-Schwarzschild metric, we can tune our theory to match onto the first excited  $0^{++}$  glueball state as calculated using lattice techniques. Having fixed the strength of this perturbation, we also find that the  $0^{-+}$  spectrum is improved. We find that in order to get the correct  $0^{++}$  spectrum we almost entirely

<i>Glueball State</i>	<i>Improved Geometry</i>	$\alpha = 0$	$N = 3$ <i>Lattice</i>
$0^{-+}$	0.35	0.29	1.61
$0^{-+*}$	1.38	1.24	2.26
$0^{-+**}$	2.48	1.84	-
$0^{-+***}$	3.71	2.42	-

Table 6.2:  $\text{QCD}_4$   $0^{-+}$  glueball masses from AdS ( $\alpha = 0$ ) and Improved ( $\alpha = 0.0855$ ) geometries along with lattice data [64]. All states are normalised to the  $0^{++}$  ground state.

remove the AdS-like region of the space. This ties in with there being only a small energy range between the mass gap and strong coupling region of QCD.

## Chapter 7

# The AdS/QCD Approach

One of the major goals of the AdS/CFT Correspondence and its variations has been to find a gravitational theory dual to QCD in order to investigate the strong coupling regime beyond the reach of perturbation theory. Some attempts towards this goal have been described in the previous two chapters. The attempts have based around finding a particular D-brane solution from 10 or 11-dimensional supergravity and interpreting the field content as dual source fields for some four-dimensional field theory. This approach has yielded some interesting general results about confining gauge theories; however, a solution has yet to be found which could truthfully be described as *the* dual theory to QCD.

We know what the field content and symmetries of this QCD gravitational theory should be. This just comes from the standard AdS/CFT operator matching. We also know that the dual theory should have a mass gap, be confining, and exhibit some form of chiral symmetry breaking. Solutions have been found which satisfy some of these

criteria and include some of the relevant dual fields, but there has yet to be found a solution with all of the correct fields and properties required for a gravity dual to QCD.

Recently, a new “bottom up” approach has been studied, known as AdS/QCD, in which one starts from QCD, and then attempts to construct a dual gravitational theory by adding the relevant dual fields by hand to a five-dimensional AdS background. The conformal invariance of the theory is broken by adding a hard cut-off in the infra-red. One then tries to constrain the properties of this dual theory by matching them to known properties of QCD. This approach has proven to be surprisingly successful in reproducing experimental meson data [66, 67] (see also [71]-[79]) .

The phenomenological approaches to describing QCD holographically are based on a 5d action of the form

$$S \sim \int d^4x dr e^\phi \sqrt{-g} \left( \mathcal{L}_\sigma + \sigma^2 \text{Tr}|DU|^2 - \frac{1}{4g_5^2} \text{Tr}(F_L^2 + F_R^2) \right), \quad (7.1)$$

where  $D_\mu U = \partial_\mu U - iA_{L\mu}U + iUA_{R\mu}$ . The field  $U(x, r) = \exp(i\pi^a(x, r)T^a)$  describes the pions produced by the breaking of a  $SU(N_f)$  chiral symmetry with generators  $T^a$ . We assume that the background value of  $U$  is the identity so we are studying  $N_f$  degenerate quarks. The non-abelian gauge fields  $A_L$  and  $A_R$  couple by left and right action on  $U$ . They will holographically describe the vector and axial vector mesons. The field  $\sigma$  is a function of  $r$  only and holographically describes the quark mass and  $\langle \bar{q}q \rangle$  expectation value. A non-zero value for this field will break the  $SU(N_f)_L \times SU(N_f)_R$  chiral symmetry of the action down to the vector  $SU(N_f)_V$ .

## Pure AdS

In the simplest approaches [66, 67], the dilaton,  $\phi$ , is taken to be constant, so drops from the action. The background metric is AdS down to some boundary at  $r_0$  which breaks the conformal symmetry and provides the theory with a mass gap.

$$ds^2 = \frac{r^2}{R^2} dx^2 + \frac{R^2}{r^2} dr^2, \quad r_0 \leq r < \infty. \quad (7.2)$$

Note that dilatation transformations in the field theory, which define the mass dimension of operators (for example if we scale  $x \rightarrow e^\alpha x$  then a scalar field of dimension one scales as  $\phi \rightarrow e^{-\alpha}\phi$ ), are mapped to a symmetry of the metric with the radial direction scaling as an energy scale.

The Lagrangian for  $\sigma$  in these models is given by

$$\mathcal{L}_\sigma = (\partial_r \sigma)^2 - 3\sigma^2, \quad (7.3)$$

with resulting solutions  $\sigma(r) = m/r + c/r^3$ . Here  $\sigma$  has does not transform under the field theory dilatations so  $m$  has dimension one and  $c$  dimension three. The two parameters  $m, c$  are fitted phenomenologically to the (degenerate) light quarks' mass and condensate.

The remaining parameter is  $g_5$ , which in string theory duals is a prediction in terms of the gauge theory 'tHooft coupling  $g_{YM}^2 N$ . In the phenomenological approach though, this relation is abandoned and the value of  $g_5$  is fitted to the vector current correlator extracted from QCD.

$$\int d^4x e^{iqx} \langle J_\mu^a(x) J_\nu^b(0) \rangle = \delta^{ab} (q_\mu q_\nu - q^2 g_{\mu\nu}) \Pi_V(-q^2), \quad (7.4)$$

where  $J_\mu^a(x) = \bar{q}\gamma_\mu T^a q$ . For QCD, the leading order contribution to  $\Pi_V(-q^2)$  is [80]

$$\Pi_V(-q^2) = -\frac{N}{24\pi^2} \ln(-q^2). \quad (7.5)$$

In order to calculate this quantity from the five-dimensional model, we appeal to the AdS/CFT correspondence. The five-dimensional vector field  $V_\mu^a(x, r) = (A_{L\mu}^a(x, r) + A_{R\mu}^a(x, r))$  acts as a source for the four-dimensional vector current  $J_\mu^a(x)$  in the limit  $r \rightarrow \infty$ . It obeys the equation of motion

$$\partial_\mu \left( \frac{1}{g_5^2} e^\phi \sqrt{-g} g^{\mu\alpha} g^{\nu\beta} (\partial_\alpha V_\beta^a - \partial_\beta V_\alpha^a) \right) = 0. \quad (7.6)$$

We look for solutions of the form  $V^\mu(x, r) = V_0^\mu(x)v(x, r)$ , with  $\lim_{r \rightarrow \infty} v(x, r) = 1$ , so that  $V_0^\mu(x)$  will act as a dimension one source for  $J_\mu^a(x)$ . Solving the equation of motion (7.6) in the  $V^r(x, r) = 0$  gauge gives

$$v(q, r) = -\frac{\pi}{2} \mathcal{Y}_1(q/r) \sim 1 - \frac{q^2}{4r^2} \ln\left(\frac{-q^2}{r^2}\right), \text{ as } r \rightarrow \infty, \quad (7.7)$$

where  $\mathcal{Y}_1$  is a Bessel function of the second kind. Substituting the solution back into the action and differentiating twice with respect to the source  $V_0^\mu$  gives the vector current correlator

$$\Pi_V(-q^2) = \left[ \frac{1}{g_5^2 q^2} r^3 \partial_r v(q, r) \right]_{r=\infty}, \quad (7.8)$$

which (up to contact terms) yields

$$\Pi_V(-q^2) = -\frac{1}{2g_5^2} \ln(-q^2). \quad (7.9)$$

Finally, comparing this to the perturbative QCD result (7.5) determines the 5d coupling

as

$$g_5^2 = \frac{12\pi^2}{N}. \quad (7.10)$$

In [67, 66] this model is used to calculate meson masses, decay constants and couplings coefficients with great success. We summarise these results in Table 7.1.

The matching in (7.10) is of course naive. One should match the gravitational theory to QCD only at the point where the QCD coupling becomes non-perturbative where gluonic corrections to the perturbative QCD result become important. It is therefore interesting to recompute the results of [67], but with  $g_5$  being a free parameter of the model in order to see how accurate this matching is. On performing a global fit on all of the parameters, we found that the optimal value for  $g_5$  is 5.19, which is 17% smaller than the result  $\sqrt{(12\pi^2)/N}$  from matching to perturbative QCD. We conclude that non-perturbative effects could have a significant effect.

## 7.1 Improving the Infra-red

The AdS/QCD models are in many ways naive. Amongst the criticisms that might be aimed at these models are:

- The use of an AdS geometry implicitly means that the background gauge configuration is conformal (and essentially that of large  $N$   $\mathcal{N} = 4$  super Yang Mills).
- The existence of a mass gap is imposed by hand through the inclusion of a boundary to the space and is not the product of a running coupling.
- The fields that holographically describe the quark bilinears are included phenomenologically and there is no rigorous (string theory) realization of the construction.

- The solution for the field which describes the quark mass and condensate is also included by hand and the quark condensate is not dynamically determined in terms of either the gauge configuration or the quark mass.
- The ultra-violet of the theory does not become asymptotically free.
- The excited meson mass spectrum typically scales like the excitation number  $n$  as opposed to the  $\sqrt{n}$  scaling predicted by a simple flux tube model [81].

In spite of these objections, the models do provide a good description of the light meson sector of QCD. The clear next step is to try to alleviate some or all of these objections. In this paper we will address this task (progress has already been made in [82, 83]).

Our main tool will be to use the more rigorous AdS/CFT description of chiral symmetry breaking in [49]. Previously it has been used as a testing ground for the generic features of chiral symmetry breaking [48], but here we will massage it to a phenomenological five-dimensional holographic description of QCD.

The geometry we will use is that on the surface of a D7 brane in a non-supersymmetric dilaton flow deformation of the AdS/CFT Correspondence. We review its origin in more detail later, but let us stress its benefits now:

- The background gauge configuration in which the quarks live is non-supersymmetric (although not purely that of QCD) and has a running coupling.
- The mass gap is a result of the non-supersymmetric gauge configuration and the geometry relevant for quark physics is smooth at all radii or energy scales.

- The holographic dual of the quark bilinear is explicit in the string construction.
- The quark condensate is a prediction of the gauge configuration and is determined as a function of the quark mass.

These points go a considerable way towards addressing the inconsistencies of the first models. We will, however, continue to adopt the phenomenological approach of treating the background as describing an  $N=3$  rather than  $N \rightarrow \infty$  theory. In addition, the string theory construction can only realise a  $U(1)$  axial symmetry, and does not provide a holographic dual of the axial vector mesons. We include by hand appropriate fields to provide a non-Abelian chiral symmetry and the axial vector states in the phenomenological spirit of [66, 67].

In this chapter we compute with our phenomenological model the masses and decay constants for the pion and the rho and  $a_1$  vector mesons, and also the  $g_{\rho\pi\pi}$  coupling. We find that the model gives comparable predictions to the pure AdS models within 16% of the QCD values. We believe these results provide support for the robustness of the predictions of these holographic models.

The geometry we propose returns to pure AdS space in the ultra-violet, so we do not address here the loss of asymptotic freedom. As we pointed out in Chapter 6, the theory should have a UV cut off corresponding to the scale at which QCD becomes non-perturbative. The correct UV dynamics should be encoded at that cut off by correcting the values of higher dimension operator couplings. In principle, these can be tuned in the AdS/CFT approach to produce the holographic equivalent of a perfect lattice action. As a small example of these ideas we consider the matching of the

five-dimensional gauge coupling in the UV. In [66, 67] this coupling is matched to the perturbative result for the vector vector correlator in QCD. Here we test how good that matching is by allowing the parameter to float and fitting it to data. We find such a fit induces roughly a 20% change in the coupling value, which provides a measure of non-perturbative corrections at the scale of matching to the strongly coupled regime of QCD. We leave attempts to further improve the UV of the theory for later work though.

Finally, it has recently been pointed out that an appropriate change to the warp factor of the metric [85] or to the IR behaviour of the dilaton [83] can correct the  $n$  scaling of the tower of excited  $\rho$  meson states. We have tested our model in this respect but find only a marginal improvement over the pure AdS case. This is a sign that, although our geometry describes a non-supersymmetric gauge configuration, it is still not a perfect description of QCD and work remains to be done on improving the geometric background.

### The New Model

Our approach in this chapter will be based around the D3/D7 brane string theory construction of [49]. In this paper the authors add a D7 brane probe to the ten-dimensional D3-brane solution of Constable and Myers [53]. The complex scalar describing the position of the D7-brane is dual to the quark mass/condensate operator  $\bar{q}q$ , and there is a nice geometrical interpretation of chiral symmetry breaking (see Chapter 5).

The Constable-Myers geometry is

$$ds^2 = H^{-1/2} \left( \frac{w^4 + b^4}{w^4 - b^4} \right)^{\delta/4} dx_4^2 + H^{1/2} \left( \frac{w^4 + b^4}{w^4 - b^4} \right)^{(2-\delta)/4} \frac{w^4 - b^4}{w^4} \sum_{i=1}^6 dw_i^2, \quad (7.11)$$

where

$$H = \left( \frac{w^4 + b^4}{w^4 - b^4} \right)^{\delta} - 1 \quad (7.12)$$

and the dilaton and four-form are given by

$$e^{2\phi} = e^{2\phi_0} \left( \frac{w^4 + b^4}{w^4 - b^4} \right)^{\Delta}, \quad C_{(4)} = -\frac{1}{4} H^{-1} dt \wedge dx \wedge dy \wedge dz. \quad (7.13)$$

There are formally two free parameters,  $R$  and  $b$ , since

$$\delta = \frac{R^4}{2b^4}, \quad \Delta^2 = 10 - \delta^2 \quad (7.14)$$

We can see that dimensionally  $b$  has energy dimension one and enters to the fourth power. The SO(6) symmetry of the geometry is retained at all  $r$ . We conclude that in the field theory a dimension four operator with no SO(6) charge has been switched on.  $b^4$  therefore corresponds to a vev for the operator  $\text{Tr}F^2$ .

Quarks are introduced by including probe D7 branes into the geometry (see section 3.4).

The DBI action for the D7-brane in the *Einstein frame* is

$$S = -\tau_7 \int d^7 \xi e^\phi \left[ -\det \left( \mathbf{P}[g_{ab}] + 2\pi\alpha' e^{-\phi/2} F_{ab} \right) \right]^{1/2}, \quad (7.15)$$

where  $\mathbf{P}[g_{ab}]$  is the 8d metric induced on the D7-brane and  $F_{ab}$  is the field strength for 8d gauge fields living on the brane. This action can be expanded (see Appendix B) to

give

$$S = -\tau_7 \int d^7 \xi e^\phi [-\det(g_{ab})]^{1/2} (1 + \dot{\sigma}^2)^{1/2} \times \left\{ 1 + \frac{1}{2} g_{rr} \sigma^2 (1 + \dot{\sigma}^2)^{-1} \partial^a U \partial_a U^\dagger - \frac{1}{4} (2\pi\alpha')^2 e^{-\phi} \text{Tr} F^2 \right\}, \quad (7.16)$$

where  $w_8 + iw_9 = \sigma(r)U(r, \xi)$ . Note that  $\text{Tr} F^2 = \mathbf{P}[g^{ac}]\mathbf{P}[g^{bd}]F_{ab}F_{cd}$ .

Since we require that our fields be the duals of non-supersymmetric operators, we can assume that  $U$  and  $F$  only have non-zero components in the  $(x, r)$  directions. We can then integrate to give a five-dimensional action

$$S = -\tau_7 (2\pi)^3 \int d^5 \xi e^\phi [-\det(g_{ab})]^{1/2} (1 + \dot{\sigma}^2)^{1/2} \times \left\{ 1 + \frac{1}{2} g_{rr} \sigma^2 (1 + \dot{\sigma}^2)^{-1} \partial^a U \partial_a U^\dagger - \frac{1}{4} (2\pi\alpha')^2 e^{-\phi} \text{Tr} F^2 \right\}. \quad (7.17)$$

If we now re-scale  $U \rightarrow R^4 \pi \sqrt{\tau_7} U$  and define the new dilaton and a five-dimensional coupling  $g_5$  as

$$e^\phi = H^{5/4} f^{5/4 - 5\delta/8 + \Delta/2} h^{5/2} r^3 (1 + \dot{\sigma}^2)^{-1/2} \sim r^{-2}, \text{ as } r \rightarrow \infty, \\ g_5^2 = \hat{g}_5^2 H^{1/2} f^{1/2 - \delta/4 + \Delta/2} h (1 + \dot{\sigma}^2)^{-1} \sim \hat{g}_5^2 r^{-2}, \text{ as } r \rightarrow \infty. \quad (7.18)$$

we can bring the action into the standard form

$$S \sim \int d^4 x \ dr \ e^\phi \sqrt{-g} \left( \mathcal{L}_\sigma + \sigma^2 \text{Tr} |DU|^2 - \frac{1}{4g_5^2} \text{Tr} F^2 \right), \quad (7.19)$$

The final step in constructing this phenomenological model is to artificially extend the symmetry group from  $SU(N_f)_V \times U(1)_A$  to the chiral  $SU(N_f)_L \times SU(N_f)_R$  and add in the axial vector gauge field in (7.1). We now have an action in the form of (7.1) with a 5d metric

$$ds^2 = H^{-1/2} f^{-\delta/4} \sum_{i=0}^3 dx_i^2 + H^{1/2} f^{1/2 - \delta/4} h \ dr^2, \quad (7.20)$$

where

$$f = \frac{(\sigma(r)^2 + r^2)^2 + b^4}{(\sigma(r)^2 + r^2)^2 - b^4}, \quad h = \frac{(\sigma(r)^2 + r^2)^2 - b^4}{(\sigma(r)^2 + r^2)^2}, \quad H = f^\delta - 1,$$

and a radially changing dilaton and 5d gauge coupling

$$e^\phi = H^{5/4} f^{5/4 - 5\delta/8 + \Delta/2} h^{5/2} r^3 (1 + \dot{\sigma}^2)^{-1/2} \sim r^{-2}, \text{ as } r \rightarrow \infty, \\ g_5^2 = \hat{g}_5^2 H^{1/2} f^{1/2 - \delta/4 + \Delta/2} h (1 + \dot{\sigma}^2)^{-1} \sim \hat{g}_5^2 r^{-2}, \text{ as } r \rightarrow \infty. \quad (7.21)$$

with  $\delta = 1/2$ ,  $\Delta = \sqrt{39}/2$ . Note that we scaled all coordinates by a factor of  $R$ . The conformal symmetry breaking scale is fixed by the parameter  $b$  which will determine the scale  $\Lambda_{QCD}$ . Since it is the only scale in the model, we set it to one for computations. At the string theory level the value of  $R$  fixes the 5d gauge coupling, but here we will fix that phenomenologically to describe an  $N_c = 3$  theory so we have also set  $R = 1$  and left  $\hat{g}_5$  free. As  $r \rightarrow \infty$ , the metric returns to  $AdS_5$ , the factor  $e^\phi/g_5^2$  goes to  $1/\hat{g}_5^2$  and we are left with exactly the pure AdS model.

### *Dynamical Quark Condensate*

The chiral symmetry breaking quark condensate is determined dynamically in this model by the background metric which represents the background gauge configuration. The Lagrangian for the field  $\sigma(r)$  in this model is

$$\mathcal{L}_\sigma = \sqrt{-g} f^{\Delta/2} g_{rr}^{3/2} \sqrt{1 + \dot{\sigma}^2}, \quad (7.22)$$

where the dot indicates differentiation with respect to  $r$ . The equation of motion for this field, which is complicated since  $\sigma$  occurs throughout the geometry, is given by

$$\frac{d}{dr} \left[ \frac{f^{\Delta/2} \mathcal{G}(\rho, \sigma)}{\sqrt{1 + (\partial_r \sigma)^2}} (\partial_r \sigma) \right] - \sqrt{1 + \partial_r \sigma^2} \frac{d}{d\bar{\sigma}} \left[ f^{\Delta/2} \mathcal{G}(\rho, \sigma) \right] = 0, \quad (7.23)$$

where

$$\mathcal{G}(\rho, \sigma) = r^3 \frac{((r^2 + \sigma^2)^2 + 1)((r^2 + \sigma^2)^2 - 1)}{(r^2 + \sigma^2)^4}. \quad (7.24)$$

The large  $r$  form of the solutions is of the AdS form (note from the metric that  $\sigma$  here enters symmetrically with  $r$  and therefore is rescaled relative to (3) and has energy dimension one)

$$\sigma(r) = m + c/r^2 + \dots, \quad (7.25)$$

where  $m$  and  $c$  are interpreted as the the quark mass and condensate respectively. We seek regular solutions that satisfy  $\dot{\sigma}(0) = 0$ . There is a single such solution for each value of  $\sigma(0)$  indicating that the condensate  $c$  is determined for a fixed asymptotic value of  $m$ . The solutions are shown in Figure 7.1.

Note that when the dynamical function  $\sigma(r)$  is included in the metric for the model there is no singularity since one cannot reach  $r + \sigma = b$ . The model therefore extends smoothly down to  $r = 0$ . We do not need to impose a hard IR cut off and the conformal symmetry breaking is expressed through the parameter  $b$  only.

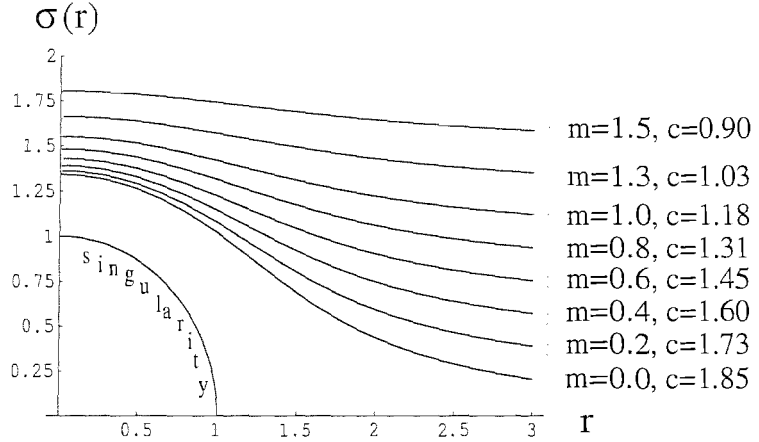


Figure 7.1: A plot of the embedding of the D7 brane as a function of the radial coordinate  $r$

### Matching the 5d Coupling

The matching occurs at the boundary  $r \rightarrow \infty$ , so the results are exactly the same as those for the pure AdS calculation, and we are led to the identification  $\hat{g}_5^2 = (12\pi^2)/N$ .

### Vector Mesons

We look for solutions to the vector equation of motion (7.6) that are of the form  $V_\mu^a(x, r) = V_\mu^a(r) \exp(iqx)$ . In the  $V_r^a(x, r) = 0$  gauge this gives the following equation of motion

$$\partial_r(K_1(r)\partial_r V_\mu^a(r)) + q^2 K_2(r)V_\mu^a(r) = 0, \quad (7.26)$$

with

$$K_1 = f^{1/2} h r^3 (1 + \dot{\sigma}^2)^{-1/2}, \quad K_2 = H f^{1-\delta/2} h^2 r^3 (1 + \dot{\sigma}^2)^{1/2}.$$

We will interpret the rho mesons as normalisable modes of this equation, with the eigenvalues corresponding to the squared rho masses  $m_\rho^2 = -q^2$ . For these modes to be

normalisable, we require that they vanish sufficiently rapidly as  $r \rightarrow \infty$ . We must also impose the gauge invariant boundary condition  $\psi'_\rho(0) = 0$  to ensure the smoothness of the solution.

The rho wavefunction  $\psi_\rho(r)$  is then a solution to (7.26) for an arbitrary component of  $V_\mu^a(r)$  subject to the boundary conditions  $\lim_{r \rightarrow \infty} \psi_\rho(r) = 0$  and  $\psi'_\rho(0) = 0$ . We solve the equation numerically to find the spectrum of rho masses.

For large  $N$ , one can write the vector current correlator as the sum over rho resonances

$$\Pi_V(-q^2) = - \sum_\rho \frac{F_\rho^2}{(q^2 - m_\rho^2)m_\rho^2}, \quad (7.27)$$

where  $F_\rho$  is the rho decay constant defined by  $\langle 0 | J_\mu^a | \rho^b \rangle = F_\rho \delta^{ab} \epsilon_\mu$ . In order to find  $F_\rho$ , we proceed by finding the Green's function solution to (7.26). Imposing the completeness relation

$$\sum_\rho K_2(r) \psi_\rho(r) \psi_\rho(r') = \delta(r - r') \quad (7.28)$$

on the set of eigenfunctions one finds

$$G(q; r, r') = \sum_\rho \frac{\psi_\rho(r) \psi_\rho(r')}{q^2 - m_\rho^2}. \quad (7.29)$$

Generalising (7.8) we have

$$\Pi_V(-q^2) = \left[ \frac{1}{\hat{g}_5^2 q^2} K_1(r) \partial_r v(q, r) \right]_{r=\infty}. \quad (7.30)$$

It can be shown that, in terms of the Green's function,  $v(q, r') = [K_1(r) \partial_r G(q; r, r')]_{r=\infty}$ .

From this, one finds

$$\Pi_V(-q^2) = - \frac{1}{\hat{g}_5^2} \lim_{r \rightarrow \infty} \sum_\rho \frac{(K_1(r) \psi'_\rho(r))^2}{(q^2 - m_\rho^2)m_\rho^2}. \quad (7.31)$$

Comparing this to (7.27) we can extract the rho decay constant

$$F_\rho^2 = \frac{1}{\hat{g}_5^2} \lim_{r \rightarrow \infty} (K_1(r)\psi_\rho'(r))^2. \quad (7.32)$$

### The Axial Sector

The action for the axial sector up to quadratic order is

$$S \sim \int d^4x dr e^\phi \sqrt{-g} \left( \frac{1}{2} \sigma^2 (\partial\pi - A)^2 - \frac{1}{4\hat{g}_5^2} \text{Tr} F_A^2 \right). \quad (7.33)$$

In the  $A_r(r, x) = 0$  gauge, letting  $A_i(r, x) = A_i^a(r, x) \exp(iqx) + \partial_i \phi^a$  the equations of motion are

$$\partial_r(K_1 \partial_r A_\mu^a) + q^2 K_2 A_\mu^a - \hat{g}_5^2 \sigma^2 K_3 A_\mu^a = 0, \quad (7.34)$$

$$\partial_r(K_1 \partial_r \phi^a) + \hat{g}_5^2 \sigma^2 K_3 (\pi^a - \phi^a) = 0, \quad (7.35)$$

$$-q_\pi^2 K_1 \partial_r \phi^a + \hat{g}_5^2 \sigma^2 K_4 \partial_r \pi^a = 0, \quad (7.36)$$

where  $K_1$  and  $K_2$  are the same as in (7.26), and  $K_3 = H f^{3/2 - \delta/2 + \Delta/2} h^3 r^3 (1 + \dot{\sigma}^2)^{-1/2}$ ,  $K_4 = f^{1+\Delta/2} h^2 r^3 (1 + \dot{\sigma}^2)^{-1/2}$ . The solutions to (7.34) represent the  $a_1$  spin 1 axial vector meson if we let  $\lim_{r \rightarrow \infty} \psi_{a_1}(r) = 0$ ,  $\partial_r \psi_{a_1}(0) = 0$ . We find the masses  $m_{a_1}^2 = -q^2$  by numerically finding the eigenvalues of this equation. The decay constant  $F_{a_1}$  is found in the same way as (7.32).

The pion can be found by solving (7.35) and (7.36) simultaneously subject to the boundary conditions  $\partial_r \phi(0) = 0$ ,  $\lim_{r \rightarrow \infty} \phi(r) = 0$  and  $\lim_{r \rightarrow \infty} \pi(r) = 0$ .

We find the pion decay constant by considering the axial current correlator.  $\langle 0 | A_\mu^a | \pi^b \rangle = i \delta^{ab} f_\pi q_\mu$ , so  $\Pi_A(-q^2)$  will have a pole at  $q^2 = m_\pi^2$ . In the limit  $m_\pi = 0$ ,  $\Pi_A(-q^2) \sim$

$-f_\pi^2/q^2$ . Using (7.8) we find

$$f_\pi^2 = \frac{1}{\hat{g}_5^2} [K_1(r)\partial_r a(0, r)]_{r=\infty}. \quad (7.37)$$

Alternatively, we could of course have used the Gell-Mann-Oakes-Renner relation

$$m_\pi^2 f_\pi^2 = 2mc \quad (7.38)$$

to find  $f_\pi$ . The two approaches are compared in Figure 7.2. We see that the two agree for small values of  $m_\pi$ , but then diverge for  $m_\pi \gtrsim 10(MeV)$ .

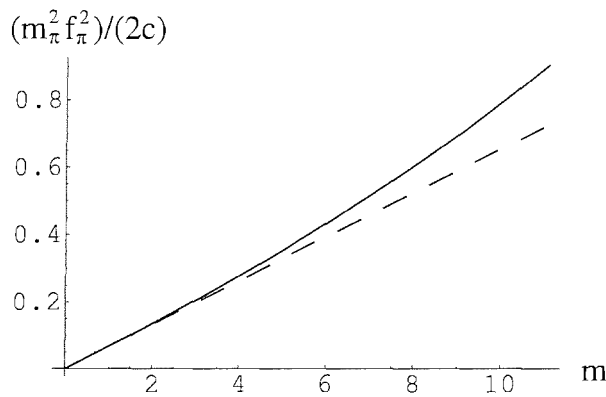


Figure 7.2: Plot of  $(m_\pi^2 f_\pi^2)/(2c)$  against  $m$ . For the Gell-Mann-Oakes-Renner relation to hold, this must be a straight line. As expected, the graph diverges from this straight line behaviour for large  $m$

### *The Coupling $g_{\rho\pi\pi}$*

The value of the  $g_{\rho\pi\pi}$  coupling can be read off from the expansion of  $|DU|^2$  in the action

$$S_{\rho\pi\pi} = \frac{1}{2} \int d^5x e^\phi \sqrt{-g} \sigma^2 \epsilon^{abc} V_\mu^a \partial^\mu \pi^b \pi^c. \quad (7.39)$$

Observable	Measured (MeV)	Model A (MeV)	AdS A (MeV)	Model B (MeV)	AdS B (MeV)
$m_\pi$	$139.6 \pm 0.0004$	$139.6^*$	$139.6^*$	$136.7$	$141$
$m_\rho$	$775.8 \pm 0.5$	$775.8^*$	$775.8^*$	$717.2$	$832$
$m_{a_1}$	$1230 \pm 40$	$1433$	$1363$	$1326$	$1220$
$f_\pi$	$92.4 \pm 0.35$	$102.5$	$92.4^*$	$96.1$	$84.0$
$F_\rho^{1/2}$	$345 \pm 8$	$324.2$	$329$	$299.6$	$353$
$F_{a_1}^{1/2}$	$433 \pm 13$	$504.4$	$486$	$464.0$	$440$
$g_{\rho\pi\pi}$	$6.03 \pm 0.07$	$4.23$	$4.48$	$4.24$	$5.29$

Table 7.1: Results for meson variables in the models discussed in the text. Model A is the new model in the paper with parameters fixed to the starred measurements. AdS A is the equivalent pure AdS model results with a hard IR cut off and the value of the condensate being fitted. Model B is a global fit in the new model and AdS B is the equivalent fit result in pure AdS.

The normalisation for  $\pi(r)$  is fixed by requiring that the pion kinetic term be canonically normalised.

Substituting the  $r$  variation of the fields from the equations of motion and integrating over  $r$  gives

$$g_{\rho\pi\pi} = \frac{1}{2} \hat{g}_5 \int dr \sigma^2(r) K_3(r) \pi(r)^2 \psi(r). \quad (7.40)$$

Note that it is entirely possible that the contribution to the coupling from an  $F^3$  term in the action not included in this model could be significant.

### 7.1.1 Results

The results of the model are displayed in Table 7.1. We compute 7 QCD meson parameters. Our model has two free parameters (after fixing  $g_5$  phenomenologically as discussed above),  $b$  corresponding roughly to the strong coupling scale  $\Lambda$  and  $m$  corresponding to the light quark mass. The model therefore has the same number of free parameters as real QCD.

In the first model,  $A$ , we match  $b$  and  $m$  by demanding that we correctly reproduce  $m_\pi$  and  $m_\rho$ . In order to do this, we must set  $\Lambda_b = 281.6(MeV)$  and  $m = 9.12(MeV)$ . This gives a prediction of  $522.7(MeV)$  for the scale of the quark condensate. The overall rms error for this model is 17.8%. For comparison we also reproduce the pure AdS fit to the same parameters found in [66]. That model has three free parameters, the value of the IR cut off, the quark mass and the quark condensate and is therefore less predictive.

In model B, we perform a global fit to all observables. This gives  $\Lambda_b = 260.0(MeV)$  and  $m = 9.48(MeV)$ , with the characteristic scale for the quark condensate  $475.9(MeV)$ . The overall rms error for this model is 15.8%. Again we reproduce the equivalent pure AdS model fit for comparison.

All global fits in these models are performed excluding the calculation of  $g_{\rho\pi\pi}$  as this is not reliable due to the lack of an  $F^3$  term in the model. The coupling is calculated in each model using the best fit parameters for the rest of the data.

It is again interesting to test how well determined the 5d gauge coupling  $g_5$  is by the phenomenological fit to the far UV expectation for  $\Pi_V$ . We therefore repeat the

fit with  $g_5$  allowed to vary. We use  $m$  and  $\Lambda$  to fix  $m_\pi$  and  $m_\rho$  to their experimental values, as these are the only two data that don't depend on  $g_5$ . We then vary  $g_5$  in order to minimise the overall rms error of the remaining parameters. The overall error for the optimum value of  $g_5$  is 16.1% for  $g_5 = 7.32$ . This is 17% greater than the value  $\sqrt{12\pi^2/N_c}$  from perturbative QCD. Note that in this model the preferred value for  $g_5$  is higher, whilst in the AdS model the fit came out lower.

### 7.1.2 Conclusions

We have adapted a string theoretic model of chiral symmetry breaking to a phenomenological description of QCD. The model we have proposed goes some way towards addressing the inconsistencies of simple AdS slice holographic QCD models [66, 67]. The background geometry of our model is non-supersymmetric, and it is the smooth variation of this geometry with the radial direction  $r$  that provides a mass gap, without the need for an artificial hard IR cut-off. In addition, the dual field to the quark mass/condensate operator is a natural part of the geometrical set-up with the value of the condensate being determined by the quark mass.

However, this is still a phenomenological approach in that we introduce extra fields and symmetries by hand into the model in order to describe the full pion and axial vector sectors. Formally there is no geometric string interpretation for this system. We also treat the background as though it describes an  $N = 3$  rather than an  $N = \infty$  field theory by matching the 5d gauge coupling to QCD.

We find that the predictions of this model match experimental results to within

16%. This model is a little more predictive than the pure AdS slice models since the condensate is dynamically determined by the geometry. The best fit is in fact a few percent worse than the AdS slice models but hopefully the theoretical improvements represent at least a moral victory. In any case one would naively have expected errors of order a few 100% in all of these models so the closeness to QCD across a range of holographic models supports the robustness of the approach.

A drawback of these models to date has been that the geometry returns to AdS for large  $r$ , meaning that the field theory is not asymptotically free in the UV. Incorrect physics in the UV will affect the strong coupling regime in the IR [84]. Here we investigated corrections to the matching of the 5d gauge coupling to naive perturbative QCD results. We found that this coupling's value should be changed at the 20% level indicating the size of non-perturbative effects. In the future one might hope to study the importance of higher dimension operators in the IR physics as well.

## 7.2 Glueballs in AdS/QCD

The AdS/QCD approach has been used to calculate the glueball spectrum [86]. In particular, in [86] the masses of the  $J^{++}$  glueballs were computed using either Dirichlet or Neumann boundary conditions on the IR brane. In both cases, the results compare favourably to lattice data. The Regge trajectory was also calculated and appears linear.

In this section, we calculate the spectrum of both the  $J^{++}$  and the  $J^{-+}$  glueballs. We assert that the source term  $\mathcal{O}(t, \mathbf{x})\phi(t, \mathbf{x}, r_0)$  is invariant under 5d parity transformations.  $\mathcal{O}(t, \mathbf{x})$  is an operator in the 4d field theory, and  $\phi(t, \mathbf{x}, r_0)$  is a 5d field evaluated at the boundary  $r = r_0$  which acts as a source for the 4d field theory operator. If  $\mathcal{O}(t, \mathbf{x})$  is odd under parity transformations,  $\mathcal{O}(t, \mathbf{x}) \rightarrow -\mathcal{O}(t, -\mathbf{x})$ , then we require that the source term also be odd  $\phi(t, \mathbf{x}, r_0) \rightarrow -\phi(t, -\mathbf{x}, -r_0)$ . The gravity duals of the  $J^{++}$  glueballs are even parity scalars, and the duals of the  $J^{-+}$  glueballs are odd parity scalars.

In section 7.2.1, we repeat the analysis of [86], but here we associate the parity of the solutions with the glueball parity.

One of the problems with the original AdS/QCD models was that the excitations of the vector mesons grew like  $M^2 \sim n^2$ . A simple flux tube argument [81] shows that this behaviour should in fact be  $M^2 \sim n$ . In [79] the hard IR cutoff was replaced and a non-constant dilaton added. It was shown that, by choosing the correct function for the dilaton, the correct  $n$  scaling of the resonances could be achieved.

In section 7.2.2, we calculate the glueball spectrum in this dilaton geometry. This geometry has the nice feature that a simple analytic formula for the glueball masses

can be derived which demonstrates the correct scaling of the masses with excitation number  $n$  and a linear Regge trajectory.

### 7.2.1 AdS/QCD Glueball Model

The dominant term in the Lagrangian for the glueballs of spin  $l$  is  $FD_{\{\mu_1} \dots D_{\mu_l\}}F$ . The dimension of this operator is  $d + l$ , where  $d$  is the dimension of spacetime. The dual AdS field to this operator is a scalar of mass  $m_l^2 = l(l + d)$ . In the AdS/QCD model, one studies this dual field in a  $d + 1$  dimensional AdS background with a hard IR cutoff

$$ds^2 = \frac{1}{z^2} \left( \sum_{i=0}^{d-1} dx_i^2 + dz^2 \right), \quad 0 < z \leq z_m. \quad (7.41)$$

Note that all coordinates have been scaled by the AdS radius  $R$  to make them dimensionless. The dual action for the glueballs is

$$S = \int d^{d+1}x \sqrt{g} \sum_l \left( \frac{1}{2} \partial_\mu \phi_l^+ \partial^\mu \phi_l^+ + \frac{1}{2} \partial_\mu \phi_l^- \partial^\mu \phi_l^- - m_l^2 \phi_l^{+2} - m_l^2 \phi_l^{-2} \right). \quad (7.42)$$

$(\phi_l^+, \phi_l^-)$  are the dual scalars to the glueballs of spin  $l$  and parity  $(+, -)$  respectively.

The equation of motion for one of these scalars is

$$\partial_\mu (\sqrt{g} g^{\mu\nu} \partial_\nu \phi) - m^2 \sqrt{g} \phi = 0. \quad (7.43)$$

We look for solutions of the form  $\phi(x, z) = f(z) \exp(ikx)$ . The mass squared of the glueball is then  $M^2 = -k^2$ . With this ansatz, parity  $\pm$  solutions are given by  $f(z) = \pm f(-z)$ . The equation of motion then becomes

$$z^2 \frac{d^2 f}{dz^2} + (1 - d)z \frac{df}{dz} + (M^2 z^2 - m^2) f = 0. \quad (7.44)$$

Rescaling the function  $f(z)$ :

$$f(z) = z^{d/2} g(z) \quad (7.45)$$

transforms this into a standard Bessel equation

$$z^2 \frac{d^2 g}{dz^2} + z \frac{dg}{dz} + (M^2 z^2 - \nu^2) g = 0 \quad (7.46)$$

with  $\nu^2 = (l + d/2)^2$ . The solutions to  $f$  are therefore

$$f(z) = \begin{cases} z^{d/2} \left( a \mathcal{J}_{l+\frac{d}{2}}(Mz) + b \mathcal{Y}_{l+\frac{d}{2}}(Mz) \right) & \text{if } (l + \frac{d}{2}) \in \mathbb{N}, \\ z^{d/2} \left( a \mathcal{J}_{l+\frac{d}{2}}(Mz) + b \mathcal{J}_{-l-\frac{d}{2}}(Mz) \right) & \text{otherwise.} \end{cases} \quad (7.47)$$

Here,  $a$  and  $b$  are arbitrary constants of integration. Using the asymptotic forms for the Bessel functions

$$\begin{aligned} \mathcal{J}_\nu(\epsilon) &= \frac{1}{\Gamma(\nu + 1)} \left( \frac{\epsilon}{2} \right)^\nu + \mathcal{O}(\epsilon^2), \\ \mathcal{Y}_\nu(\epsilon) &= -\frac{\Gamma(\nu)}{\pi} \left( \frac{\epsilon}{2} \right)^{-\nu} + \mathcal{O}(\epsilon^2), \end{aligned}$$

we can see that the two independent solutions scale like

$$f(z) \sim az^{l+d} + bz^{-l} \quad (7.48)$$

as  $z \rightarrow 0$ . We take the solution  $b = 0$  which corresponds to the value for  $\text{Tr}F^2$  in the field theory (as opposed to the solution  $a=0$  corresponding to the coupling of the  $\text{Tr}F^2$  operator).

The final solution is

$$f(z) = az^{d/2} \mathcal{J}_{l+\frac{d}{2}}(Mz). \quad (7.49)$$

In order to get a discrete mass spectrum, we impose a fixed IR cutoff at  $z = z_m$ . This breaks the conformal symmetry of the geometry. As the value of  $z_m$  is arbitrary, we identify even parity solutions, corresponding to the  $J^{++}$  glueballs, as those which obey Neumann boundary conditions on the IR brane. The odd parity solutions, corresponding to the  $J^{-+}$  glueballs, will be those which obey Dirichlet boundary conditions.

A Dirichlet boundary condition  $f(z_m) = 0$  gives

$$\mathcal{J}_{l+\frac{d}{2}}(Mz_m) = 0, \quad M_i = \frac{\chi_{l+\frac{d}{2},i}}{z_m}, \quad (7.50)$$

where  $\chi_{l+\frac{d}{2},i}$  are the Bessel function zeroes.

A Neumann boundary condition  $f'(z) = 0$  gives

$$Mz_m \mathcal{J}_{l+\frac{d}{2}-1}(Mz_m) - l \mathcal{J}_{l+\frac{d}{2}}(Mz_m) = 0. \quad (7.51)$$

The results for  $d = 4$  for the first three resonances up to spin 4 are shown in Table 7.2, and a comparison to lattice data made in Table 7.3. The results give a total rms error of 12.9%.

### 7.2.2 Dilaton Geometry

In [79] the metric is AdS<sub>5</sub>,

$$ds^2 = \frac{1}{z^2} \left( \sum_{i=0}^{d-1} dx_i^2 + dz^2 \right), \quad 0 < z < \infty, \quad (7.52)$$

but instead of a hard IR cut-off, there is a non-constant dilaton<sup>1</sup>

$$e^\Phi = e^{-cz^2}, \quad (7.53)$$

---

<sup>1</sup>Note that in [79], the sign of  $cz^2$  was positive. Although both signs give the same Schrödinger potential, it was argued that for negative  $cz^2$  there was a massless solution for the rho meson.

where  $c$  is an arbitrary constant which sets the scale of the conformal symmetry breaking which we will set to 1 for convenience - note that all masses will implicitly be in units of this energy scale.

The inclusion of this non-constant dilaton gives the correct  $M^2 \sim n$  scaling of the meson resonances. We will now investigate the glueball spectrum in this geometry.

The equation of motion for a scalar in this background is

$$\partial_\mu (e^{-\Phi} \sqrt{g} g^{\mu\nu} \partial_\nu \phi) - m^2 e^{-\Phi} \sqrt{g} \phi = 0. \quad (7.54)$$

As in section 7.2.1, we look for solutions of the form  $\phi(x, z) = f(z) \exp(ikx)$ .

$$\frac{d^2 f}{dz^2} + [(1-d)z^{-1} + z] \frac{df}{dz} + (M^2 - m^2 z^{-2}) f = 0. \quad (7.55)$$

We can bring this equation into Schrödinger form by rescaling the function  $f(z)$ :

$$f(z) = z^{\frac{1}{2}(d-1)} e^{-\frac{1}{2}z^2} g(z). \quad (7.56)$$

The equation of motion then becomes

$$-\frac{d^2 g}{dz^2} + \left[ z^2 + \frac{m^2 - 1/4}{z^2} \right] g = E g, \quad (7.57)$$

where we have defined  $m = (l + d/2)$  and  $E = M^2 + (d - 2)$ . The solution to this equation which  $\sim z^{l+d}$  as  $z \rightarrow 0$  is

$$g(z) = a e^{-\frac{1}{2}z^2} z^{m+1/2} L_n^m(z^2), \quad (7.58)$$

which gives

$$f(z) = a e^{-z^2} z^{l+d} L_n^m(z^2), \quad (7.59)$$

where  $L_n^m$  are the associated Laguerre polynomials. The eigenvalues of this system are

$$E = 4n + 2m + 2. \quad (7.60)$$

The function  $f(z)$  is an even function for all values of  $n$  and therefore, according to our prescription must correspond to the  $J^{++}$  glueballs. The masses can be read from (7.60) as

$$M^2 = 4n + 2l + 4. \quad (7.61)$$

The error on the two predicted masses compared to lattice data is slightly larger than the pure AdS model at around 13.4%. However, this model does have some interesting properties:

- The mass spectrum is given by an extremely simple analytic formula
- The masses scale as  $\sqrt{n}$  as is predicted from a simple flux tube argument
- The Regge trajectory is linear

Rearranging (7.61) for  $n = 0$  we can read off the Regge parameters

$$l = -2 + \frac{1}{2c}M^2, \quad (7.62)$$

where we have reinstated the parameter  $c$ . This gives a string tension of  $\alpha' = 1/(2c)$ , and  $\alpha_0 = -2$ . This value of  $\alpha_0$  is much too low for the glueball to play the role of a pomeron. This agrees with a recent lattice study [87] for (2+1) dimensional glueballs where a negative value of  $\alpha_0$  was also found.

Interestingly, if we arbitrarily decide to identify the even  $n$  solutions with the even parity  $J^{++}$  glueballs and the odd  $n$  solutions with the odd parity  $J^{-+}$  glueballs, the

fit to lattice data is extremely good with an overall rms error of less than 4% (see table 7.7). It is possible that some higher order effects may cause the even(odd)  $n$  solutions to have even(odd) parity. For example, one can imagine that including the effects of some higher dimensional operator in the spirit of Chapter 5 would leave us with a modified metric of the form

$$ds^2 = \frac{1}{z^2} \left( h(z)^{-1/2} \sum_{i=0}^{d-1} dx_i^2 + h(z)^{1/2} dz^2 \right), \quad 0 < z < \infty, \quad (7.63)$$

where for instance  $h(z) = (1 + \epsilon z^\gamma + \dots)$ . It turns out that the solution to the scalar equation of motion with this modified metric takes the form

$$f(z) = a e^{-z^2} z^{l+d} L_n^m(z^2 + \epsilon(\gamma + 1)^{-1} z^\gamma) + \epsilon q(z) + \mathcal{O}(\epsilon^2) \quad (7.64)$$

for some function  $q(z)$ . Our parity arguments tell us that the  $J^{++}$  glueballs should be even around  $r = 0$  ( $r=1/z$ ). For large  $x$   $L_n^m(x) \sim (-1)^n \frac{1}{n!} x^n$ , so if  $\gamma$  is odd then it is plausible that the solutions for even  $n$  have even parity, and the solutions for odd  $n$  have odd parity. This argument is, however, speculative and it would be interesting to investigate this model further.

### 7.2.3 Conclusions

We have demonstrated that the spectrum of  $J^{P+}$  glueballs can be successfully calculated by solving a gravitational dual theory of scalars in AdS and identifying the parity of the glueballs with the parity of the scalars under a change in the radial coordinate  $r \rightarrow -r$ . The error for this model was 13% when compared to lattice data.

If we modify the geometry by adding a non-constant dilaton, an extremely simple

analytic formula for the glueball masses can be derived which predicts a linear Regge trajectory and gives the correct  $M^2 \sim n$  scaling of the resonances. This model, however, only predicts the  $J^{++}$  glueballs and give a similar error to the pure AdS model of around 13%. We showed, however, that it may be possible to modify this model slightly in such a way that the masses of both the  $J^{++}$  and the  $J^{-+}$  glueballs could be derived to within 4% of lattice data.

state	mass	state	mass
$0^{++}$	1.00	$0^{-+}$	1.34
$0^{*++}$	1.83	$0^{*-+}$	2.20
$0^{**++}$	2.66	$0^{***-+}$	3.03
$1^{++}$	1.28	$1^{-+}$	1.67
$1^{*++}$	2.16	$1^{*-+}$	2.55
$1^{**++}$	3.01	$1^{***-+}$	3.40
$2^{++}$	1.56	$2^{-+}$	1.98
$2^{*++}$	2.49	$2^{*-+}$	2.89
$2^{**++}$	3.35	$2^{***-+}$	3.75
$3^{++}$	1.84	$3^{-+}$	2.29
$3^{*++}$	2.81	$3^{*-+}$	3.22
$3^{**++}$	3.69	$3^{***-+}$	4.09
$4^{++}$	2.11	$4^{-+}$	2.59
$4^{*++}$	3.12	$4^{*-+}$	3.55
$4^{**++}$	4.02	$4^{***-+}$	4.44

Table 7.2: 4d glueball masses from simple AdS slice model. All masses are normalised to  $m(0^{++})$ .

State	AdS	$N_c = 3$ Lattice
$m(0^{++})$	1.00*	1.00*
$m(0^{*++})$	1.83	1.74(11)
$m(2^{++})$	1.56	1.39(4)
$m(0^{-+})$	1.34	1.50(4)
$m(0^{*-+})$	2.55	2.11(6)
$m(2^{-+})$	1.98	1.79(5)

Table 7.3: 4d glueball masses from AdS slice compared to  $N_c = 3$  lattice data [64]. All masses are normalised to  $m(0^{++})$ . The total rms error is 12.9%

state	mass
$0^{++}$	1.00
$0^{*++}$	1.34
$0^{***++}$	1.83
$1^{++}$	1.28
$1^{*++}$	1.67
$1^{***++}$	2.16
$2^{++}$	1.56
$2^{*++}$	1.98
$2^{***++}$	2.49
$3^{++}$	1.84
$3^{*++}$	2.29
$3^{***++}$	2.81
$4^{++}$	2.11
$4^{*++}$	2.59
$4^{***++}$	3.12

Table 7.4: 4d glueball masses from AdS plus dilaton geometry. All masses are normalised to  $m(0^{++})$

State	AdS	$N_c = 3$ Lattice
$m(0^{++})$	1.00*	1.00*
$m(0^{*++})$	1.41	1.74(11)
$m(2^{++})$	1.41	1.39(4)

Table 7.5: 4d glueball masses from AdS plus dilaton geometry compared to  $N_c = 3$  lattice data [64]. All masses are normalised to  $m(0^{++})$ . The total rms error is 13.4%

state	mass	state	mass
$0^{++}$	1.00	$0^{-+}$	1.34
$0^{*++}$	1.83	$0^{*-+}$	2.20
$0^{**++}$	2.66	$0^{**-+}$	3.03
$1^{++}$	1.28	$1^{-+}$	1.67
$1^{*++}$	2.16	$1^{*-+}$	2.55
$1^{**++}$	3.01	$1^{**-+}$	3.40
$2^{++}$	1.56	$2^{-+}$	1.98
$2^{*++}$	2.49	$2^{*-+}$	2.89
$2^{**++}$	3.35	$2^{**-+}$	3.75
$3^{++}$	1.84	$3^{-+}$	2.29
$3^{*++}$	2.81	$3^{*-+}$	3.22
$3^{**++}$	3.69	$3^{**-+}$	4.09
$4^{++}$	2.11	$4^{-+}$	2.59
$4^{*++}$	3.12	$4^{*-+}$	3.55
$4^{**++}$	4.02	$4^{**-+}$	4.44

Table 7.6: 4d glueball masses from AdS plus dilaton geometry, identifying even(odd) parity solutions with even(odd) values of  $n$ . All masses are normalised to  $m(0^{++})$

State	AdS	$N_c = 3$ Lattice
$m(0^{++})$	1.00*	1.00*
$m(0^{*++})$	1.73	1.74(11)
$m(2^{++})$	1.41	1.39(4)
$m(0^{-+})$	1.41	1.50(4)
$m(0^{*-+})$	2.00	2.11(6)
$m(2^{-+})$	1.73	1.79(5)

Table 7.7: 4d glueball masses from AdS plus dilaton geometry, identifying even(odd) parity solutions with even(odd) values of  $n$ , compared to  $N_c = 3$  lattice data [64]. All masses are normalised to  $m(0^{++})$ . The total rms error is 3.9%

# Chapter 8

## Conclusions

We have provided many examples of the usefulness of the AdS/CFT correspondence as a tool for studying non-perturbative aspects of QCD-like theories. We have also demonstrated ways of modifying the correspondence in order to get closer to a dual theory of QCD.

In Chapter 4 we studied a dual geometry which went from  $\mathcal{N} = 4$  supersymmetric Yang-Mills in the UV region and was broken down to an  $\mathcal{N} = 1$  theory through the inclusion of a mass term. We were able to demonstrate an explicit matching between the field theory and its gravity dual at fixed points along a particular renormalisation group flow off of moduli space.

In Chapter 5 we were able to find a pleasing geometric picture of chiral symmetry breaking and produced a simple test to determine whether a supergravity theory would exhibit chiral symmetry breaking in its dual field theory. Out of the geometries that we tested, only geometries that were non-supersymmetric in the IR with a running dilaton

passed the chiral symmetry breaking test.

A major downside to supergravity duals of QCD-like theories is that they all flow to the conformal  $\mathcal{N} = 4$  SYM at high energy. In QCD, the theory flows to a non-interacting fixed point as the energy goes to infinity. Even if properties of the dual theory are similar to QCD in the IR limit, the fact that the UV of the two theories is different will affect IR predictions through loop effects.

In Chapter 6 we demonstrated a systematic way of removing these unwanted effects by introducing a hard UV cut-off into the dual theory and tuning the coefficients of higher dimensional operators much like the improved action techniques of lattice QCD. We applied this technique to calculating the glueball spectrum in finite temperature  $\text{QCD}_4$ . The results showed a marked improvement over the original AdS/CFT calculations.

Finally, in Chapter 7 we introduced the AdS/QCD bottom-up approach to finding a dual QCD gravity theory. Using this phenomenological approach we were able to calculate meson data to within 18% of experimental data and glueball masses to within 14% of lattice data. It would be interesting to combine the improved action ideas of Chapter 5 within the AdS/QCD framework to see if an even better dual theory of QCD could be achieved.

# Appendices

## A: Calculating the Schrödindger Potential

In this appendix we will demonstrate how to transform a second order eigenvalue equation

$$\mathcal{L}f = \lambda f \quad (\text{A.1})$$

into Schrödinger form

$$-\frac{d^2f}{dx^2} + Vf = \lambda f \quad (\text{A.2})$$

in the special case that the operator  $\mathcal{L}$  is in self-adjoint form

$$\mathcal{L}(x) = -\frac{d}{dx} \left( p(x) \frac{d}{dx} \right) + q(x). \quad (\text{A.3})$$

First, we make a change of variables  $x \rightarrow z$ , where

$$z(x) = \int^x dx' p(x')^{-\frac{1}{2}}. \quad (\text{A.4})$$

Using this change of variables, the equation (A.1) becomes

$$-\frac{d^2f}{dz^2} - \frac{1}{2p} \frac{dp}{dz} \frac{df}{dz} + qf = \lambda f. \quad (\text{A.5})$$

Now, we let  $f(z) = h(z)g(z)$ . Assuming  $h(z) \neq 0$ , this gives an equation in terms of  $g$ :

$$-g'' - \left(2h^{-1}h' + \frac{1}{2}p^{-1}p'\right)g' + \left(-h^{-1}h'' - \frac{1}{2}p^{-1}p'h^{-1}h' + q\right)g = \lambda g, \quad (\text{A.6})$$

where ' indicates differentiation with respect to  $z$ . In order to get this equation into Schrödinger form, we must choose the function  $h$  so that

$$2h^{-1}h' + \frac{1}{2}p^{-1}p' = 0. \quad (\text{A.7})$$

This implies that

$$h = p^{-\frac{1}{4}} \quad (\text{A.8})$$

giving the Schrödinger potential

$$V(z) = \frac{1}{4}p(z)^{-1}\frac{d^2p}{dz^2} - \frac{3}{16}p^{-2}(z)\left(\frac{dp}{dz}\right)^2 + q(z), \quad (\text{A.9})$$

or, in terms of  $x$

$$V(x) = \frac{1}{4}\frac{d^2p}{dx^2} - \frac{1}{16}p(x)^{-1}\left(\frac{dp}{dx}\right)^2 + q(x). \quad (\text{A.10})$$

A slight variation of this problem is finding the Schrödinger potential of the equation

$$\mathcal{L}(y)f(y) = \lambda s(y)f(y) \quad (\text{A.11})$$

This can be brought into self-adjoint form by letting

$$\begin{aligned} x(y) &= \int^y dy' s(y'), \\ \tilde{p} &= sp, \\ \tilde{q} &= q/s. \end{aligned} \quad (\text{A.12})$$

This means that the equation can be brought into Schrödinger form with a change of variables  $y \rightarrow z$

$$z(y) = \int^y dy' \left( s(y')/p(y') \right)^{\frac{1}{2}} \quad (\text{A.13})$$

and a scaling  $f(z) = h(z)g(z)$ , where

$$h = \tilde{p}^{-\frac{1}{4}} = (ps)^{-\frac{1}{4}}. \quad (\text{A.14})$$

The potential in terms of  $y$  is

$$V(y) = \frac{1}{4}s(y)^{-2} \frac{d^2\tilde{p}}{dy^2} - \frac{1}{4}s(y)^{-3} \frac{ds}{dy} \frac{d\tilde{p}}{dy} - \frac{1}{16}s(y)^{-2}\tilde{p}(y)^{-1} \left( \frac{d\tilde{p}}{dy} \right)^2 + \tilde{q}(y). \quad (\text{A.15})$$

## B: Expanding the D-Brane Action

The action for a Dp-brane in the string frame is

$$S = -T_p \int d^{p+1}\xi e^{-\Phi} [-\det (\mathbf{P}[G]_{ab} + 2\pi\alpha' F_{ab})]^{1/2}, \quad (\text{B.1})$$

where  $\xi^a, a = 0, \dots, p$  are coordinates on the brane. The fields on the brane are the embedding  $X^m(\xi), m = 0, \dots, D-1$  and the gauge fields  $A_a(\xi)$ .  $\mathbf{P}[G]_{ab}$  is the pullback of the background metric on the Dp-brane

$$\mathbf{P}[G]_{ab}(\xi) = \frac{\partial X^m}{\partial \xi^a} \frac{\partial X^n}{\partial \xi^b} G_{mn}(X(\xi)). \quad (\text{B.2})$$

Let  $X^8, X^9$  be the two directions transverse to the brane and choose coordinates  $\xi^a$  to be aligned along the directions  $X^a$ . With these choices, the pullback can be written as

$$\mathbf{P}[G]_{ab} = G_{ab} + G_{ij} \partial_a X^i \partial_b X^j. \quad (\text{B.3})$$

Now, if the metric  $G_{ij}$  is diagonal  $G_{ij} = G\delta_{ij}$  then we may write

$$X = X^8 + iX^9 \quad (\text{B.4})$$

and

$$\mathbf{P}[G]_{ab} = G_{ab} + G \partial_a X \partial_b X^\dagger. \quad (\text{B.5})$$

Let  $X(\xi) = \sigma(r)U(\xi)$ . We can assume that  $\partial U$  and  $\partial A$  will be small. We will now expand the action up to order  $(\partial U)^2, (\partial A)^2, \partial U \partial A$ .

We have

$$\begin{aligned} \mathbf{P}[G]_{ab} + 2\pi\alpha' F_{ab} &= G_{ab} + G \partial_a X \partial_b X^\dagger + 2\pi\alpha' F_{ab}, \\ &= G_{ac} \left[ \delta^c_b + G \partial^c X \partial_b X^\dagger + 2\pi\alpha' F^c_b \right]. \end{aligned} \quad (\text{B.6})$$

The second term inside the brackets can be re-written in terms of  $\sigma$  and  $U$

$$\begin{aligned}
G\partial_a X \partial_b X^\dagger &= G \begin{pmatrix} \partial^r X \partial_r X^\dagger & \partial^r X \partial_\nu X^\dagger \\ \partial^\mu X \partial_r X^\dagger & \partial^\mu X \partial_\nu X^\dagger \end{pmatrix}, \\
&= G \begin{pmatrix} \partial^r \sigma \partial_r \sigma & 0 \\ 0 & 0 \end{pmatrix} + G\sigma \begin{pmatrix} 0 & \partial^r \sigma U \partial_\nu U \\ \partial_r \sigma U \partial^\mu U & 0 \end{pmatrix} + G\sigma^2 \partial^a U \partial_b U^\dagger,
\end{aligned} \tag{B.7}$$

where  $\mu = \{\xi\} - r$ . Using this we can now write

$$\det(\mathbf{P}[G]_{ab} + 2\pi\alpha' F_{ab}) = \det(G_{ab}) \det(A + B + C + D), \tag{B.8}$$

where

$$\begin{aligned}
A &= \begin{pmatrix} (1 + G\partial^r \sigma \partial_r \sigma) & 0 \\ 0 & 1 \end{pmatrix}, \quad B = G\sigma \begin{pmatrix} 0 & \partial^r \sigma U \partial_\nu U \\ \partial_r \sigma U \partial^\mu U & 0 \end{pmatrix}, \\
C &= G\sigma^2 \begin{pmatrix} \partial^r U \partial_r U^\dagger & \partial^r U \partial_\nu U^\dagger \\ \partial^\mu U \partial_r U^\dagger & \partial^\mu U \partial_\nu U^\dagger \end{pmatrix}, \quad D = 2\pi\alpha' \begin{pmatrix} 0 & F_\nu^r \\ F_r^\mu & F_\nu^\mu \end{pmatrix}.
\end{aligned} \tag{B.9}$$

Now

$$\begin{aligned}
\det(A + B + C + D) &= \det(A) \det(1 + A^{-1}B + A^{-1}C + A^{-1}D), \\
&= (1 + G\partial^r \sigma \partial_r \sigma) \det(1 + \tilde{B} + \tilde{C} + \tilde{D}),
\end{aligned} \tag{B.10}$$

where

$$\begin{aligned}
\tilde{B} &= G\sigma \begin{pmatrix} 0 & (1 + G\partial^r\sigma\partial_r\sigma)^{-1}\partial^r\sigma U\partial_\nu U^\dagger \\ \partial_r\sigma U^\dagger\partial^\mu U & 0 \end{pmatrix}, \\
\tilde{C} &= G\sigma^2 \begin{pmatrix} (1 + G\partial^r\sigma\partial_r\sigma)^{-1}\partial^r U\partial_r U^\dagger & (1 + G\partial^r\sigma\partial_r\sigma)^{-1}\partial^r U\partial_\nu U^\dagger \\ \partial^\mu U\partial_r U^\dagger & \partial^\mu U\partial_\nu U^\dagger \end{pmatrix}, \\
\tilde{D} &= 2\pi\alpha' \begin{pmatrix} 0 & (1 + G\partial^r\sigma\partial_r\sigma)^{-1}F_\nu^r \\ F_r^\mu & F_\nu^\mu \end{pmatrix}. \tag{B.11}
\end{aligned}$$

This is now in a form that can be expanded using

$$\begin{aligned}
[\det(1 + X)]^{1/2} &= \exp \left[ \frac{1}{2} \text{Tr} \ln(1 + x) \right], \\
&= \exp \left[ \frac{1}{2} \text{Tr} \left( X - \frac{1}{2}X^2 + \dots \right) \right], \\
&= 1 + \frac{1}{2} \text{Tr} X - \frac{1}{4} \text{Tr} X^2 + \mathcal{O}(X^3). \tag{B.12}
\end{aligned}$$

This gives

$$\begin{aligned}
[-\det(\mathbf{P}[G]_{ab} + 2\pi\alpha' F_{ab})]^{1/2} &= [-\det(G_{ab})]^{1/2} (1 + GG^{rr}\dot{\sigma}^2)^{1/2} \\
&\times \left\{ 1 + \frac{1}{2} \text{Tr}(\tilde{B} + \tilde{C} + \tilde{D}) - \frac{1}{4} \text{Tr}(\tilde{B} + \tilde{C} + \tilde{D})^2 + \dots \right\}, \tag{B.13}
\end{aligned}$$

where we have defined  $\dot{\sigma} \equiv \partial_r\sigma$ . Note that  $\tilde{B} \sim \partial U$ ,  $\tilde{C} \sim (\partial U)^2$  and  $\tilde{D} \sim \partial A$  so we only need to keep the terms linear in  $\tilde{C}$  and quadratic in  $\tilde{B}$  and  $\tilde{D}$ . Also note that  $\text{Tr}\tilde{B} = \text{Tr}\tilde{D} = 0$ .

Using (B.11) the action becomes

$$\begin{aligned}
S = & -T_p \int d^p \xi e^{-\Phi} [-\det(G_{ab})]^{1/2} (1 + GG^{rr} \dot{\sigma}^2)^{1/2} \\
& \times \left\{ 1 + \frac{1}{2} G \sigma^2 (1 + GG^{rr} \dot{\sigma}^2)^{-1} \partial^a U \partial_a U^\dagger \right. \\
& \left. - \frac{1}{4} (2\pi\alpha')^2 [(1 + GG^{rr} \dot{\sigma}^2)^{-1} F_{r\mu} F^{r\mu} + F_{\mu\nu} F^{\mu\nu}] \right\}. \quad (\text{B.14})
\end{aligned}$$

Define the *Einstein frame* metric,  $g$ , and dilaton,  $\phi$ , as

$$g_{ab} = e^{-\phi/2} G_{ab}, \quad \phi = \Phi - \Phi_0 \quad (\text{B.15})$$

and let the effective string tension in the presence of a constant background dilaton field  $\Phi_0$  be

$$\tau_p = T_p e^{-\Phi_0} \quad (\text{B.16})$$

then the action in the Einstein frame is

$$\begin{aligned}
S = & -\tau_p \int d^p \xi e^\phi [-\det(g_{ab})]^{1/2} (1 + gg^{rr} \dot{\sigma}^2)^{1/2} \\
& \times \left\{ 1 + \frac{1}{2} g \sigma^2 (1 + gg^{rr} \dot{\sigma}^2)^{-1} \partial^a U \partial_a U^\dagger \right. \\
& \left. - \frac{1}{4} (2\pi\alpha')^2 e^{-\phi} [(1 + gg^{rr} \dot{\sigma}^2)^{-1} F_{r\mu} F^{r\mu} + F_{\mu\nu} F^{\mu\nu}] \right\}. \quad (\text{B.17})
\end{aligned}$$

# Bibliography

- [1] R. P. Feynman, “QED. The Strange Theory Of Light And Matter,” <http://www.slac.stanford.edu/spires/find/hep/www?irn=1631209>
- [2] A. Hocker, “The hadronic contribution to  $(g-2)(\mu)$ ,” arXiv:hep-ph/0410081.
- [3] G. W. Bennett *et al.* [Muon g-2 Collaboration], “Measurement of the negative muon anomalous magnetic moment to 0.7-ppm,” Phys. Rev. Lett. **92** (2004) 161802 [arXiv:hep-ex/0401008].
- [4] S. Weinberg, *The Quantum Theory of Fields, Vol. 1,2*, Cambridge University Press (1995)
- [5] P. W. Higgs, “Broken Symmetries and the Masses of the Gauge Bosons,” Phys. Rev. Lett. **13** (1964) 508.
- [6] S. Eidelman *et al.* [Particle Data Group], “Review of particle physics,” Phys. Lett. B **592** (2004) 1.
- [7] S. P. Martin, “A supersymmetry primer,” arXiv:hep-ph/9709356.

[8] J. B. Kogut, “A Review Of The Lattice Gauge Theory Approach To Quantum Chromodynamics,” *Rev. Mod. Phys.* **55** (1983) 775.

[9] J. Polchinski, *String Theory, Vol. 1,2*, Cambridge University Press (1998)

[10] M. B. Green, J. H. Schwartz and E. Witten, *Superstring theory, Vol. 1,2*, Cambridge University Press (1987)

[11] J. D. Lykken, “Introduction to supersymmetry,” arXiv:hep-th/9612114.

[12] S. R. Coleman and J. Mandula, “All Possible Symmetries of the S Matrix,” *Phys. Rev.* **159** (1967) 1251.

[13] <http://lhc.web.cern.ch/lhc/>

[14] J. M. Maldacena, “The large N limit of superconformal field theories and supergravity,” *Adv. Theor. Math. Phys.* **2** (1998) 231 [*Int. J. Theor. Phys.* **38** (1999) 1113] [arXiv:hep-th/9711200].

[15] M. E. Peskin and D. V. Schroeder, *An Introduction to Quantum Field Theory*, Reading, USA: Addison-Wesley (1995).

[16] D. J. Gross and F. Wilczek, “Asymptotically Free Gauge Theories. 1,” *Phys. Rev. D* **8** (1973) 3633.

[17] H. D. Politzer, *Phys. Rev. Lett.* **26** (1973) 1346.

[18] Y. Nambu and G. Jona-Lasinio, “Dynamical model of elementary particles based on an analogy with superconductivity. I,” *Phys. Rev.* **122** (1961) 345.

[19] K. Fujikawa, “Path Integral For Gauge Theories With Fermions,” *Phys. Rev. D* **21** (1980) 2848 [Erratum-*ibid. D* **22** (1980) 1499].

[20] G. ’t Hooft, “A Planar Diagram Theory for Strong Interactions,” *Nucl. Phys. B* **72** (1974) 461.

[21] E. Witten, “String theory dynamics in various dimensions,” *Nucl. Phys. B* **443** (1995) 85 [[arXiv:hep-th/9503124](https://arxiv.org/abs/hep-th/9503124)].

[22] C. V. Johnson, “D-brane primer,” [arXiv:hep-th/0007170](https://arxiv.org/abs/hep-th/0007170).

[23] J. Polchinski, “Dirichlet-Branes and Ramond-Ramond Charges,” *Phys. Rev. Lett.* **75** (1995) 4724 [[arXiv:hep-th/9510017](https://arxiv.org/abs/hep-th/9510017)].

[24] I. R. Klebanov, “From threebranes to large N gauge theories,” [arXiv:hep-th/9901018](https://arxiv.org/abs/hep-th/9901018).

[25] J. H. Schwarz, “Introduction to M theory and AdS/CFT duality,” [arXiv:hep-th/9812037](https://arxiv.org/abs/hep-th/9812037).

[26] L. Susskind and E. Witten, “The holographic bound in anti-de Sitter space,” [arXiv:hep-th/9805114](https://arxiv.org/abs/hep-th/9805114).

[27] E. Witten, “Anti-de Sitter space, thermal phase transition, and confinement in gauge theories,” *Adv. Theor. Math. Phys.* **2** (1998) 505 [[arXiv:hep-th/9803131](https://arxiv.org/abs/hep-th/9803131)].

[28] L. Girardello, M. Petrini, M. Petrini, M. Petrini and A. Zaffaroni, “Novel local CFT and exact results on perturbations of  $N = 4$  super Yang-Mills from AdS dynamics,” *JHEP* **9812** (1998) 022 [[arXiv:hep-th/9810126](https://arxiv.org/abs/hep-th/9810126)].

[29] L. Girardello, M. Petrini, M. Petrati and A. Zaffaroni, “The supergravity dual of  $N = 1$  super Yang-Mills theory,” *Nucl. Phys. B* **569** (2000) 451 [arXiv:hep-th/9909047].

[30] D. Z. Freedman, S. S. Gubser, K. Pilch and N. P. Warner, “Continuous distributions of D3-branes and gauged supergravity,” *JHEP* **0007** (2000) 038 [arXiv:hep-th/9906194].

[31] A. Karch and E. Katz, “Adding flavor to AdS/CFT,” *JHEP* **0206** (2002) 043 [arXiv:hep-th/0205236].

[32] J. L. Petersen, “Introduction to the Maldacena conjecture on AdS/CFT,” *Int. J. Mod. Phys. A* **14** (1999) 3597 [arXiv:hep-th/9902131].

[33] S. S. Gubser, I. R. Klebanov and A. M. Polyakov, “Gauge theory correlators from non-critical string theory,” *Phys. Lett. B* **428** (1998) 105 [arXiv:hep-th/9802109].

[34] E. Witten, “Anti-de Sitter space and holography,” *Adv. Theor. Math. Phys.* **2** (1998) 253 [arXiv:hep-th/9802150].

[35] R. G. Leigh and M. J. Strassler, “Exactly Marginal Operators And Duality In Four-Dimensional  $N=1$  Supersymmetric Gauge Theory,” *Nucl. Phys. B* **447** (1995) 95 [arXiv:hep-th/9503121].

[36] C. V. Johnson, K. J. Lovis and D. C. Page, “Probing some  $N = 1$  AdS/CFT RG flows,” *JHEP* **0105** (2001) 036 [arXiv:hep-th/0011166].

[37] C. V. Johnson, K. J. Lovis and D. C. Page, “The Kaehler structure of supersymmetric holographic RG flows,” *JHEP* **0110** (2001) 014 [[arXiv:hep-th/0107261](https://arxiv.org/abs/hep-th/0107261)].

[38] N. Evans, T. R. Morris and O. J. Rosten, “Gauge invariant regularization in the AdS/CFT correspondence and ghost D-branes,” *Phys. Lett. B* **635** (2006) 148 [[arXiv:hep-th/0601114](https://arxiv.org/abs/hep-th/0601114)].

[39] J. Babington, D. E. Crooks and N. J. Evans, “A non-supersymmetric deformation of the AdS/CFT correspondence,” *JHEP* **0302** (2003) 024 [[arXiv:hep-th/0207076](https://arxiv.org/abs/hep-th/0207076)].

[40] K. Pilch and N. P. Warner, “ $N = 2$  supersymmetric RG flows and the IIB dilaton,” *Nucl. Phys. B* **594** (2001) 209 [[arXiv:hep-th/0004063](https://arxiv.org/abs/hep-th/0004063)].

[41] N. J. Evans, C. V. Johnson and M. Petrini, “The enhancon and  $N = 2$  gauge theory/gravity RG flows,” *JHEP* **0010** (2000) 022 [[arXiv:hep-th/0008081](https://arxiv.org/abs/hep-th/0008081)].

[42] A. Buchel, A. W. Peet and J. Polchinski, “Gauge dual and noncommutative extension of an  $N = 2$  supergravity solution,” *Phys. Rev. D* **63** (2001) 044009 [[arXiv:hep-th/0008076](https://arxiv.org/abs/hep-th/0008076)].

[43] J. Babington, D. E. Crooks and N. J. Evans, “A stable supergravity dual of non-supersymmetric glue,” *Phys. Rev. D* **67** (2003) 066007 [[arXiv:hep-th/0210068](https://arxiv.org/abs/hep-th/0210068)].

[44] M. Gunaydin, L. J. Romans, and N. P. Warner, “Gauged  $N = 8$  supergravity in five-dimensions,” *Phys. Lett. B* **154** (1985) 268.

[45] M. Gunaydin, L. J. Romans, and N. P. Warner, “Compact and noncompact gauged supergravity theories in five-dimensions,” *Nucl. Phys. B* **272** (1986) 598.

[46] L. Girardello, M. Petrini, M. Petrini and A. Zaffaroni, “Confinement and Condensates Without Fine Tuning in Supergravity Duals of Gauge Theories,” *JHEP* **9905** (1999) 026 [hep-th/9903026](#).

[47] J. Babington, N. J. Evans and J. Hockings, “Secrets of the metric in  $N = 4$  and  $N = 2^*$  geometries,” *JHEP* **0107** (2001) 034 [[arXiv:hep-th/0105235](#)].

[48] N. J. Evans and J. P. Shock, “Chiral dynamics from AdS space,” *Phys. Rev. D* **70** (2004) 046002 [[arXiv:hep-th/0403279](#)].

[49] J. Babington, J. Erdmenger, N. J. Evans, Z. Guralnik and I. Kirsch, “Chiral symmetry breaking and pions in non-supersymmetric gauge / gravity duals,” *Phys. Rev. D* **69** (2004) 066007 [[arXiv:hep-th/0306018](#)].

[50] N. J. Evans, C. V. Johnson and M. Petrini, “Clearing the throat: Irrelevant operators and finite temperature in large  $N$  gauge theory,” *JHEP* **0205** (2002) 002 [[arXiv:hep-th/0112058](#)].

[51] K. A. Intriligator, “Maximally supersymmetric RG flows and AdS duality,” *Nucl. Phys. B* **580** (2000) 99 [[arXiv:hep-th/9909082](#)].

[52] A. Hashimoto, “Holographic description of D3-branes in flat space,” *Phys. Rev. D* **60** (1999) 127902 [[arXiv:hep-th/9903227](#)].

[53] N. R. Constable and R. C. Myers, “Exotic scalar states in the AdS/CFT correspondence,” *JHEP* **9911** (1999) 020 [[arXiv:hep-th/9905081](#)].

[54] A. Brandhuber and K. Sfetsos, “An  $N = 2$  gauge theory and its supergravity dual,” *Phys. Lett. B* **488** (2000) 373 [[arXiv:hep-th/0004148](#)].

[55] R. Apreda, D. E. Crooks, N. J. Evans and M. Petrini, “Confinement, glueballs and strings from deformed AdS,” *JHEP* **0405** (2004) 065 [[arXiv:hep-th/0308006](#)].

[56] J. Babington, D. E. Crooks and N. J. Evans, “A non-supersymmetric deformation of the AdS/CFT correspondence,” *JHEP* **0302** (2003) 024 [[arXiv:hep-th/0207076](#)].

[57] G. T. Horowitz and A. Strominger, “Black strings and P-branes,” *Nucl. Phys. B* **360** (1991) 197.

[58] O. Aharony, S. S. Gubser, J. M. Maldacena, H. Ooguri and Y. Oz, “Large  $N$  field theories, string theory and gravity,” *Phys. Rept.* **323** (2000) 183 [[arXiv:hep-th/9905111](#)].

[59] N. Itzhaki, J. M. Maldacena, J. Sonnenschein and S. Yankielowicz, “Supergravity and the large  $N$  limit of theories with sixteen supercharges,” *Phys. Rev. D* **58** (1998) 046004 [[arXiv:hep-th/9802042](#)].

[60] C. Csaki, H. Ooguri, Y. Oz and J. Terning, “Glueball mass spectrum from supergravity,” *JHEP* **9901** (1999) 017 [[arXiv:hep-th/9806021](#)].

[61] P. Hasenfratz and F. Niedermayer, “Perfect Lattice Action For Asymptotically Free Theories,” *Nucl. Phys. B* **414** (1994) 785 [[arXiv:hep-lat/9308004](#)].

[62] M. Lüscher, “Improved Lattice Gauge Theories,” *Phys. Lett.* **158B** (1985) 250.

[63] P. Kraus, F. Larsen and S. P. Trivedi, “The Coulomb branch of gauge theory from rotating branes,” *JHEP* **9903** (1999) 003 [[arXiv:hep-th/9811120](https://arxiv.org/abs/hep-th/9811120)].

[64] C. J. Morningstar and M. J. Peardon, “The glueball spectrum from an anisotropic lattice study,” *Phys. Rev. D* **60** (1999) 034509 [[arXiv:hep-lat/9901004](https://arxiv.org/abs/hep-lat/9901004)].

[65] B. Lucini and M. Teper, “ $SU(N)$  gauge theories in four dimensions: Exploring the approach to  $N = \infty$ ,” *JHEP* **0106** (2001) 050 [[arXiv:hep-lat/0103027](https://arxiv.org/abs/hep-lat/0103027)].

[66] J. Erlich, E. Katz, D. T. Son and M. A. Stephanov, “QCD and a holographic model of hadrons,” *Phys. Rev. Lett.* **95** (2005) 261602 [[arXiv:hep-ph/0501128](https://arxiv.org/abs/hep-ph/0501128)].

[67] L. Da Rold and A. Pomarol, “Chiral symmetry breaking from five dimensional spaces,” *Nucl. Phys. B* **721** (2005) 79 [[arXiv:hep-ph/0501218](https://arxiv.org/abs/hep-ph/0501218)].

[68] G. F. de Teramond and S. J. Brodsky, “The hadronic spectrum of a holographic dual of QCD,” *Phys. Rev. Lett.* **94** (2005) 201601 [[arXiv:hep-th/0501022](https://arxiv.org/abs/hep-th/0501022)].

[69] C. Csaki, Y. Oz, J. Russo and J. Terning, “Large  $N$  QCD from rotating branes,” *Phys. Rev. D* **59** (1999) 065012 [[arXiv:hep-th/9810186](https://arxiv.org/abs/hep-th/9810186)].

[70] J. A. Minahan, “Glueball mass spectra and other issues for supergravity duals of QCD models,” *JHEP* **9901** (1999) 020 [[arXiv:hep-th/9811156](https://arxiv.org/abs/hep-th/9811156)].

[71] N. Evans and T. Waterson, “Improving the infra-red of holographic descriptions of QCD,” [arXiv:hep-ph/0603249](https://arxiv.org/abs/hep-ph/0603249).

[72] K. Ghoroku and M. Yahiro, “Holographic model for mesons at finite temperature,” *Phys. Rev. D* **73** (2006) 125010 [[arXiv:hep-ph/0512289](https://arxiv.org/abs/hep-ph/0512289)].

- [73] T. Hambye, B. Hassanain, J. March-Russell and M. Schvellinger, “On the Delta(I) = 1/2 rule in holographic QCD,” *Phys. Rev. D* **74** (2006) 026003 [[arXiv:hep-ph/0512089](https://arxiv.org/abs/hep-ph/0512089)].
- [74] K. Ghoroku, N. Maru, M. Tachibana and M. Yahiro, “Holographic model for hadrons in deformed AdS(5) background,” *Phys. Lett. B* **633** (2006) 602 [[arXiv:hep-ph/0510334](https://arxiv.org/abs/hep-ph/0510334)].
- [75] L. Da Rold and A. Pomarol, “The scalar and pseudoscalar sector in a five-dimensional approach to chiral symmetry breaking,” *JHEP* **0601** (2006) 157 [[arXiv:hep-ph/0510268](https://arxiv.org/abs/hep-ph/0510268)].
- [76] J. Hirn and V. Sanz, “Interpolating between low and high energy QCD via a 5D Yang-Mills model,” *JHEP* **0512** (2005) 030 [[arXiv:hep-ph/0507049](https://arxiv.org/abs/hep-ph/0507049)].
- [77] J. Hirn, N. Rius and V. Sanz, “Geometric approach to condensates in holographic QCD,” *Phys. Rev. D* **73** (2006) 085005 [[arXiv:hep-ph/0512240](https://arxiv.org/abs/hep-ph/0512240)].
- [78] J. P. Shock and F. Wu, “Three flavour QCD from the holographic principle,” *JHEP* **0608** (2006) 023 [[arXiv:hep-ph/0603142](https://arxiv.org/abs/hep-ph/0603142)].
- [79] A. Karch, E. Katz, D. T. Son and M. A. Stephanov, “Linear confinement and AdS/QCD,” *Phys. Rev. D* **74** (2006) 015005 [[arXiv:hep-ph/0602229](https://arxiv.org/abs/hep-ph/0602229)].
- [80] M. A. Shifman, A. I. Vainshtein and V. I. Zakharov, “QCD And Resonance Physics. Sum Rules,” *Nucl. Phys. B* **147** (1979) 385.

[81] M. Shifman, “Highly excited hadrons in QCD and beyond,” arXiv:hep-ph/0507246.

[82] K. Ghoroku, N. Maru, M. Tachibana and M. Yahiro, “Holographic model for hadrons in deformed AdS(5) background,” *Phys. Lett. B* **633** (2006) 602 [arXiv:hep-ph/0510334].

[83] A. Karch, E. Katz, D. T. Son and M. A. Stephanov, “Linear confinement and AdS/QCD,” *Phys. Rev. D* **74** (2006) 015005 [arXiv:hep-ph/0602229].

[84] N. Evans, J. P. Shock and T. Waterson, “Towards a perfect QCD gravity dual,” *Phys. Lett. B* **622** (2005) 165 [arXiv:hep-th/0505250].

[85] O. Andreev, “ $1/q^{**2}$  corrections and gauge / string duality,” *Phys. Rev. D* **73** (2006) 107901 [arXiv:hep-th/0603170].

[86] H. Boschi-Filho, N. R. F. Braga and H. L. Carrion, “Glueball Regge trajectories from gauge / string duality and the pomeron,” *Phys. Rev. D* **73** (2006) 047901 [arXiv:hep-th/0507063].

[87] H. B. Meyer and M. J. Teper, “Glueball Regge trajectories in (2+1) dimensional gauge theories,” *Nucl. Phys. B* **668** (2003) 111 [arXiv:hep-lat/0306019].